General Disclaimer

One or more of the Following Statements may affect this Document

- This document has been reproduced from the best copy furnished by the organizational source. It is being released in the interest of making available as much information as possible.

- This document may contain data, which exceeds the sheet parameters. It was furnished in this condition by the organizational source and is the best copy available.

- This document may contain tone-on-tone or color graphs, charts and/or pictures, which have been reproduced in black and white.

- This document is paginated as submitted by the original source.

- Portions of this document are not fully legible due to the historical nature of some of the material. However, it is the best reproduction available from the original submission.

ORI

Operations Research, Inc.

TABLE OF CONTENTS

TABLE OF CONTENTS (Continued)

TABLE OF CONTENTS (Continued)

LIST OF FIGURES

LIST OF FIGURES (continued)

LIST OF FIGURES (Continued)

LIST OF TABLES

LIST OF TABLES (Continued)

GLOSSARY

α = Index for one of five noise processes ($-2 \leq \alpha \leq 2$)

ATS = Applications Technology Satellite

B_L = Phase lock loop noise bandwidth

$B_1(N, r, \mu)$, $B_2(N, r, \mu)$ = Bias functions

c = Speed of light

D = Drift rate of oscillator

δf = Frequency offset of oscillator

$\delta\tau$ = Additional path delay error

$\delta\tau_V$ = Additional vertical path delay error

ε = Time error

E_b/N_0 = Energy per bit to noise density ratio at the receiver

f = Frequency

f_0 = Oscillator frequency

h_α = Oscillator constant for noise process α

h_m = Height at which N_m occurs

i = Index denoting one of eight operational modes

ℓ = Path length

M = System margin

μ = Index for one of five noise processes ($-2 \leq \mu \leq 1$)

$n(t)$ = Oscillator noise process

N = Refractive index in Section V; Number of samples in Section VI.

$N_{\bar{e}}$ = Total electron content per square meter along the ray path

N_g = Group refractive index

N_m = Maximum density of electrons

N_T = Number of electrons per square meter

P = Pressure

$\phi(t)$ = Oscillator phase output at time t

$\phi_\varepsilon(t)$ = Oscillator phase error at time t

r = T/τ

R = Data rate

S/N = Signal to noise density ratio at the bit synchronizer

$Sy(f)$ = Spectral density of fractional frequency fluctuations

$S_{z_\alpha}(f)$ = Spectral density of individual noise process

σ = Standard deviation of timing error source

σ_B = Standard deviation of the bit synchronizer timing error

σ_{c_i} = Standard deviation of clock error for operational mode i

$\sigma_c(\tau)$ = Standard deviation of clock timing error during an interval τ

σ_D = Standard deviation of TDRS timing delay error

$\sigma_{\delta f}$ = Standard deviation of user frequency offset error

$\sigma_{\delta\tau}$ = Standard deviation of path delay error caused by propagation effects

σ_e = Standard deviation of total equipment error

σ_ε = Standard deviation of total timing error

σ_{GD} = Standard deviation of the ground station data delay measurement

σ_{GS} = Standard deviation of the ground station systematic timing error

σ_{PN} = Standard deviation of pseudo-random code timing error

σ_{POS} = Standard deviation of position error

σ_ϕ = Standard deviation of phase error

$\sigma_r(2, T, \tau)$ = Standard deviation of ranging error

σ_{TP} = Standard deviation of transponder delay error

$\sigma(\tau_{cg}, \tau)$ = Standard deviation of ground clock error during τ

$\sigma(\tau_{cs}, T_s)$ = Standard deviation of user clock error during T_s

σ_{TC} = Standard deviation of the ground station time code error

$\sigma(\tau_c, T_B)$ = Standard deviation of time error during an interval T_B following a τ_c calibration interval

$\sigma_{t_\varepsilon} = \sigma_t(2, T, \tau)$ = Standard deviation of ground clock time error caused by two-way propagation delay z

$\sigma_v(2, T, \tau)$ = Standard deviation of range rate error

$\sigma_y(N, T, \tau)$ = Standard deviation of fractional frequency fluctuations

$\sigma_y(\tau)$ = Manufacturer's frequency stability

σ_o = Calibration timing error

T = Time between successive samples in $\sigma_y(N, T, \tau)$; propagation delay in σ_{t_ε}

τ = Sampling or averaging interval

T_B = Time between end of calibration to beginning of next calibration

T_c = Time between recalibrations

τ_c = Calibration interval

τ_{c_g} and τ_{c_s} = Calibration intervals of the ground and satellite clocks respectively.

TDRS = Tracking and Data Relay Satellite

$t_\varepsilon(\tau)$ = Clock timing error during interval τ

t_o = Thickness of electron density

τ_p = Signal propagation delay

T_s = User data storage time

θ_o = Elevation angle

$U(\beta)$ = Mean Square Value of $\chi(t)$

$\chi(t)$ = Random time fluctuations

$y(t)$ = Normalized fractional frequency deviation

$z_\alpha(t)$ = Individual noise processes

I. INTRODUCTION AND SUMMARY

STATEMENT OF THE PROBLEM

For many satellites there is a requirement for precise time correlation of scientific and operational data. This correlation must be performed for many sources, collected by either single or multiple satellites and supported by the Tracking and Data Relay Satellite System (TDRSS), together with networks of ground stations and user laboratories. Since the user applications are quite varied, the necessary timing accuracies vary from milliseconds to microseconds, and possibly even as far as the sub-microsecond region. As we presently anticipate user requirements, our upper (most stringent) bound in the measurement of precise time is on the order of a few microseconds.

The TDRSS will be used by the Spacecraft Tracking and Data Network (STDN) to relay data from low orbit satellites to a ground station in the U.S. This service will commence during the 1980's.

The TDRSS will consist of a ground station and two operational relay satellites as shown in Figure 1.1. There will also be an in-orbit spare satellite not shown in the figure. A number of satellites will be supported by the TDRSS through the multiple TDRS antennas. Data will be transmitted by the user to a TDRS which will relay the data to the ground station. The TDRS's will be located in synchronous orbit such that, between them, they will be capable of maintaining almost continuous communications with the users. In fact at some altitudes, user satellites will always be visible to one of the TDRS's. Details of the TDRSS are given in the Users Guide and Technical Memorandum (References 1, 2). Only those details necessary to the timing study will be discussed herein.

There are many definitions of data timing error. One possible definition is absolute data timing error which would correspond to the accuracy of the user event data relative to some absolute national standard time reference. A second possible definition is relative data timing error

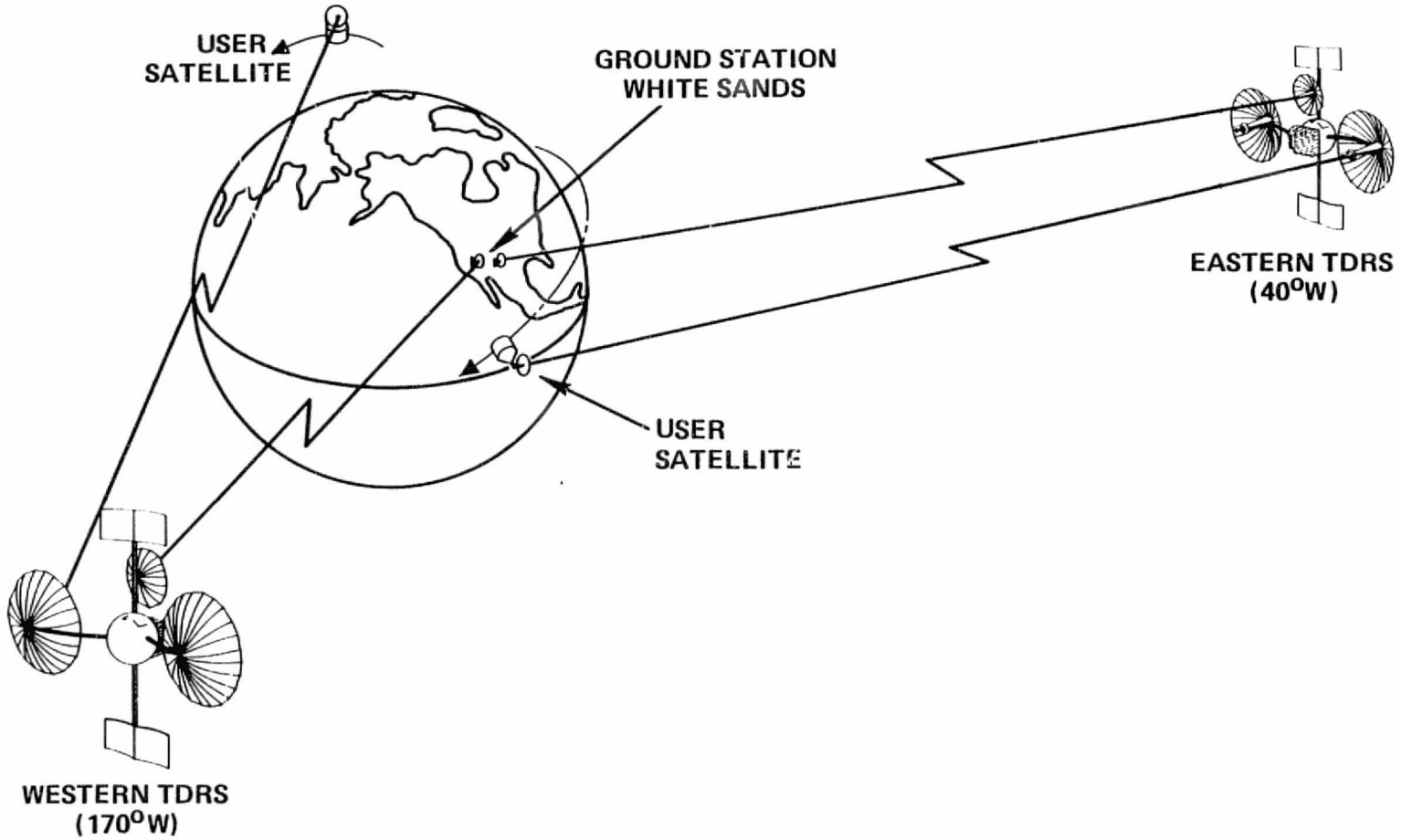

FIGURE 1.1. TDRSS CONFIGURATION

which corresponds to a user event data accuracy based on a specifically located time reference point. Based on these definitions it is clear that relative timing error will be less than or equal to absolute timing error depending on the reference point time standard and the necessary calibration with a national timing standard.

For this study effort the relative data timing error concept has been adopted. Data timing error is therefore defined as the difference between the actual sample time of some phenomenon or time reference of some event at a user satellite and the corresponding sample time or time reference of that event as calculated by a ground data processing facility using information available from the TDRSS. Typical data timing errors are derived in this report for the various items of equipment within the system (including the user and TDRSS satellites). Also, the effects of propagation anomalies on path length variations are examined. The established error analysis framework will allow for more accurate data timing error calculations when more precise information on equipment time delay variations becomes available for the TDRSS and user satellites, possibly through calibration measurements.

There are many alternative concepts for accomplishing precise time correlation, ranging from the use of highly stable clocks on each satellite to on-the-ground processing. Depending on where the actual time tagging occurs, each concept has a unique set of error sources and tradeoffs which vary with each configuration of satellites and ground stations. A need exists to:

- Analyze these alternative time tagging concepts within the range of their expected use
- Ultimately implement an optimum system which would provide highly accurate time correlation to various users.

This report attempts to satisfy the first need by presenting a timing analysis for data readout through the TDRSS. Various time tagging approaches have been considered and the resulting accuracies delineated. A general methodology now exists to analyze different users to determine the timing accuracy that can be provided by the TDRSS. The second need (to implement an optimum system to provide accurate timing to various users) is not within the scope of the present contract and represents a potential future study effort.

CONCLUSIONS

Numerous tradeoff analyses are performed in this report. These analyses focus around three basic timing areas:

- General equipment timing errors (exclusive of clocks used for time tagging user event data)
  - User satellite
  - TDRS
  - Ground station

- Propagation effect timing error
  - S-band
  - Ku-band
- Clock timing error (dependent on time tagging approach)
  - Real time data transfer of user event data (time tag at ground station)
  - Non-real time data transfer of user event data (time tag at user satellite)

Each of the above problem areas have been extensively analyzed within this report. Our general conclusions regarding these effects are discussed in the following paragraphs.

General Equipment Timing Errors

In Sections III and VII the specific implementation and contributing error sources are described and summarized. The user satellite transponder and data delay root sum squared (RSS) timing error is equal to approximately 20 nanoseconds. Similarly, the TDRS itself will have a timing error of approximately 17 nanoseconds. The ground station, however, has a much larger overall timing error equivalent to 645 nanoseconds. This is due to both data delay measurement accuracy and time code resolution. When combining all these effects, the total RSS general equipment (exclusive of clocks used for time tagging user data) timing error is about 647 nanoseconds. The dominant error source for this present TDRSS design is due to the ground station itself. If both more accurate data delay and time code measurements can be obtained, the overall general equipment timing error could be significantly reduced. As indicated in Section VII, the upper bound on general equipment timing error for a TDRSS/USER design is approximately 52 nanoseconds, assuming sufficient sophistication in the ground station equipment to cause negligible data delay and time code errors. This upper bound represents a reasonable and probable limit on any time tagging satellite-to-TDRS-to-ground scheme. It is composed of the basic user and TDRS equipment errors and the ground station bit synchronizer error. For higher data rates (than envisioned through TDRS) the bit synchronizer timing error can be decreased leaving an overall equipment timing error of 32 nanoseconds. This value of 32 nanoseconds then represents the upper limit of user event time tagging and assumes a near perfect ground station implementation.

Propagation Effects Timing Error

The effects of propagation are considered in Section V for both the ionosphere and troposphere at S-band and Ku-band frequencies. At these frequencies our estimate of the timing error is equal to a maximum of 10 nanoseconds under normal conditions. This error will increase during a rain storm,

for example, and accurate timing data may be difficult to achieve under severe and undesirable weather conditions.

Clock Timing Error

The effect of this error is primarily dependent on where the time tagging of the user event data is done as well as the frequency standard used for this purpose. Basically, two broad categories of time tagging have been considered; real time (RT) and non-real time (NRT) data transfer of user event data. These two broad classes of time tagging have each been further subdivided into four categories:

- Continuous 2-Way Range & Range Rate (R&RR) Tracking
- Continuous 1-Way RR Tracking with R&RR Calibration
- R&RR Calibration With Orbit Ephemeris Data
- One-Way Only Tracking

These time tagging approaches are discussed in detail in Sections 7 through 9. In the first above category, the forward link (from ground to TDRS to user satellite) is available so that 2-way R&RR or coherent 2-way RR can be made through the contact period. For the second time tagging above category, the forward link is generally available only at the start of a pass for 2-way R&RR measurements. For the balance of the pass one-way RR measurement data is available. The third time tagging category is similar to the previous case with the difference being that position data from orbit computations is used to determine the propagation delay between calibrations instead of one-way RR measurement data. In the final one-way only tracking mode, the user satellite is assumed to be equipped with a transmitter only. Hence, a forward link to the user (for calibration or any other purpose) is never available. Time tagging, however, is still performed on the ground for the RT data. It is necessary to have ephemeris data from the satellite to accurately determine the propagation delay.

The methodology for obtaining the timing error associated with each of these operational modes is given in Sections VIII and IX. Results are given for the clock timing error for each of these eight operational modes in Tables 8.1 through 8.3 and 9.1 through 9.4. Since there are so many possible cases of interest, refer to Sections VIII and IX for specific details and results.

RT Data Transfer of User Event Data (Ground Time Tagging). Depending on the operational mode of interest, using atomic standards on the ground for time tagging will provide a timing error by itself on the order of nanoseconds or fractions of nanoseconds. Use of crystal oscillators in the ground station will provide an error ranging from tens of nanoseconds to tens of microseconds depending on the quality of the crystal and the operational mode. Use of orbit position data will enable time tagging of RT events to an accuracy of microseconds to fractions of microseconds depending on the type of user orbit and inclination angle.

NRT Data Transfer of User Event Data (User Time Tagging). For this case the use of atomic standards in the user satellite will allow for highly accurate event time tagging ($\leq$ 10 nanoseconds) when 2-way links are available. If a nominal crystal is used in the user satellite, a worst case clock error on the order of 620 microseconds will exist when 2-way links are available. Using a higher quality crystal in the user satellite will decrease this timing error down to 2 microseconds or less. Using orbit position data will not affect a user satellite which uses a crystal oscillator for time tagging, but would severely degrade a user satellite which has an atomic standard on-board for event time tagging. The resulting timing error for this last case would be the same as for the RT operational mode discussed above. If a 1-way only link is available from the user, use of a nominal crystal in the satellite will result in a maximum timing error of 750 microseconds, whereas using either a high quality crystal or an atomic standard will yield a maximum clock timing error of 24 microseconds.

Summary of User/TDRS Timing Errors

Table 10.1 presents a summary of the total system timing error, σ_ε, including the various contributing effects. The results are based on a representative worst case analysis of each operational mode. For convenience, this table is repeated in this section as Table 1.1. In order to understand these results more completely, reference to Sections VIII and IX is necessary. The shaded areas in Table 1.1 represent "practical and reasonable" system implementations using appropriate ground and/or user satellite frequency standards.

In terms of satisfying our initial goal of $\sigma_\varepsilon \leq 1$ μsecond timing error, only operational modes 1 and 2 are fully acceptable using an atomic standard as the ground clock and at least a high quality crystal clock in the user satellite for mode 2. Modes 3 and 4 would also be acceptable for certain high inclination orbits. All of these first 4 modes deal with time tagging real-time event data only. For non real-time event time tagging, the next 4 modes are basicly unacceptable (for σ_ε = 1 μsec) without some modifications of parameters, such as reducing the user data storage time or placing an atomic standard aboard the user spacecraft. One additional comment worth noting is that one-way links from the user through TDRS generally provide either poor timing accuracy or small data storage time. The primary reason for this poor accuracy is the determination of the frequency offset error component.

RECOMMENDATIONS FOR FURTHER STUDY

Two specific areas of further study are recommended. The first topic deals with improvements of this report and the second is directed towards satisfying our second need (discussed earlier) of an optimum system implementation.

Current Study Improvements

Our major conclusions have just been outlined for three basic areas of investigation; equipment, propagation and clock timing errors. In two of these study areas, further effort is warranted to improve the overall timing accuracy. First, attempts should be made to reduce the ground equipment error from 647 nanoseconds to approximately 50 nanoseconds by using a more accurate time code and obtaining a better data delay measurement accuracy. Secondly,

TABLE 1.1

SUMMARY OF USER/TDRSS TIMING ERRORS

Operational Mode	Equipment Timing Error, σ_e	Clock Timing Error, σ_{c_i}				Total System Timing Error, σ_ε			
		Nominal Crystal	High Quality Crystal	Rubidium	Cesium	Nominal Crystal	High Quality Crystal	Rubidium	Cesium
1*	647 nsec.	$\leq$ 3.3 μsec	$\leq$ 12 nsec	$\leq$ 0.6 nsec	$\leq$ 0.9 nsec	$\leq$ 3.4 μsec	$\leq$ .65 μsec	$\leq$ .65 μsec	$\leq$ .65 μsec
2*	647 nsec.	$\leq$ 90 μsec	$\leq$ 0.3 μsec	$\leq$ 3 nsec	$\leq$ 2 nsec	$\leq$ 90 μsec	$\leq$ .71 μsec	$\leq$ .65 μsec	$\leq$ .65 μsec
3* and 4*	647 nsec.	← $\leq$ .34** (1.9) μsec*** →				← $\leq$ .73** (2.02) μsec*** →			
5* and 6*	647 nsec.	$\leq$ 620 μsec	$\leq$ 2.1 μsec	$\leq$ 10 nsec	$\leq$ 6 nsec	$\leq$ 620 μsec	$\leq$ 2.2 μsec	$\leq$ .65 μsec	$\leq$ .65 μsec
7*	647 nsec.	$\leq$ 620 μsec	$\leq$ 2.9 μsec	$\leq$ .34** (1.9) μsec***		$\leq$ 620 μsec	$\leq$ 3.0 μsec	$\leq$ .73** (2.02) μsec***	
8*	647 nsec.	$\leq$ 750 μsec	$\leq$ 24.1 μsec			$\leq$ 750 μsec	$\leq$ 24.2 μsec		

*1 - RT Continuous 2-way R&RR
2 - RT Continuous 1-way RR with R&RR Calibration
3 - RT R&RR Calibration with Position Data
4 - RT One Way Only Tracking
5 - NRT Data Transfer - Continuous 2-way R&RR
6 - NRT Data Transfer - Continuous 1-way RR with R&RR Calibration
7 - NRT Data Transfer - R&RR Calibration with Position Data
8 - NRT Data Transfer - One Way Only Tracking

** For High inclination orbits.

*** For Low inclination orbits.

a detailed technical effort is required to precisely determine the frequency offset error for one-way only tracking of stored data. This quantity was treated parametrically during our study effort with bounds based on practical knowledge of spacecraft systems. Both of these study efforts could have an impact on the results shown in Table 1.1. In particular, a reduction in the ground timing error to 50 nanoseconds would reduce the values of σ_ε shown in Table 1.1 for the first seven operational modes. Any reductions in the frequency offset error would then reduce the value of σ_ε for the eighth operational mode shown in Table 1.1.

Optimum Timing System Implementation - Users Timing Guide

The above second objective of implementing an optimum system to provide accurate timing to various users has not been analyzed to date. In order to satisfy this second objective. two broad areas of system analysis and engineering are warranted; (1) user satellite(s) and (2) TDRSS. One cannot analyze and determine the resulting user satellite timing accuracy without similarly examining the total impact on the TDRS system and its various components. Based on these analyses it will then be possible to develop a user's timing guide and TDRSS ground system timing guide document. These efforts coupled with subsequent tradeoffs and system engineering analysis will then allow for an optimum system design, thereby satisfying the second need expressed earlier in this section.

This study should encompass the following tasks:

- Task 1 - Definitions and standards of timing error sources
- Task 2 - Development of broad ranges of user characteristics (orbit, application, real-time or stored timing need, communication capability, timing accuracy requirement)
- Task 3 - Ground data processing error analysis
- Task 4 - Development of user satellite timing guide
- Task 5 - Development of ground station timing guide
- Task 6 - Optimum design of TDRSS/USER time correlation system with various performance options.

ORGANIZATION OF THE REPORT

This report is divided into ten major sections. Section II discusses the general system timing concept. In Section III the various equipment time delay error sources are determined. These include ground station, TDRS, and user error sources exclusive of the clock error associated with time tagging user event data. This particular clock timing problem is addressed specifically in Section VI. Section IV discusses some operational considerations with respect to user satellites and the TDRSS. Propagation effect timing error is described in Section V. Ionospheric and tropospheric effects are considered. Section VII indicates the approach taken to determine the total system timing error. In Sections VIII and IX the computation of the clock timing error is described for a total of eight operational modes. Finally, Section X summarizes the overall timing error to be expected for the various User/TDRS operational modes.

II. GENERAL TIMING SYSTEM CONCEPT

USER SATELLITE EQUIPMENT

A simplified block diagram of the configuration of a typical user satellite is shown in Figure 2.1. The diagram is intended to show the relationship between the flow of the data, carrier and ranging signals. It is not expected that acquisition operations will have a direct bearing on data timing so that acquisition functions are not included in the diagram.

The user satellite will contain a data reference oscillator or an overall satellite reference oscillator which will be used as a reference for data timing within the data processor. Satellite clock signals will also be derived from the same oscillator. Phenomenon of interest or events occurring at the satellite will be detected by a number of detectors, depending on the satellite mission. The detector outputs will be sampled and digitized or event times assigned and the information organized into a data frame. The clock signals will be sampled at some predetermined point in the frame and the time combined with the data. The binary data will be convolutionally encoded to allow bit error rate improvement when received at the TDRSS ground station. The data is combined with the pseudo-random ranging code, if necessary, to provide the spread spectrum characteristic. The data then modulates a signal from the frequency synthesizer and is transmitted.

Equipment is provided to synchronize with the received carrier and the pseudo-random ranging code in the forward link from a TDRS to provide a coherent carrier and ranging code in the return link. The carrier PLL is locked to and tracks the received carrier. Local oscillator signals are then generated in the frequency synthesizer for up and down conversion such that the transmitted carrier is a constant multiple factor of the received carrier. The pseudo-random code bit rate is tracked by a separate PLL or by an incremental phase modulator which uses an output of the frequency synthesizer as a reference. A locally generated code is synchronized with the received code and provides a noise free signal for coherent range code transmission in the return link and for spread spectrum data modulation.

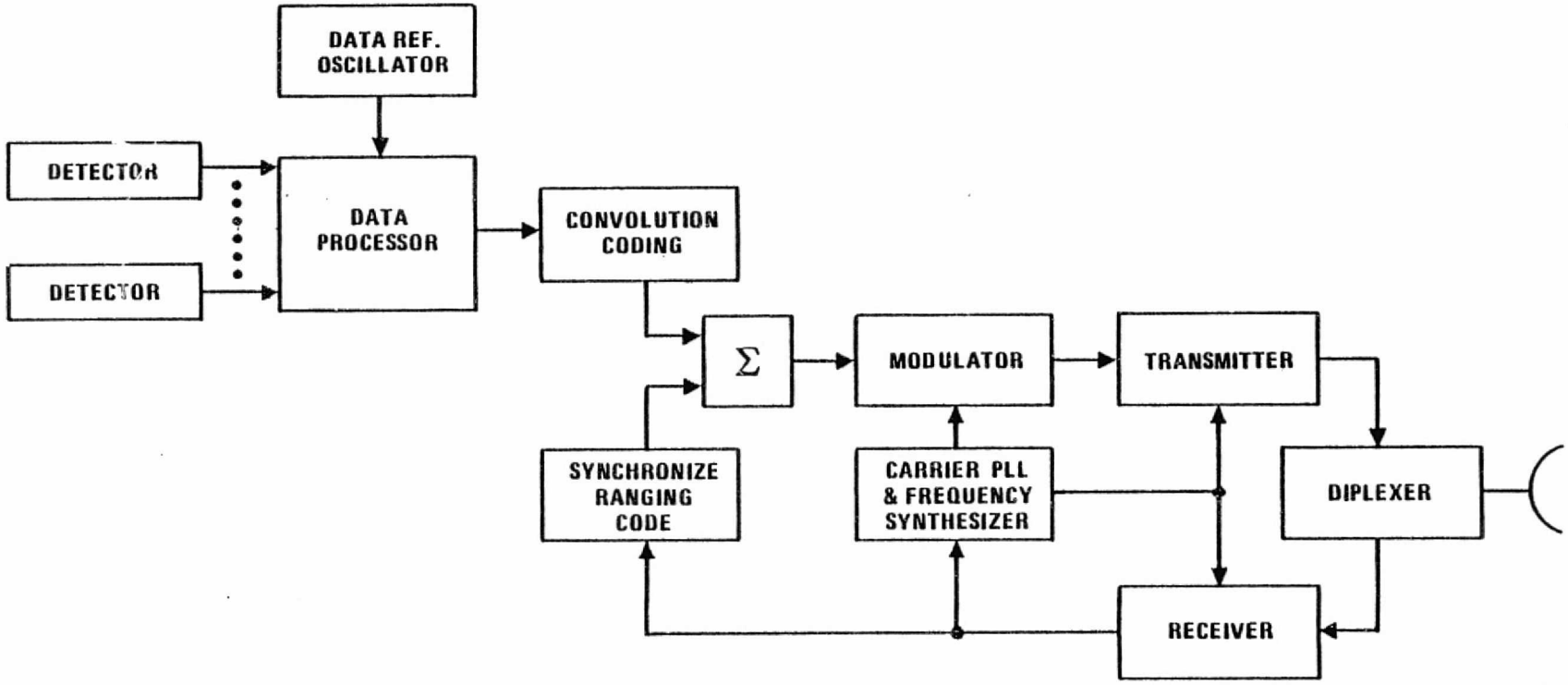

FIGURE 2.1. SIMPLIFIED BLOCK DIAGRAM OF TYPICAL USER EQUIPMENT

The equipment can be operated in a one-way transmit only mode. In this case the frequency synthesizer frequencies may be generated from the free-running PLL oscillator or from a separate fixed frequency oscillator to provide greater precision in the return carrier frequency. If a separate oscillator is required then this may be a satellite reference oscillator used as a reference for all satellite operations including data processing.

TDRS

A simplified block diagram of a TDRS is shown in Figure 2.2. The TDRS essentially performs frequency translations in the forward and return links. A frequency synthesizer can be locked to the received signal in the forward link and provides all up and down conversion frequencies to the RF equipment so that coherent operation is possible for ranging operations.

TDRSS GROUND STATION

A simplified block diagram of the TDRSS ground station equipment is shown in Figure 2.3. The ground station generates a pseudo-random code for ranging and frequency spreading and transmits this code on the forward link to the user satellite.

Return-link signals from the user satellite are down converted and the data and/or pseudo-random ranging code demodulated in a receiver which phase locks to the carrier components of the received signal. A ranging code synchronizer synchronizes with the pseudo-random ranging code and provides a data output with the code removed. A receiver frequency component and a ranging code synchronizer timing signal connect to the range and range rate (R&RR) equipment where the two-way range delay and range rate measurements are made.

The data signal enters a bit synchronizer which synchronizes with the data bit rate and provides a noise-free data output. The convolution code is then decoded to provide an output at the user clock rate. A ground station time tag is generated for the bit which will become the first bit of a data block. The data and time tag are assembled into data blocks and then transmitted to the user facility. Note that, at the point the data is assembled into blocks, further time referencing is impossible, particularly since the data may also be held in buffer storage. This means that the user has only those time references applied prior to data blocking for data timing.

The method of handling multi-megabit data at the ground station and transmission of this data to the user facility has not been defined at this time. A similar time tagging scheme may be used or a time signal could be transmitted in parallel with the data. The analysis in this document determines the data timing accuracy with the time tag scheme described in this paragraph and may require modification when multi-megabit operations are defined.

DATA TIMING METHOD

The method relating user satellite time to ground time will be

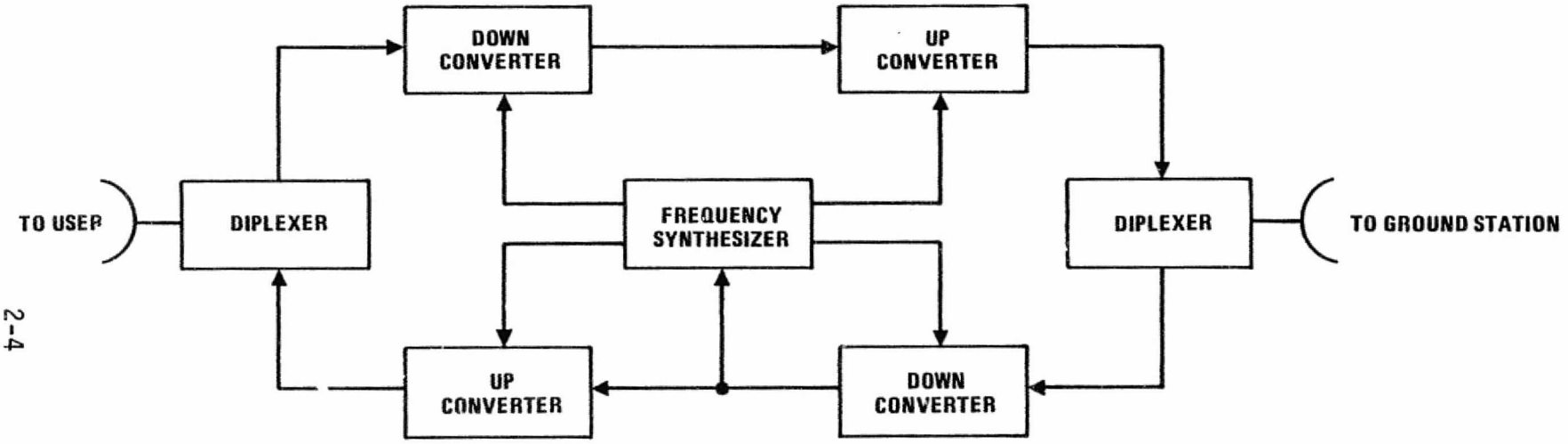

FIGURE 2.2. SIMPLIFIED BLOCK DIAGRAM OF TDRS

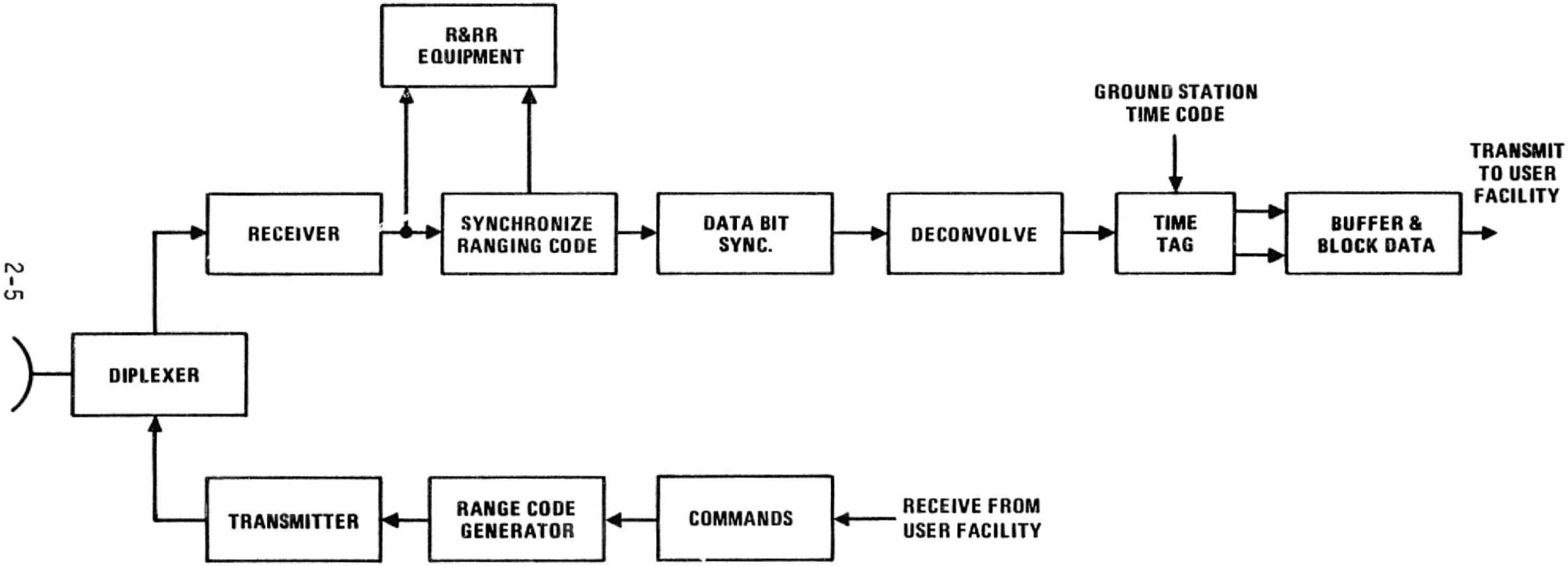

FIGURE 2.3. SIMPLIFIED BLOCK DIAGRAM OF GROUND STATIONS EQUIPMENT

described. The data timing problem becomes one of correlating the user satellite time reference with ground time.

When the user facility receives the data and time tags from the TDRSS ground station, it must perform a computation to determine the original data timing at the user satellite. Figure 2.4 will help to explain the operations involved.

The data delay time is computed for the time of the tagged bit and then the delay time is subtracted from the time tag to give the actual time that the bit occurred in the user satellite. The number of bits to the next sync word are counted and the equivalent delay time is calculated with a knowledge of the user satellite bit rate. The delay time from the time tagged bit to the sync word is added to the time of occurrence of the tagged bit in the user satellite to determine the time of occurrence of the sync word in the user satellite. Once a time reference has been established for a sync word, the timing of any data can be determined from the position of the data in the frame and the known user bit rate. The timing error between time tags, neglecting other error contributions, is dependent on the user satellite data oscillator stability.

Using the user satellite clock time transmitted with the data, it is possible to correlate satellite time with ground time and establish the drift rate. This would enhance the data timing accuracy and only occassional delay computation may be required, depending on the user satellite data oscillator stability and the data timing accuracy requirements.

The method for data timing, as described above, can be utilized with the planned TDRSS configuration, and is the method given prime consideration in this report. Other possible timing methods were seen as possible during the analysis. One of these methods was to correlate the user satellite through direct communications to ground stations, bypassing the TDRSS. No general advantage can be seen to this method since time correlation would only be possible when the user satellite was visible to a ground station which, for low orbit satellites, would be only occassionally. Also the delay time from the ground station to the user satellite would be required to a high degree of accuracy. The TDRSS can provide frequent observations of the user satellite, at least once per orbit during prime operating times, and has precise ranging capability.

Another method of correlating user satellite time with ground time, which does appear to have some merit, is to use the pseudo-random ranging code for time correlation. The time that some particular pattern in the code occurred at the user satellite, such as the all ones pattern, would be transmitted with the data. The TDRSS ground station then records the times that the all ones pattern is received at the ground station and transmits this information to the user data reduction facility. The user satellite time and ground time can then be correlated by computing the communications delay.

An alternate scheme, using the pseudo-random ranging code, is to use the forward link for time correlation. In this case, the ground station records the transmission time for the all ones pattern. The user satellite

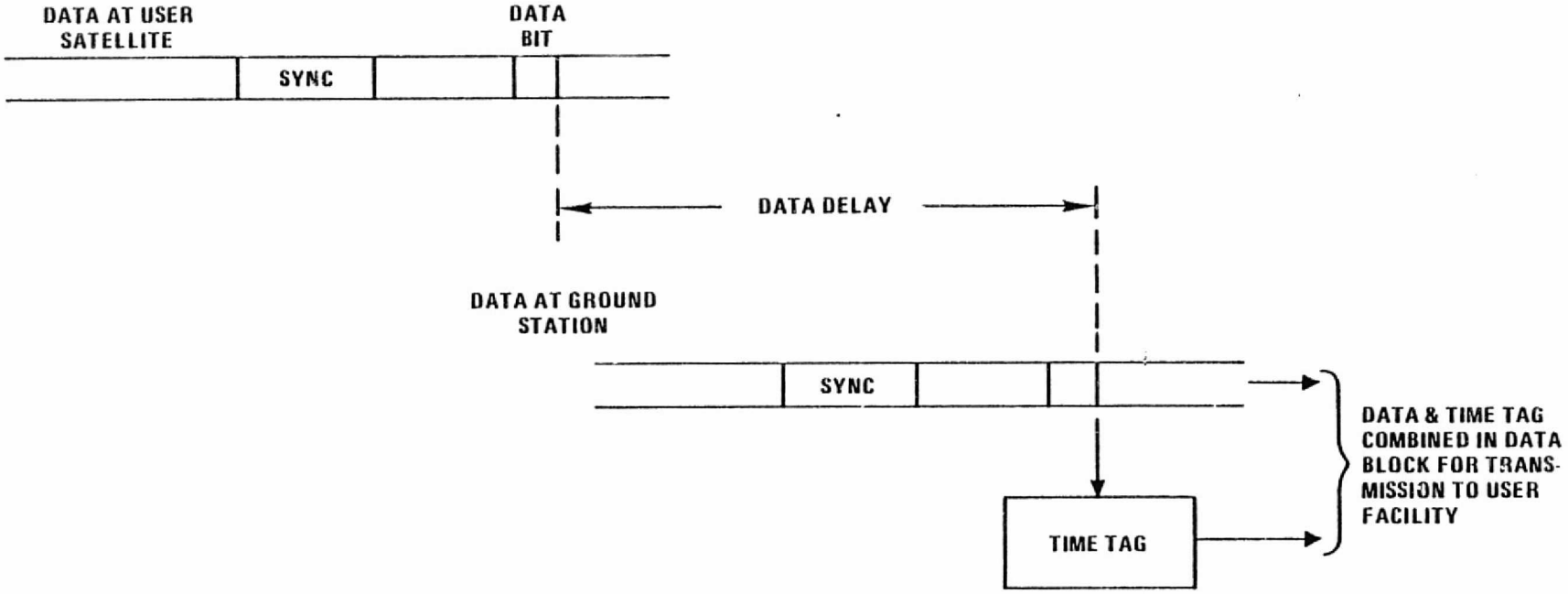

FIGURE 2.4. DATA FLOW & TIMING

records the time that the all ones pattern is received and transmits the time with the data to the ground station. If the forward delay is computed, it is possible to calibrate the user time reference against ground station time. This may be more easily accomplished since the code is transmitted from the ground station at precise intervals and may be at the same time for all satellites, whereas the received times vary with satellite range.

The potential disadvantage of using the pseudo-random code is that it may not always be available, as will be discussed in Section IV.

PARAMETERS CONTRIBUTING TO TIMING ERROR

Figure 2.5 shows the various elements of the system which contribute to timing error. When 2-way ranging data is used in computation of data delays, then all equipment contributes to data timing errors, including the forward link equipment. If 1-way Doppler data is used then the forward links will not contribute to data timing errors.

It is seen that ranging computations play a big part in time correlation and the data timing error. The availability and quality of ranging data is therefore important to the analysis and will be emphasized.

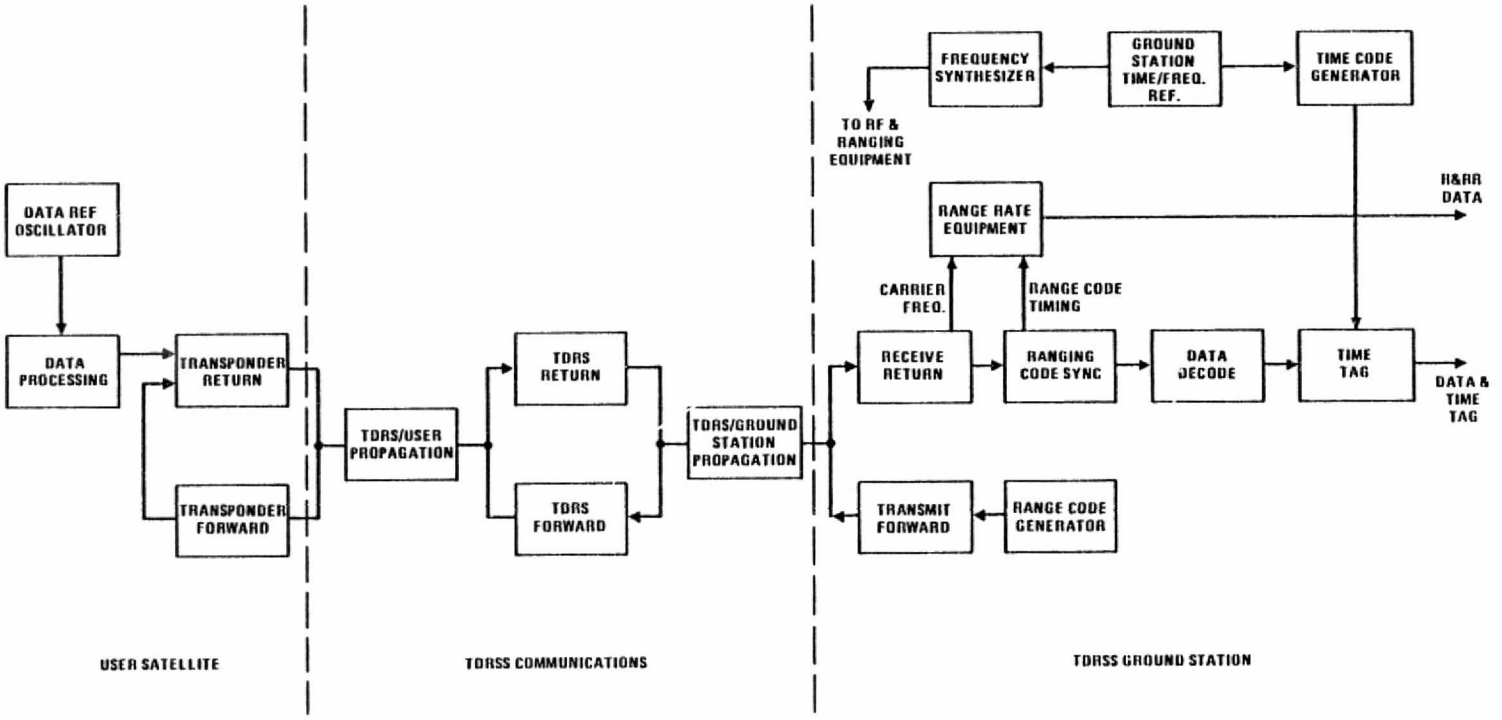

FIGURE 2.5. ELEMENTS OF SYSTEM CONTRIBUTING TO TIMING ERROR

III. EQUIPMENT TIME DELAY ERROR SOURCES

USER SATELLITE TIMING ERRORS

General Considerations

Data timing errors in the user satellite will depend directly on the timing errors and delay variations in the data equipment and indirectly on the delay variations in the transponder which will affect the range delay computation accuracy. In this subsection, estimates will be made of data equipment errors. Tracking and Data Relay Experiment (T&DRE) transponder calibration data will be used to provide estimates of transponder delay errors.

Data Equipment Timing Errors

To provide accurate system data timing, the user satellite must provide accurate data timing and transmit the data in a format that allows accurate data timing computation at the user data reduction facility. Two basic implementations will be discussed; namely, a sampled data system and a discrete event data system. The two systems will be briefly discussed first; then particular segments of the systems, followed by timing errors for a single logic gate, and finally, overall timing error estimates will be made. Note that the reference oscillator, which provides the reference for data system operations, is not covered here but will be analyzed in detail in Section 6.

Sampled Data System. The essential elements of a sampled data system are shown in Figure 3.1. A number of detectors monitor the phenomena of interest and provide electrical outputs. An oscillator provides the basic time reference and drives a time code generator. Format timing signals are generated, using the reference oscillator output as a clock signal, which control the sequencing of the sampling and data formatting functions. The detector outputs are sampled and digitized and the digital data, together with the time code generator output, are formatted in a predetermined sequence. The detectors provide continuous data or data in synchronism with timing signals from the formatting circuitry.

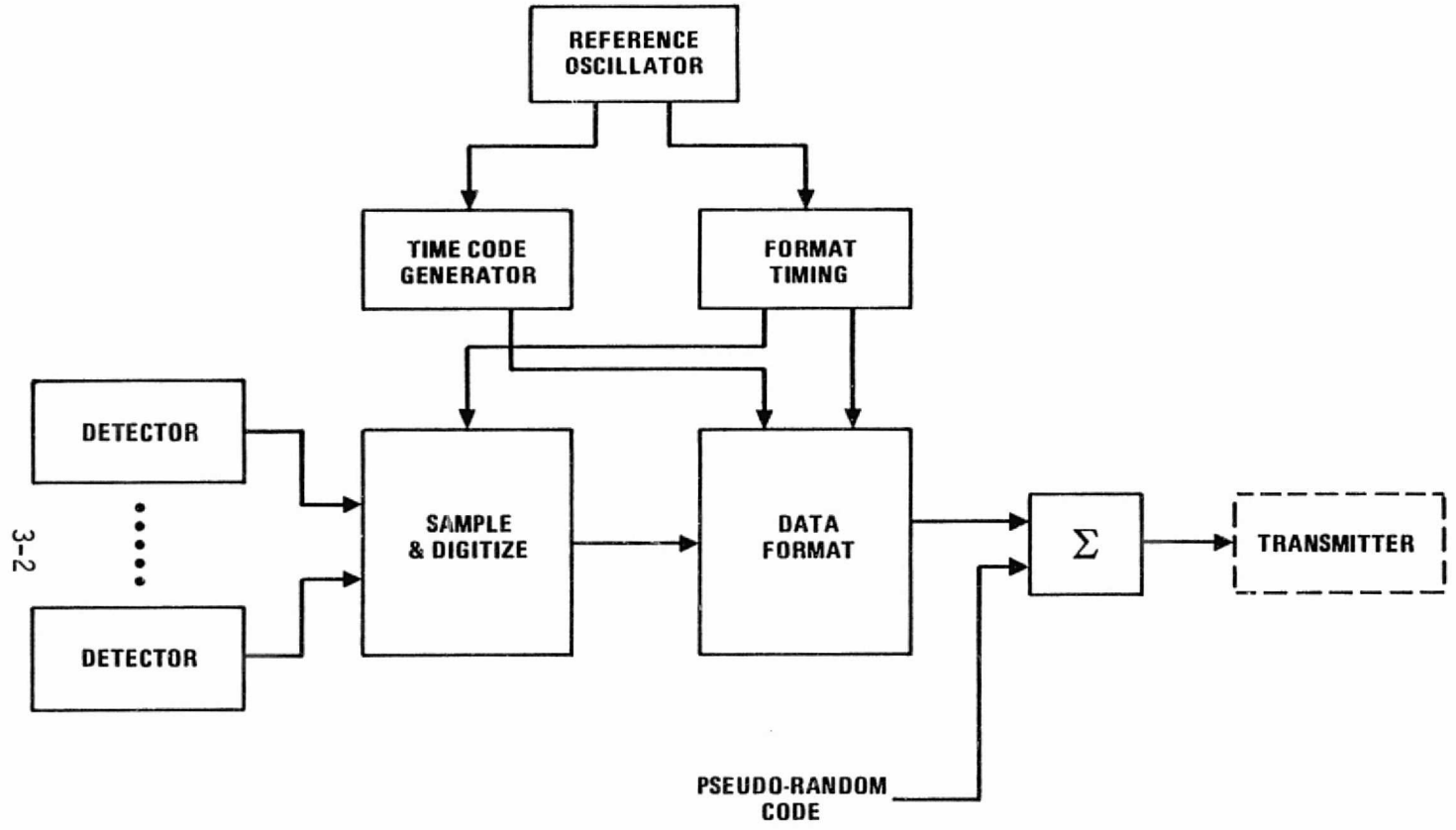

FIGURE 3.1. BLOCK DIAGRAM OF SAMPLED DATA SYSTEM

All timing depends on the bit timing. The ground station tags a particular bit and the user satellite time code generator is advanced at the bit rate.

Discrete Event Data System. This system is shown in Figure 3.2. Here, event detectors detect discrete events and provide an output signal to a time selector which stores the time of the events until sampled by the data formatter. The buffer storage is necessary to hold the information until entered into the data stream by the data formatter.

Time Code Generator. There are different methods for implementing the time code generator circuitry and sampling of the output depending on the system accuracy requirement and data rates. The simplest case is that of the sampled data system where the time code output is inserted in the data once per frame so that the user data reduction facility can correlate user satellite time with ground station time. The time code generator would include a count down chain, which for the simplest case, would be a binary ripple counter. The counter would count at the bit rate and the output would be inserted in the data for a particular bit each frame. It is assumed here that the counter completes the ripple count and allows time for sampling within the bit period to avoid ambiguous timing. With this arangement it may be possible to interpolate the times of data samples within a bit period.

Accomplishing the ripple count may not be possible within one bit period. If the data rate is 1 Mbps and for example a 20 stage counter is required to provide a 1 second count (it may be possible to keep track of any timing beyond 1 second during data reduction to avoid ambiguity), then each stage must have a propagation time of less than 50 nanoseconds which requires fairly fast logic. Alternate counter configurations are possible. For instance, each stage can include a gate which checks for the all ones state in previous stages and the stage only changes state when the all ones condition is detected. With this arrangement all stages change state simultaneously and the propagation delay is nearly the same as for one stage.

With the discrete event data scheme the requirements for code insertion for correlation of user satellite time are the same as for the sampled data system. If event times are required to a resolution of less than one bit then the counter must count at a higher rate than the bit rate and change state at a more rapid rate. It is therefore more likely that the simple ripple counter could not be used and more complex arrangements would be required.

Format Timing Generation. The format timing generation is shown in Figure 3.3. The reference oscillator is counted down to the highest rate required for formatting. A series of count downs then provide the bit word and frame timing and will probably be a combination of series and parallel counters. The various counter outputs are clocked from the same time to provide the final outputs. This final clocking provides outputs with accurate relative timing. Timing errors will occur primarily in the initial count down, fixed delay and the output gates so that the major part of the circuitry will not influence timing errors. The fixed delay can be obtained from different phases of the initial count down output.

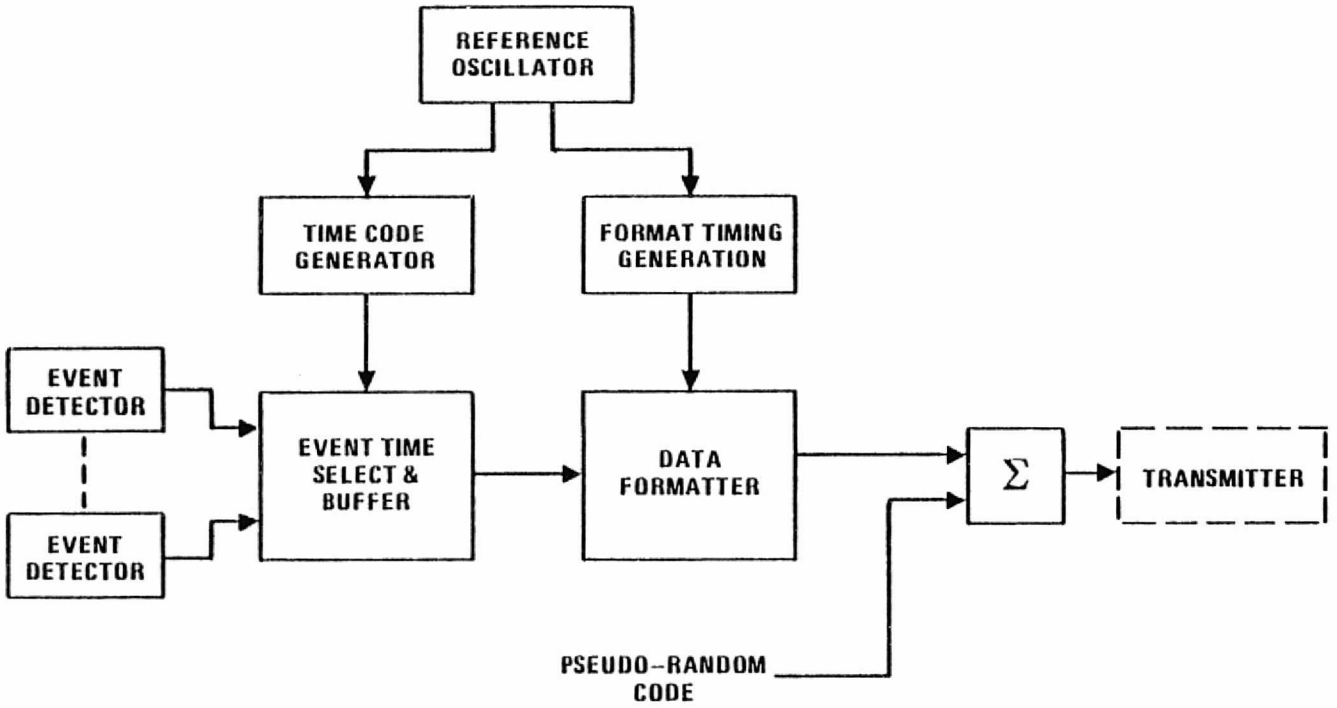

FIGURE 3.2. DISCRETE EVENT DATA SYSTEM

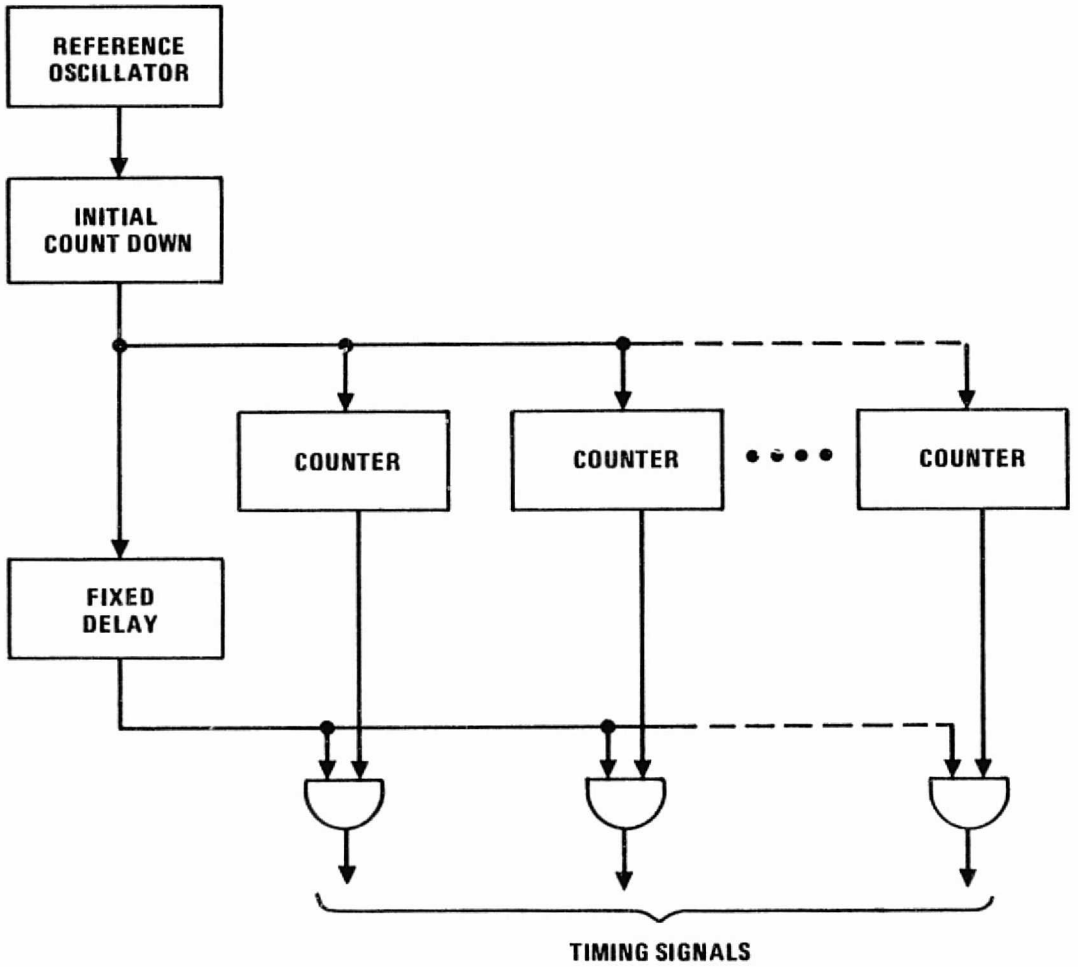

FIGURE 3.3. FORMAT TIMING GENERATION

Timing Errors for a Single Logic Gate. Timing errors will be calculated for a single logic gate to demonstrate the method for deriving errors and to indicate the order of magnitude of logic timing errors which will constitute the major portion of the timing errors within the user satellite data system.

C-MOS logic is often used for spacecraft hardware and will be used as a basis for determining time delays and jitter variations. Information from the RCA Solid State Databook 74 Series will be used. This logic is not very high speed and should represent worst case delays. Typical characteristics for a nor-gate are listed below:

- Propagation delay — 35 nsec
- Transition Time — 65 nsec (10 to 90%)
- Temperature Coef. for the above — 0.3%/^{o}C
- Variation with Supply Voltage — 3.2 nsec/volt at 5 volts

The variation of propagation delay with temperature will be 35 x .003 = 0.1 nsec/^{o}C. If a long term supply variation of 0.1V is assumed then the delay variation will be 0.3 nsec. Short term variations may be caused by noise in the return lines to communicating devices causing timing variations through the finite rise time and short term variations in the supply voltage. If 0.05V rms variations is assumed for the return line noise and supply voltage variation the jitter will be:

$$\sigma = \frac{.05}{4} \times 65 = 0.8 \text{ nsec for return noise.}$$

(transient delays are for 10 to 90% of the voltage swing, i.e. 4V)

$$\sigma = .05 \times 32 \approx .2 \text{ nsec for supply voltage variation}$$

Thus, the variations for a single gate are fractions of a nanosecond.

Estimation of Data System Delays and Timing Errors. Figure 3.4 shows the time delays for a sampled data system. The detector output passes through a gate to a sample and hold circuit. The stored sample is then converted to digital form and clocked into the data stream through a parallel to serial register. It is assumed that direct digital data will also be combined with the data requiring equipment equivalent of two gates. The data is then combined with the pseudo-random code through an exclusive -or circuit. The digitizing time is variable depending on the speed of the A/D converter. A period equivalent to one word period may be allowed for this function. The total delay will be the summation of time delays shown which is 195 nsec plus one word time.

The circuit functions contributing to timing variations are shown in Figure 3.5. If most functions are clocked at the bit rate then some functions will not affect timing. For instance, if the count down to the word rate is clocked at the bit rate, then it will not cause delay variations. In Table 3.1

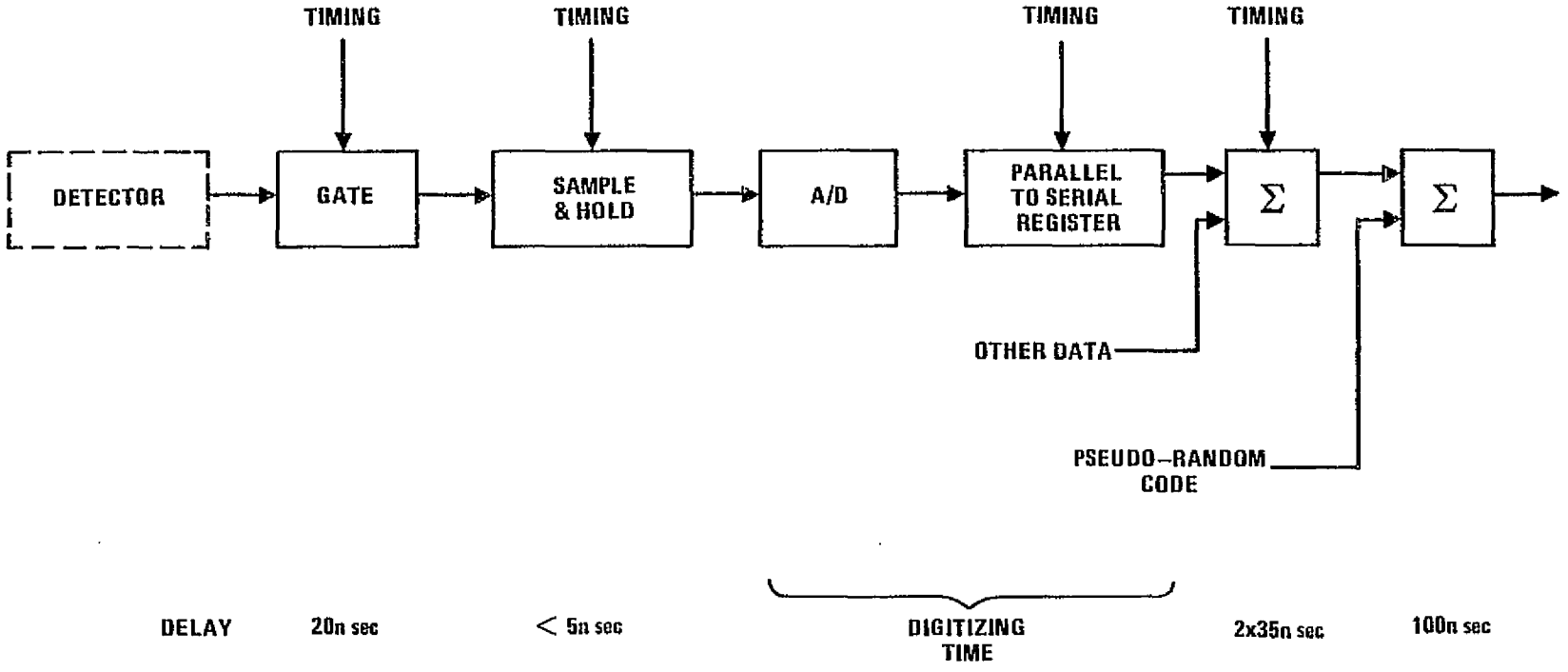

FIGURE 3.4. SAMPLE DATA SYSTEM TIME DELAYS

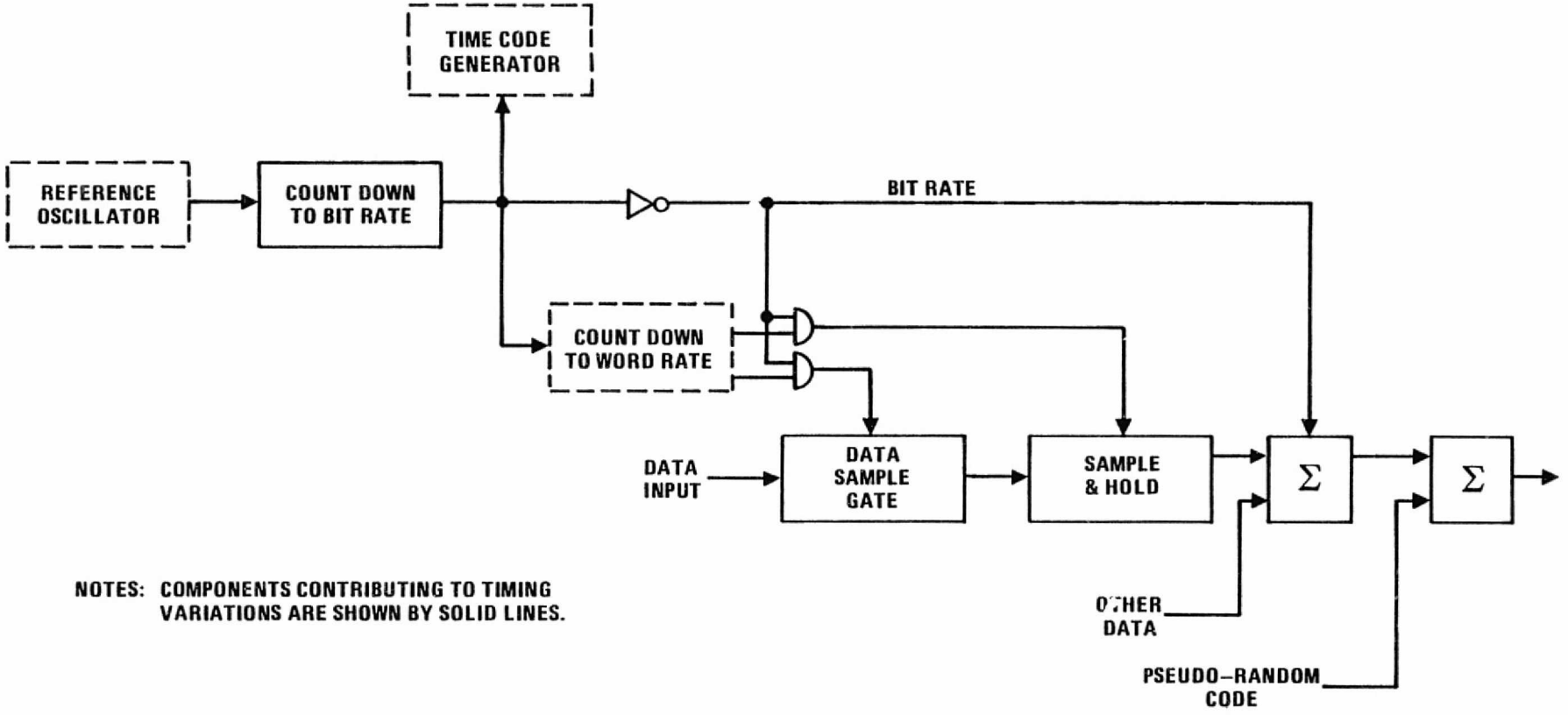

FIGURE 3.5. SAMPLED DATA SYSTEM TIMING VARIATIONS

TABLE 3.1. SAMPLED DATA SYSTEM DELAY VARIATIONS (NSEC)

Circuit Function	Total Delay	Transition Time	Temperature* Delay Variation (1°C)	Return Noise** Variation (.05V rms)	Supply Voltage* Variation (.05V rms)
Count Down to Bit Rate, 3 Stages	3 x 175	3 x 175	1.6	2.2	.4
Inverter	15	20	0	.3	.2
Gate	35	65	.1	.8	.2
Sample Gate	20	-	.1	-	-
Sample and Hold	5	-	0	-	-
Data Combining Gates	2 x 35	2 x 65	.2	.8	.4
Exclusive -or	100	70	.3	.9	1.0

RSS of Variations~3.3 nsec

* Based on total delay
** Based on one transition time for multiple devices

an attempt is made to estimate the overall delay variations. The temperature delay variation in obtained by multiplying the total delay by the factor of 0.3%/°C, given in the previous paragraph. It is assumed that the short term temperature variation would not be greater than 1°C. Return noise variation is the delay variation due to circuit return noise of .05V rms. Series devices, such as in the bit rate count down which may be on one chip, are considered to experience the same instantaneous level of return voltage and only one transition time is considered in the calculation. A supply voltage variation of .05V rms is assumed and considered to affect all devices. The RSS variation is 3.2 nsec and this can only be considered a very rough approximation. Actual circuit implementation might require more complexity, particularly in gates and buffer inverters. Also, it was noted that the device delay variation is very susceptible to supply voltage variation at lower voltages. Average variations were used in the computation, however, the maximum variation of the exclusive -or gate, for instance, increases by an order of magnitude at about 5 volts.

Figure 3.6 shows the discrete data system components contributing to time delay variations. Timing variations would occur in the time code generator, selecting the event times and clocking the data out, and would be of similar order of magnitude as for the sampled data system. The resolution of event timing would depend on the time code generator resolution and it would be possible to resolve the time to less than one bit period.

Transponder Delays

Calibration data for the Nimbus-6 T&DRE equipment was reviewed to obtain data on transponder delays. The Nimbus-6 T&DRE equipment operates at S-band in conjunction with the ATS-6 relay satellite. The experiment uses a 100 kHz tone for range measurements which directly modulates the carrier on the forward link and modulates a 2.4 MHz subcarrier on the return link. TDRSS user transponders require a wider bandwidth, particularly on the forward link, to accomodate the 3 or 6 Mbps pseudo-random ranging code. This means that TDRSS user transponder delay variations should be less than those for the Nimbus-6 T&DRE transponder and the values presented will be conservative.

Many calibration measurements were made of the Nimbus-6 T&DRE transponder characterisitcs for variations in signal level, frequency and temperature. The total delay averaged about 2.7 μsecs for strong signal conditions. Approximate total variations are listed below:

Parameter	Total Maximum Variation
Temperature Variation (0 to 40°C)	25 nsec
Received Signal Level Variation (50 dB dynamic range)	60 nsec
Frequency Uncertainty (± 100 kHz)	30 nsec

It is possible to correct for these variations if necessary, provided sufficient calibration data is available. However, this may not be necessary since the variation in the user satellite may not be as great. The temperature

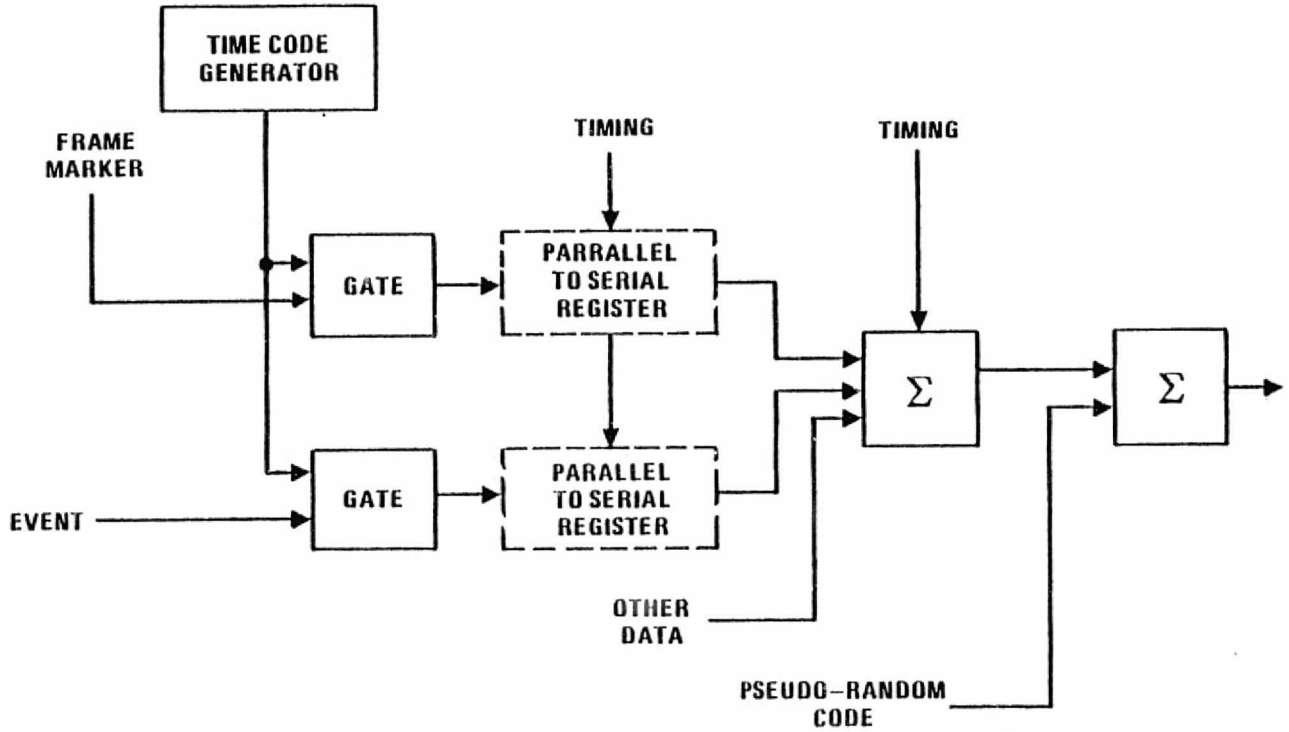

FIGURE 3.6. DISCRETE EVENT SYSTEM TIME DELAY COMPONENTS

variation would be expected to be much less than 40°C. The received signal level variation may be of the order of 10 dB for a low orbit satellite. The wider bandwidth of the TDRSS user transponder would be less sensitive to frequency uncertainty which will be due primarily to Doppler shift.

A total delay variation may be determined for the variations given in the previous paragraph. If it is assumed that the variables are uniformly distributed for the range of variation shown, then the total delay variation, σ_{TP} is of the order of 20 nsec.

A variation, not present in the Nimbus-6 T&DRE transponder, is the detection of the pseudo-random ranging code in the TDRSS user transponder. This function will add a delay variation, σ_{PN}, of 2.4 nsec with expected signal to noise ratios and a multimode ranging code chip rate of 3.07 Mcps (Ref. 3).

The delay considered here is the total transponder delay used for range and range rate computations of satellite position. If the one way data delay is required from two-way range delay data then the delays in the forward receiving equipment and return transmitting equipment would be required separately. If this is the case, the transponder should be calibrated so that the delays can be separated.

TDRS DELAY ERRORS

The TDRSS office has specified that the TDRS contribution to range delay error shall be less than $\pm$ 30 nsec. In order to combine the error values of the various contributors it is necessary to convert them to a common form and the standard deviation is most convenient. To determine the standard deviation the distribution must be known or a distribution assumed. A conversative assumption is a uniform distribution between the limits $\pm$ 30 nsec which results in a σ_D of 17.3 nsec.

TDRSS GROUND STATION DATA TIMING ERRORS

General TDRSS Characteristics

Characteristics of the TDRSS ground station have been obtained from TDRSS documentation and coordination with the TDRSS Program Office to clarify details. These characteristics will be given and discussed in this subsection. One factor which was considered to require analysis, is the clock timing accuracy generated by the data bit synchronizer which will provide the reference for ground station time tagging. The data bit synchronizer clock timing accuracy will be analyzed in the next subsection.

The TDRSS characteristics considered applicable to the data timing analysis are listed in Table 3.2. A range of data rates are available in the different modes. Details are given for the range measurement data available and accuracies. The range measurement systematic error is the two-way delay error for all ground station equipment involved in handling ranging signals. The ground station time code will be a 46-bit binary microsecond code and this

TABLE 3.2

SUMMARY OF TDRSS CHARACTERISTICS FROM TDRSS DOCUMENTATION AND COORDINATION

DATA CHANNEL CAPACITY

MA: I & Q channels - Sum of bit rates - 50 kbps

SSA & KSA, Group 1: I & Q channels - Sum of bit rates - 300 kbps

SSA Group 2: I & Q channels - Sum of bit rates - 6 Mps

KSA Group 2: I & Q channels - Sum of bit rates - 300 Mbps

Groups 1 and 2 can be combined with some loss of EIRP for both. Use of this option would allow continuous two-way ranging data for Group 2 users that do not require the pseudo-random code for frequency spreading.

RANGE MEASUREMENTS

RMS Error:

MA:	<1 kbps 20 nsec	Based on signal to noise ratio
	>1 kbps 10 nsec	
SA:	5 nsec	

Systematic Error: Ground Terminal ± 20 nsec

Granularity: <1 nsec

Ambiguity: 67 msec, minimum

Measurement Timing, R&RR:

Absolute Accuracy; Within ± 5 usec of NRL time standards

Data Sampling Accuracy; Within ± 25 nsec of local standard

Sample Rates; .1, 1, 5, 10, 60 and 300 sec/sample

Duty Factor:

One-way RR - Any 10 channels

Two-way R&RR, MA - 1 channel/TDRS (Forward link is shared)

Two-way R&RR, SA - 6 or 9 channels (Effectively all users)

Note: Scheduling exercises have assumed 2 minutes of R&RR per pass though if code is available through the pass measarements can be continued.

Staleness: Available within 2 sec of acquisition

Bilateration: Transponders will be available at White Sands and two other locations

TIME CODE REFERENCE & TIME TAGGING

Time Code Data: 46-bit binary microsecond code

Time Reference Accuracy: Accuracy ± 5 usec to NRL time standard

Tagging Accuracy: Dependent on bit rates

DATA DELAY MEASUREMENT

The Data delay through the ground to station, from the antenna to the government interface shall be measured to an accuracy of ± 1 usec. The measurement shall be prior to and following each support period.

DATA INTERFACE

Bit synchronized decoded data. Each data channel shall consist of bit synchronized Viterbi decoded data, where applicable, at the spacecraft data rate.

will be used for time tagging data. The time tag resolution will be ± 1 μsec. The total data delay through the ground station will be measured to an accuracy of ± 1 μsec. The ground station time standard will be referenced to NRL standards with an accuracy of ± 5 μsec. Figure 3.7 is a diagram of the TDRSS ground station with the most pertinent delay parameters shown.

As for the TDRS delay variation, standard deviations will be derived for those errors not given in terms of a standard deviation. The ground terminal systematic error of ± 20 nsec. will be assumed to be uniformly distributed so that σ_{GS} = 11.5 nsec. Treating the ground station data delay measurement of ± 1 μsec similarly gives σ_{GD} of 577 nsec. The time code resolution of 1 μsec will result in an average error of 500 nsec. with an even distribution over ± 500 nsec. Thus, the σ_{TC} about the mean error will be σ_{TC} = 289 nsec.

Bit Synchronizer Clock Timing Accuracy

The clock signal generated in the data bit synchronizer will be used for clocking data in subsequent operations and for time tagging. Variations in the clock timing will directly affect the data timing accuracy.

The bit synchronizer phase lock loop (PLL) phase jitter is given by

$\sigma_\phi^2 = \frac{B_L}{S/N_0}$ radians where S/N_0 is the signal to noise density ration and B_L is the loop noise bandwidth. This result is based on the inherent assumption of additive white Gaussian noise. For narrow bandwidths, however, other noise effects may be present or even mask the Gaussian noise. Some of these noise processes are discussed in Section 6 and include flicker of phase and frequency effects. The impact of these various noise processes upon bit synchronizer clock timing accuracy is a subject requiring further detailed analysis. Our efforts will be based on the assumption of additive white Gaussian noise.

Link calculations are given in the TDRSS User's Guide from which the signal to noise density can be obtained. This can be used to determine the signal to noise density ratio at the bit synchronizer,

$$\frac{S}{N} = R + \frac{E_b}{N_0} + M \text{ (in dB)}$$

$$= R + 7.7 \text{ (dB)}$$

where $\frac{E_b}{N_0}$ is the required energy per bit to noise density ratio (4.7 dB) and M is the system margin (3 dB). The bit synchronizer PLL will synchronize on data transitions. With NRZ data the transitions depend on the information content and several bits may occur without a transition. It will be assumed that as a worst case, there will be one transition in at least 10 bits so that the transition energy will be reduced 10 dB. The effective S/N_0 will now be:

$$(S/N_0)_{eff} = R - 2.3 \text{ (dB)}$$

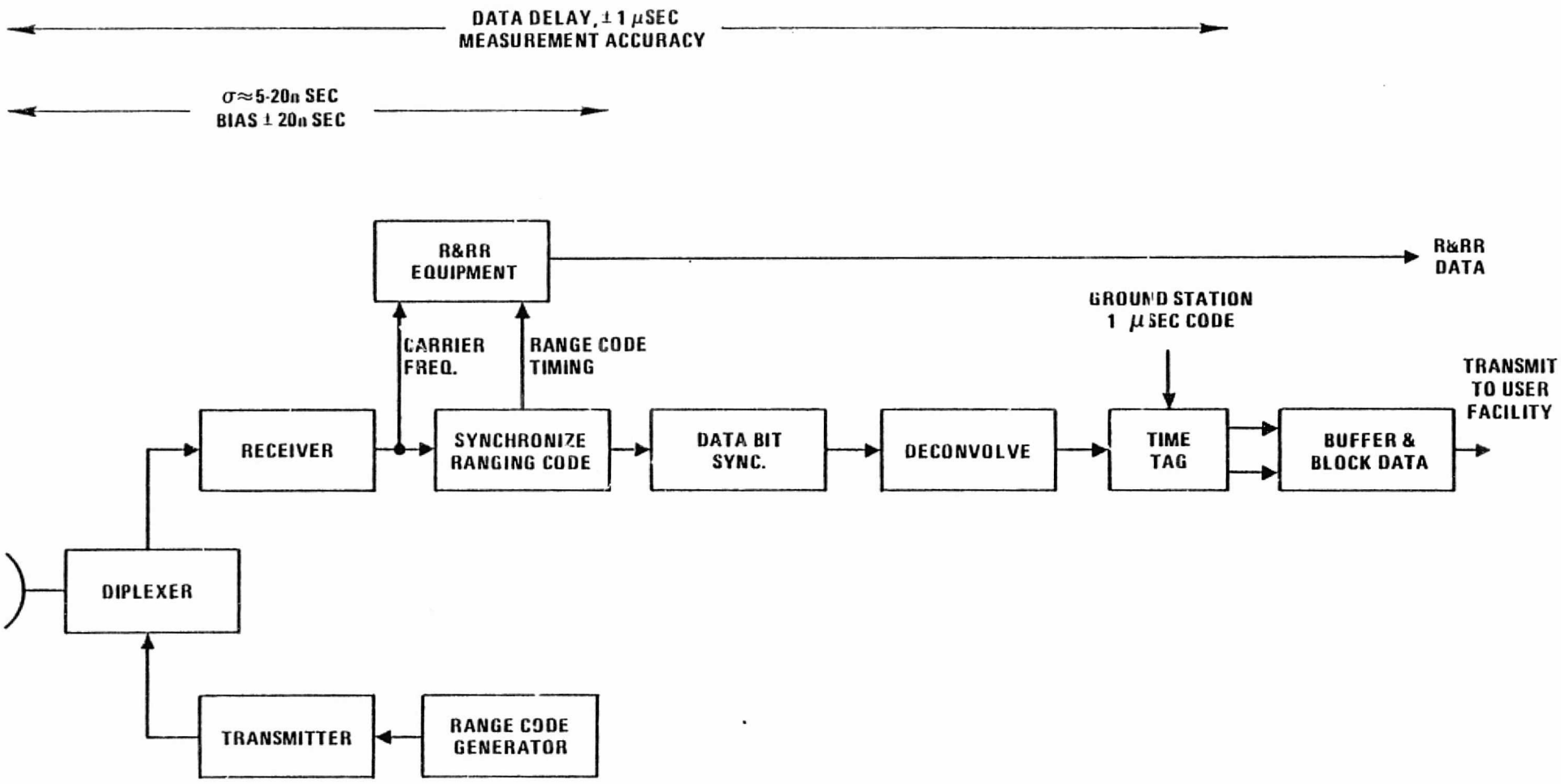

FIGURE 3.7. SIMPLIFIED BLOCK DIAGRAM OF GROUND STATION EQUIPMENT

Combining these results in the equation for PLL phase jitter:

$$\sigma_\phi^2 = B_L - (S/N_o)_{eff}$$

$$= B_L - R + 2.3 \text{ (dB)}$$

A typical loop bandwidth will conservatively be on the order of $B_L = R \times 10^{-4}$ yielding a rms phase error of $\sigma_\phi = 0.013$ radians. Thus, the bit timing error as a part of a bit period will be $\sigma_B = \frac{.013}{2\pi} = .00207$ bits. At the highest MA rate of 50kbps this becomes 41 nsec and at a bit rate of 5kbps would be 410 nsec.

Calculations of σ_ϕ^2 for SSA and KSA are within 1 dB of those for the MA mode so that the above results can be used with reasonable accuracy for all modes. Since the SSA and KSA modes use bit rates in excess of 50 kbps the timing error will be less than 41 nsec.

IV. OPERATIONAL CONSIDERATIONS

INTRODUCTION

Timing accuracy will depend on the periods available for user satellite time correlation and acquisition of ranging data. The availability of such periods will depend on mutual visibility of user satellites with TDRSS and TDRSS scheduling of communications with user satellites. The type of operations will also have a bearing. Two-way operations allows accurate time delay measurement and correlation of the user satellite oscillator timing. In one-way operation, one-way Doppler measurements may be used to calculate variations in time delay. In this case timing accuracy will depend on user clock stability, or position data may be used which will depend on the accuracy of tracking data and orbit computations. During periods of no contact with the TDRS, required data will be recorded and timing accuracy will be completely dependent on the user satellite oscillator stability in addition to equipment limitations.

MUTUAL VISIBILITY PERIODS

Periods of mutual visibility will depend on satellite altitude and orbital inclination. Orbital altitudes were determined by ORI in a TDRSS mission model (Reference 4) and the number of satellites versus orbital altitude and period are shown in Figure 4.1b. It is seen that the majority of satellites have an orbital altitude of less than 1000km. All those shown are within the pointing range of the TDRS's. Also, all were assumed to have circular orbits except for two where the perigee and apogee are 256 and 3466km respectively.

The user visibility of TDRSS, given in the User's Guide (Reference 1), is as follows:

a. Minimum of 85% at 200km altitude

b. 100% at 1,200 to 2,000km MA and to 12,000km SA

c. Decreasing towards zero at synchronous altitudes.

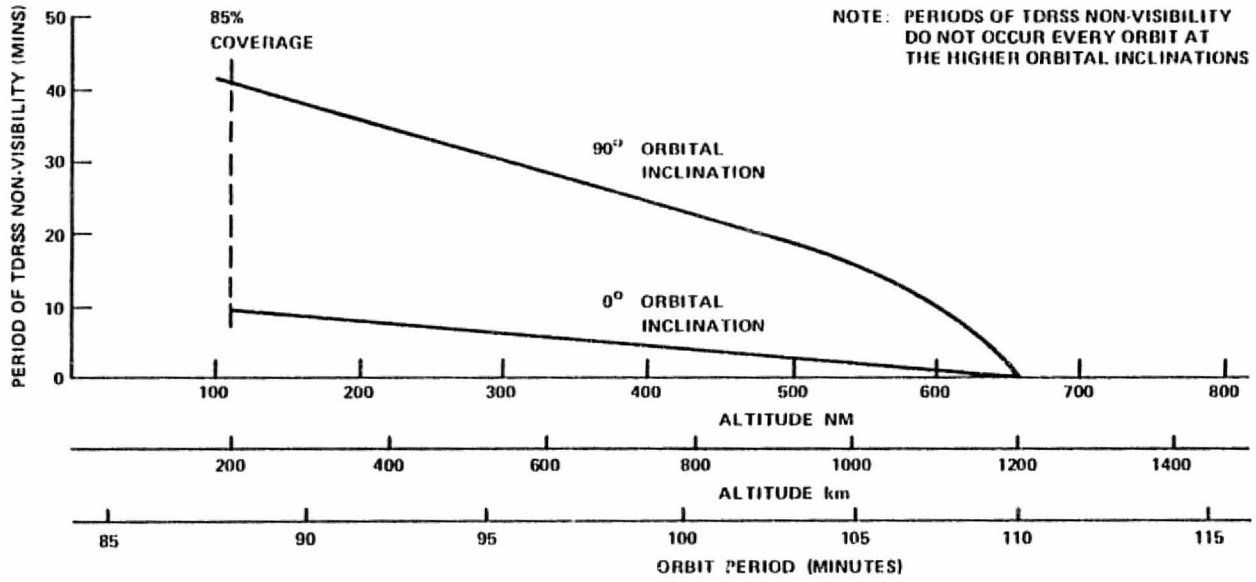

FIGURE 4.1-a PERIODS OF USER/TDRSS NON-VISIBILITY

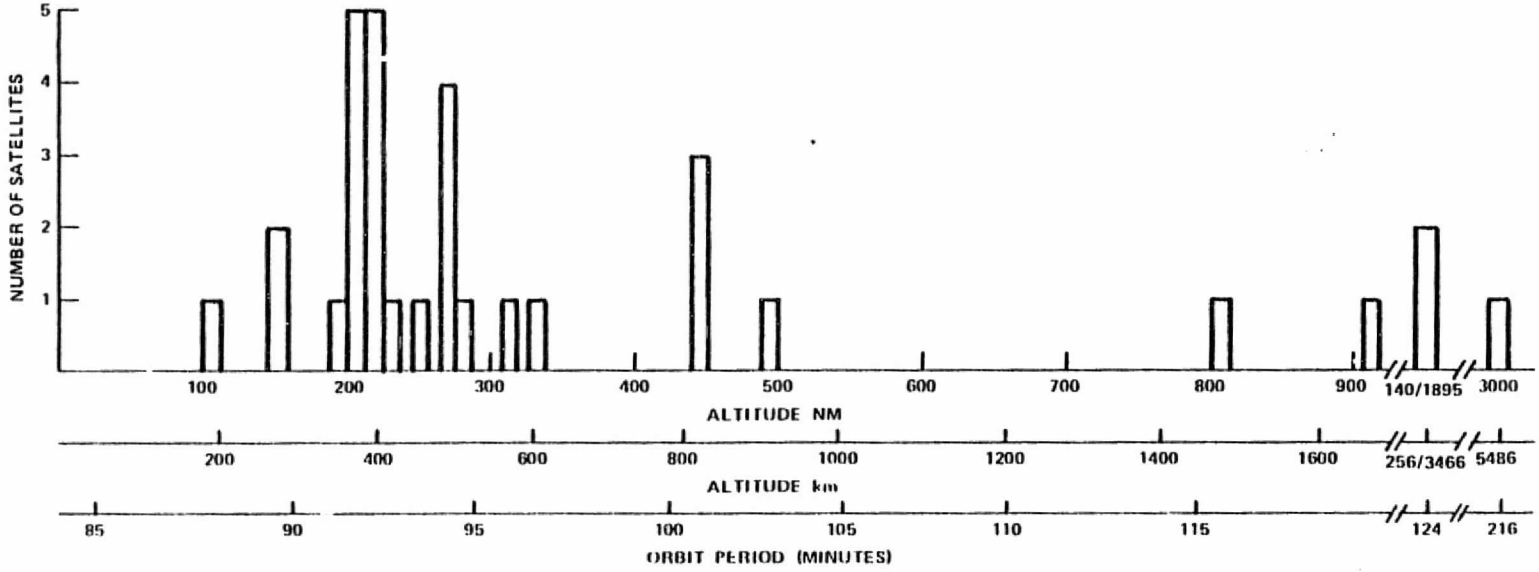

FIGURE 4.1-b NUMBER OF SATELLITES VS. ORBITAL ALTITUDE AND ORBIT PERIOD

Periods of non-visibility are of interest for estimation of timing accuracy since no contact will be possible with the user satellite during these periods. The information in items a and b above and visibility diagrams in the TDRSS User's Guide were used to generate curves of periods of User/TDRSS non-visibility shown in Figure 4.1a.

Periods of non-visibility vary with orbital inclination. For a satellite in a 200km circular orbit and zero degrees orbital inclination, a period of non-visibility occurs each orbit and is 15% of the orbital period. If the orbital inclination is 90^0, then a period of non-visibility will occur during certain orbits and will be as much as 40% of the orbital period. The periods of non-visibility decrease to zero as the orbital altitude varies from 200 to 1,200km.

In comparing Figures 4.1a and b, it is seen that there will be periods of User/TDRSS non-visibility for the majority of user satellites. The orbital inclinations of the satellites vary so the frequency and period of non-visibility will vary from user satellite to user satellite.

AVAILABILITY OF RANGING DATA

Ranging data may be used in two ways. The data may be used to determine the data delay directly for correlation of the user satellite oscillator or the orbital position may be computed through an orbital program and the propagation delays calculated from the position data. A Wolf report (Reference 5) discusses an orbit determination system and indicates that most accurate position information can be obtained with ranging data samples taken every 2 hours. It will be assumed that ranging data will be available at this frequency for all satellites. It is also assumed here that determining the data delay directly will give the best timing accuracy provided ranging data is available frequently. The accuracy of position data is greatly affected by the particular orbit parameters so that it may only be usable where the orbit parameters are most advantageous or insufficient data is available for direct computation of data delay.

MA users will have a return link available continuously during periods of visibility with the TDRSS. The forward link will be shared between users and will be available for transmission of command data and two-way ranging measurements with the return link for a part of each pass. Thus MA users will have two-way range and range rate data available for short periods and one-way range rate data using the user oscillator reference for nearly the balance of time.

In the case of SA users, scheduling of all SA satellites may limit contact periods to 10 or 15 minutes each pass. For the low rate SA users two-way range and range rate data will be available for the contact period, less a short initial period for acquisition. High data rate users that do not have simulataneous low data rate capability will only have two-way range and range rate data available during the period of a contact where the low data rate is used, possibly during acquisition and a period for readout of satellite housekeeping data. The high data rate information will be non-coherent with the forward link and will only provide one-way Doppler data.

Thus, routine scheduling of TDRSS operations will only provide the most useful range measurements, two-way, on an intermittent basis, about once for a TDRS pass for all users. In special cases more data may be taken. For instance, if schedule allows, a number of forward link contacts may be made with a particular MA user through a TDRS pass. Also, continuous two-way operations may be performed with particular SA users when in view of TDRSS. Such operations will only be possible with a small number of SA users and for limited periods. The TDRSS load will vary from year-to-year so that a satellite that has special requirements should schedule its operation in years of low TDRSS loading.

V. PROPAGATION ANALYSIS

GENERAL

Three distinct types of propagation anomalies must be considered in this analysis. These effects include:

- Ionospheric Fluctuations
- Tropospheric Fluctuations
- Multipath.

Figure 5.1 depicts some typical TDRS/user satellite geometrical configurations. In Figure 5.1 user satellites #1 and #3 are at high altitudes, but at different inclination angles. At near ninety degrees inclination the path traversed by user #1 will pass through the ionosphere and troposhere as will the multipath signal. For highly inclined orbits (user #3), only the multipath signal on the user to TDRS link is subject to ionospheric and tropospheric fluctuations. For a low altitude satellite (user #2) both the direct and reflected signals are subject to tropospheric and ionospheric effects. For all of these users the downlink (TDRS to ground) is corrupted by the tropospheric and ionospheric anomalies.

Multipath effects will be considered negligible for the MA users since they employ a PN spectrum spreading technique. If the multipath delay is greater than one chip duration (fractions of 1 μsec), then the multipath signal is discriminated against and is merely treated as additive noise. For nearly all of our geometrical configurations, the multipath delay is much greater than 1 μsec which indicates that multipath effects can be ignored for the MA users.

In the next two paragraphs ionospheric and tropospheric effects are considered. Average path delays and fluctuations are developed for the frequencies of interest.

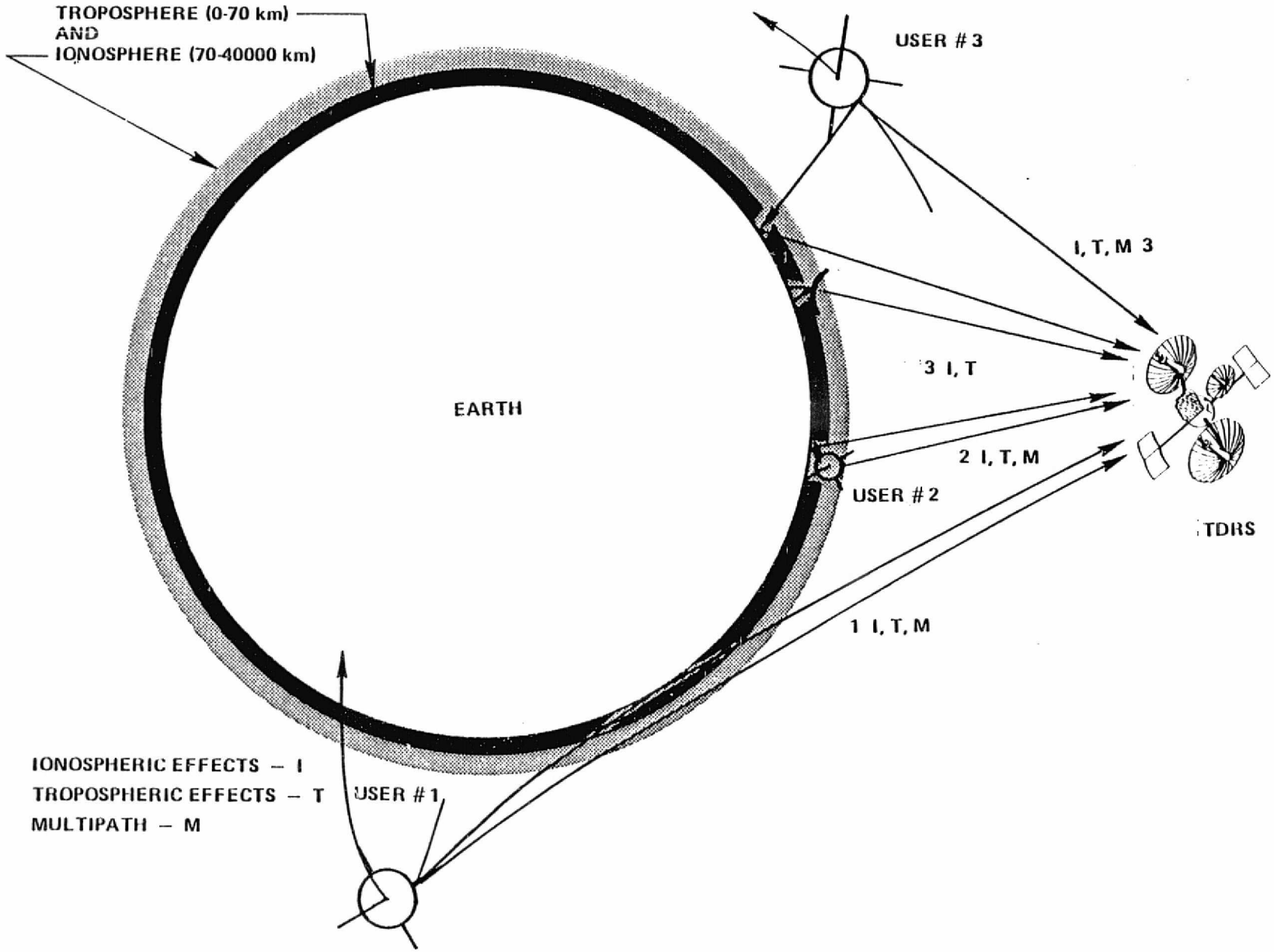

FIGURE 5.1. TYPICAL TDRS/USER GEOMETRICAL CONFIGURATIONS

IONOSPHERIC EFFECTS

The effects of the ionosphere are considered separately for Ku-band and S-band signals.

Ku-Band Ionospheric Effects

Additional Path Delay Time, $\delta\tau$. To date, no direct measurements of the total time delay through the ionosphere have been made at Ku-band. In fact, the best measurements to a synchronous satellite to date have been the ATS-6 radio beacon experiment results (References 6,7). These investigators use the Appleton-Hartree equation to evaluate the expected delay due to electrons in the atmosphere. The resulting formula is:

$$\delta\tau = \frac{40.3}{cf^2} \; N_T \text{ seconds}$$

where $c = 3 \times 10^8$ m/sec., f = frequency in Hz and $N_T = \int_o^s N_e \, ds$ is the number of electrons per square meter along the incremental signal path ds between the observer (o) and the satellite (s).

Typical values for N_T range from 3×10^{16} electrons/m^2 at local sunrise to 30×10^{16} electrons/m^2 at local sunset. The resulting values of $\delta\tau$ are

$$\delta\tau \approx 0.2 \text{ nanosecond (sunset)}$$

$$\delta\tau \approx 0.02 \text{ nanosecond (sunrise)}$$

All of these measurements are made during a low sunspot period (1974-1975), and so some increase during solar maximum periods (1979-1980) may be expected. However, increasing N_T by a factor of 10 during high sunspot periods only results in a $\delta\tau$ of the order of 2 nanoseconds.

There is also a slant path contribution. For an earth-satellite path at elevation angle θ_o, an upper bound for the ionospheric path delay is given by $\delta\tau_v \csc\theta_o$, where $\delta\tau_v$ is the delay for a vertical path. This $\csc\theta_o$ expression is only accurate for $\theta_o \geq 10^o$, but it does indicate that the above estimates for ionospheric delay, $\delta\tau$, might be increased by a factor of approximately ten for elevation angles as low as 5^o. Similar increases in $\delta\tau$ could occur for satellite - satellite signals that travel significant distances through the ionosphere.

Fluctuations in Path Delay Time, $\sigma_{\delta\tau}$. Two types of path delay variations have been observed. These are:

- Rapid fluctuations (1 Hz to 150 Hz)
- Slow fluctuations (0.01 to 1 Hz)

The rapid fluctuations have been observed in the amplitude of 20 GHz ATS-6 signals (Reference 8) and undoubtedly correspond to changes in $\delta\tau$. However, no quantitative $\sigma_{\delta\tau}$ data appears to exist in the range from 1 to 150 Hz.

Slow fluctuations have been observed on the 162 and 324 MHz GEOS-1 satellite (Reference 9). These correspond to $\Delta N_T \approx 0.1 \times 10^{16}$ electrons/m^2.

The corresponding $\Delta\tau = 6 \times 10^{-4}$ nanoseconds. Using a stratified turbulence model (Reference 10) and typical estimated numbers for the turbulence parameters, a standard deviation, $\sigma_{\delta\tau}$, was calculated of 6×10^{-9} nanoseconds.

S-Band Ionospheric Effects

Additional Path Delay Time, $\delta\tau$. Many users of the TDRS will be operating via the 2.2 to 2.3 GHz user-to-TDRS data link and the 2.025 to 2.12 GHz TDRS-to-user link (Reference 1). Unlike the TDRS Ku-band signals, these S-band signals can experience significant delays through the ionosphere. This is particularly true for those paths which transit thousands of kilometers of ionosphere. Using a very simplified model, calculated delays of 40 to 50 nanoseconds (one-way) may be experienced. At Ku-band, signals transiting the same path will experience only 0.8 to 1 nanosecond delays because the delay time decreases as f^{-2}, ie.,

$$\text{Ku-band delay} = (0.022)\text{x}(\text{S-band delay}).$$

The total electron content of the ionosphere has been modeled by NASA (Reference 11) and others (Reference 12). The accuracy of these models is dependent on many parameters such as latitude and longitude of ground station, time of day, season of year, solar flux number, etc. These parameters and others are being updated on a regular basis in the GSFC ionosphere model and are in use in ongoing experiments for spacecraft operations. However, the present programs do not include the geometric effects required to calculate time delays between two satellites (Reference 13), such as TDRS to a user satellite. The modification of the current program to do this would not be expected to require a large expenditure of time and would yield total time delay results within 80% of the correct value over the continental U.S.

Lacking the availability of an accurate satellite-to-satellite ray path ionospheric model, an approximate calculation has been done in order to size the effect of the TDRS-to-user time delay due to the ionosphere. For this calculation the 2.2 GHz TDRS frequency was assumed along with the worst-case geometry shown in Figure 5.2. However, certain orbits which have user-TDRS longitudinal displacements of 80° to 90° may closely approximate the geometry in Figure 5.2.

The distribution of the electrons in the ionosphere was modeled by a uniform distribution which approximates the actual distribution as shown in Figure 5.3. The values selected for the maximum density of electrons N_m, the height h_m where N_m occurs, and the thickness t_o of the uniform distribution were

$$N_m = 5 \times 10^{11} \text{ electrons/m}^3$$

$$h_m = 300 \text{ km}$$

$$t_o = 200 \text{ km}$$

$$= (\text{total electron content to synchronous orbit})/N_m$$

which are typical of those observed. Using this simple uniform distribution, the ionospheric path length ℓ may be calculated for the worst case. The resulting length is $\ell = 3300$ km as shown in Figure 5.4. Using the assumed profile model for the ionosphere, the resulting one-way delay through the ionosphere is 46 nanoseconds at 2.2 GHz and about 1 nanosecond at 15 GHz with

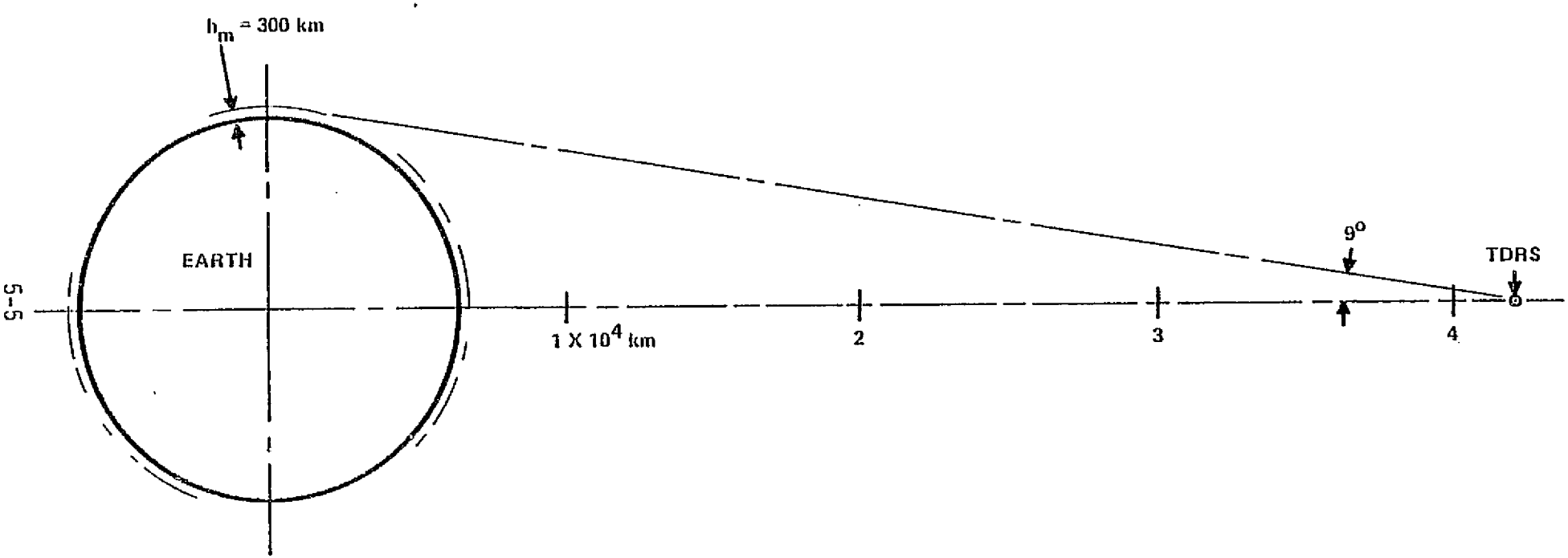

ASSUME $N_m = 5 \times 10^{11}$ e/m^3

h_m = 300 km

$t_o = TEC/N_m = 10^{17}/5 \times 10^{11} = 2 \times 10^5$m = 200 km

FIGURE 5.2. SATELLITE TO SATELLITE GEOMETRY FOR IONOSPHERIC MODEL

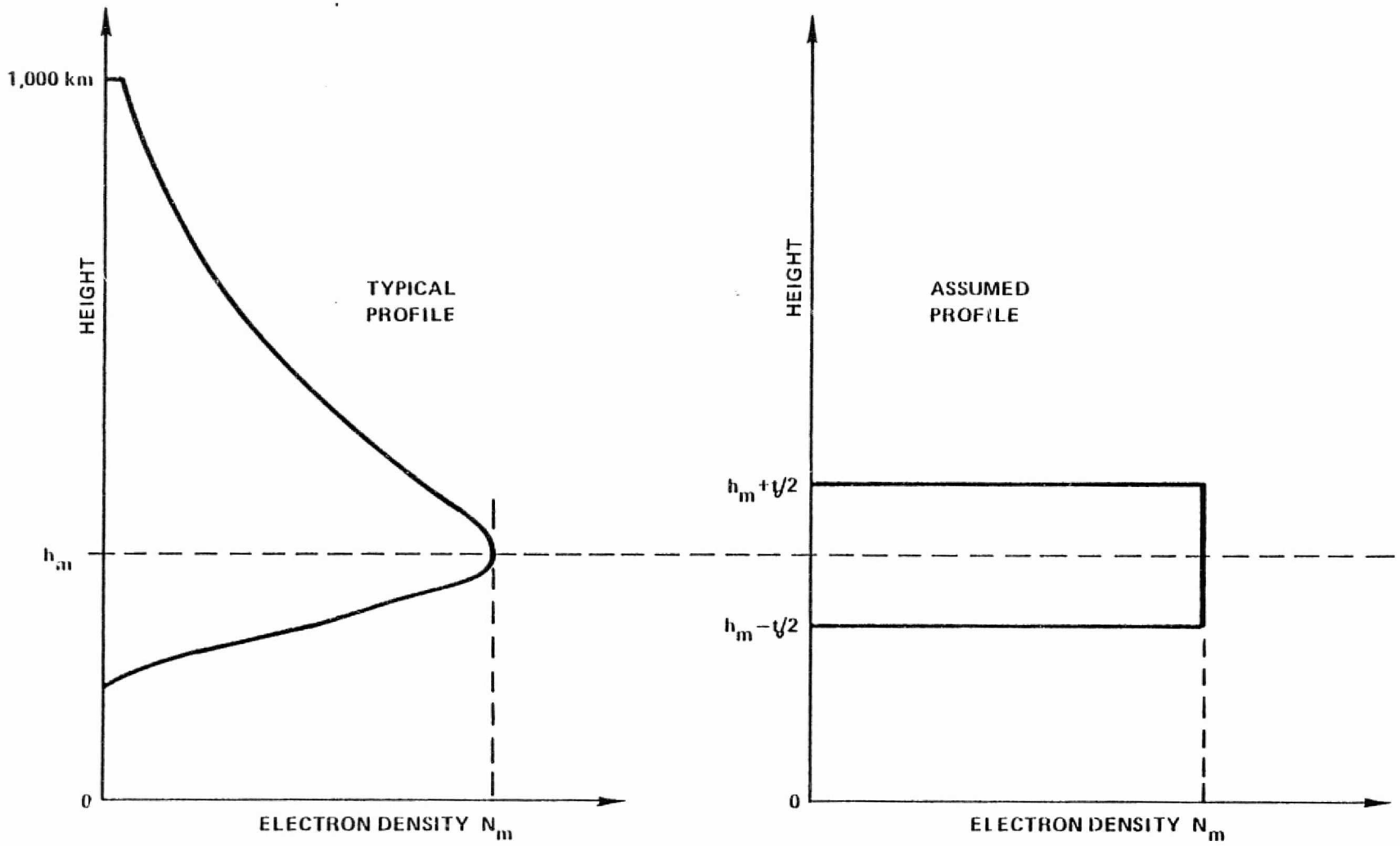

KEY: h_m = HEIGHT OF MAXIMUM ELECTRON DENSITY

t = THICKNESS OF UNIFORM MODEL

FIGURE 5.3. VERTICAL PROFILE OF FREE ELECTRONS IN IONOSPHERE

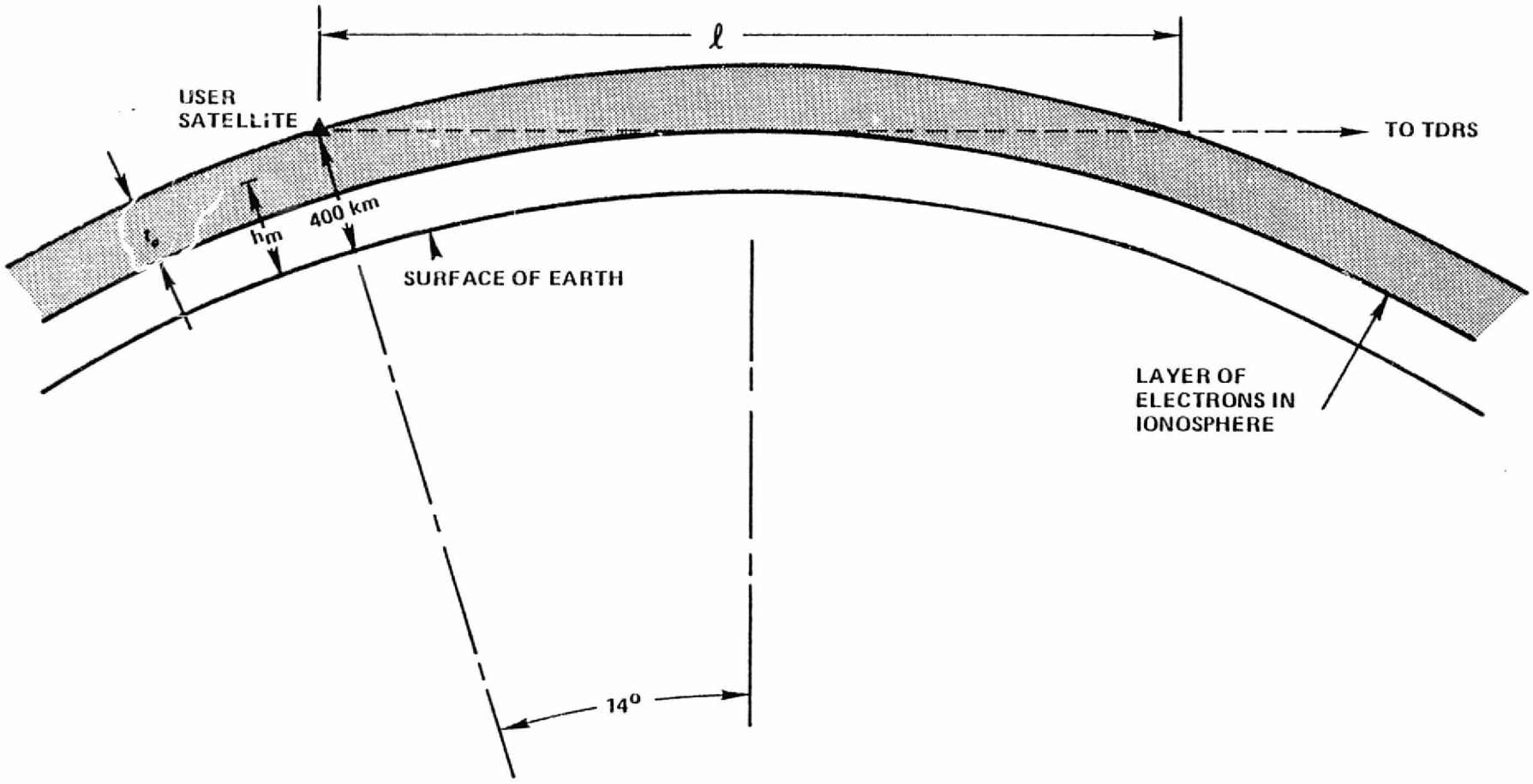

NOTE: FOR ASSUMED PROFILE

h_m = 300 km

t_o = 200 km

FIGURE 5.4. WORST-CASE IONOSPHERIC PATH FROM USER SATELLITE TO TDRS

approximately ±20% error (Reference 12). These results were arrived at using the relation

$$\delta\tau = \frac{(40.3)\ (N_e)}{cf^2}$$

where N_e is the total electron content per square meter along the ray path ($N_e = N_m \ell$), $c = 3 \times 10^8$ m/sec, and f is the frequency in Hz.

These ionospheric delays may be considerable during those periods when the satellite-TDRS path is scanning the limb of the earth. Therefore, the calculation of the S-band time delay from the user satellite to TDRS may vary from the 46 nanoseconds to less than 0.1 nanosecond when the user satellite is on the line passing from the center of the earth to TDRS.

Fluctuations in Path Delay Time, $\sigma_{\delta\tau}$. Fluctuations of the ionospheric delay time can be considered to extend from periods of 0.01 second (the highest measured to date, Reference 14) to 11 years (sunspot cycle period). However, for the purposes of this study, fluctuations occurring over time periods comparable to the period required to make a timing measurement will be considered. That is, time periods less than 1 second are considered most critical. However, fluctuations in the total electron content within the radio beam with periods greater than 1 second are also important, but can be included in the ionospheric model (Reference 11) or can be measured and removed as a source of error.

(a) Slow Fluctuations

The slow fluctuations (fluctuations with periods greater than 1 second) have been recorded by numerous investigators. For example, Davies, et al (Reference 15) have observed the ATS-6 Radio Beacon Experiment signals from July 1974 to April 1975. They recorded the maximum and minimum total electron content for each month during the July 1974 to April 1975 time period. The results in terms of the time delay and total electron content at 2.2 GHz from synchronous orbit are shown in Figure 5.5. Note the wide variations which occur during the period of a month. About 80% of these variations may be removed from the experimental data by ionospheric modeling (Reference 12). Thus, it appears that ionospheric modeling is necessary unless direct measurements of the delay can be made. Other variations in the time delay with periods greater than 1 second are:

(1) diurnal variations

(2) variations due to the ray path passing through the mid-latitude trough

(3) sun spot conditions.

These variations are part of the ionospheric models (Reference 12) which exist today and thus it is assumed that they will be subtracted out of the measured time delay data. However, the uniformly distributed error of ±20% remains and must be considered in any error analysis.

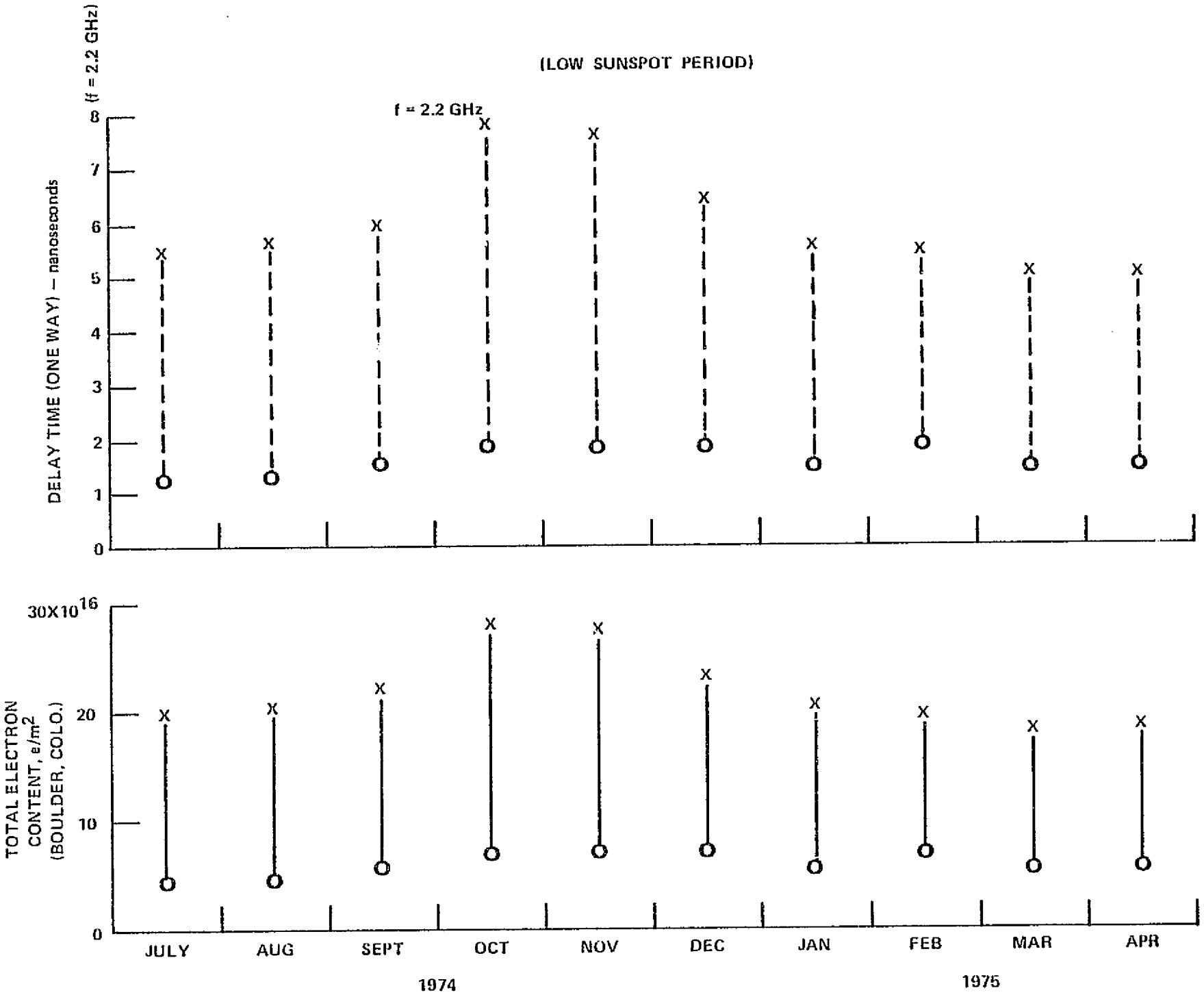

FIGURE 5.5. DELAY TIME AND TOTAL ELECTRON CONTENT VERSUS MONTH

(b) Rapid Fluctuations

Fluctuations in the ionospheric delay of less than one second are being measured by GE investigators (Reference 14) using low orbiting satellites. They have observed phase scintillations with periods of 0.01 second, which is the limit of the bandwidth of their phase-lock-loop receivers. Of course they also observe the slower fluctuations such as when the satellite passes through the mid-latitude trough. The results of these observations are not yet complete, but preliminary results indicate that the standard deviation for fluctuations with periods less than 1 second at 2.2 GHz is less than 1 nanosecond (Reference 14). This number is probably the most reasonable value to use since it is based on experimental data rather than a mathematical model which yields $\sigma_{\delta\tau} = 3.4 \times 10^{-4}$ nanoseconds. However, if in doing the timing measurement, it is necessary to rely on the ionospheric model for a calculation of the time delay $\delta\tau$, then depending on the orbit geometry, the model will probably introduce an error much larger than $\sigma_{\delta\tau} = 1$ nanosecond. Again, we observe that the errors to be expected are highly dependent on, among other things, the orbital geometry with respect to TDRS and the method of operating the system. A summary of the above comments is given in Table 5.1 below:

TABLE 5.1

TIME DELAY ERROR BUDGET AT 2.2 GHz THROUGH THE IONOSPHERE

Fluctuations:	typically $\sigma_{\delta\tau} = 1$ nanosecond, linearly dependent on ionospheric path length
Ionospheric Model Errors:	vary between ±1 and ±10 nanoseconds, ±20% of time delay, highly dependent on orbit/TDRS geometry.

TROPOSPHERIC EFFECTS

Ku-Band Tropospheric Effects

Additional Path Delay Time, $\delta\tau$. The major signal delay between a ground station and a satellite at Ku-band frequencies occurs in the troposphere. This arises due to the reduced velocity of a radio wave compared to the speed of light and the increase in path length brought about by refractive bending of the propagated ray (Reference 10). In general, the velocity factor is the main contribution to the delay except at low elevation angles. The magnitude of the delay time $\delta\tau$ is a function of elevation angle, path length, humidity of the air, and dielectric constant of the dry air.

The refractivity of the air (non-ionized) has been expressed by several formulas (References 16, 17), but the results are relatively independent of the formula. Typical of these are

$$N = \frac{77.6P}{T + 273.15} + \frac{3.73 \times 10^5 e}{(T + 273.15)^2}$$

where N is the refractivity [$N = (N_g - 1) \times 10^6$, where N_g is the group refractive index], P is the pressure in millibars, T is the temperature in ^oC, and e is the partial pressure of water vapor in millibars. This expression for N may sensibly be considered independent of frequency over the range 0.1 - 30 GHz, and is therefore applicable to the TDRSS. For optical wavelengths dispersion effects begin to enter into N and so a frequency dependent N is obtained (Reference 16).

The difference in delay time between the actual ray path and the direct path, $\delta\tau$, is a complicated calculation. However, the formulas have been worked out by Marini (References 18, 19) and approximations are available. Typical results for N = 313 (a ground station at sea level, 51^o elevation angle) were $\delta\tau$ = 9 nanosec. The maximum $\delta\tau$ through the above atmosphere is 16.4 nanosecond at 1.7 degrees elevation angle. Another formulation by Millman (Reference 10) gives a maximum $\delta\tau$ = 38 nanosec at zero degrees elevation angle and 100% relative humidity. Millman quotes 9 nanoseconds at 5^o elevation angle and 100% humidity.

Additional delays can be expected on satellite - ground station signal paths that pass through rain. The magnitude of the rain delay is determined by the nature of the rain (dropsize distribution, rainrate, etc.) and the path length through the rain. Typically, rain delays are an order of magnitude less than those due to the clear troposphere (Reference 20). Hence, rain delays can generally be ignored for TDRS - ground station links.

Fluctuations in Tropospheric Path Delay Time. Delay time fluctuations for signal paths through the troposphere are primarily caused by clear air turbulence, although variations can also be caused by rain and clouds along the path. For TDRSS frequencies, variations due to rain will generally be an order of magnitude less than those due to tropospheric turbulence (Reference 21), but for periods of a minute or so, the fluctuations have approximately the same magnitude (Reference 20). However, combined clear troposphere and rain variation for a one-minute period should not exceed a few tenths of a nanosecond.

Delay fluctuations due to clouds are more difficult to estimate, since apparently there is no data for this effect. However, an estimate can be made of the largest fluctuation that might occur. For instance, the radio refractive index of a cloud can be 40-45 N-units larger than the nearly clear air (Reference 22). If a cumulonimbus cloud of thickness 10 km moves in to fill the beam of a vertically-pointing antenna, the path delay for this signal path can therefore increase by 1.5 ns. If the cloud top is at 12 km, and the horizontal velocity of the cloud is 50 km/h, the beam of a 1^o beamwidth antenna will be filled in less than 1.5 s. For slant paths, the magnitude of the delay variation can be larger, but the time for the beam to be filled will be longer.

SUMMARY OF PROPAGATION EFFECTS

Table 5.2 presents a summary of the propagation effects to be encountered in obtaining precise user time. The additional path delay through the ionosphere will be less than 1 nanosecond at Ku-band and vary from 1 to 50 nanoseconds at S-band. The estimated standard deviation will be approximately 10 nanoseconds at S-band due to the model inaccuracy of ±20 percent. At Ku-band the variation in delay can be considered negligible in this analysis. The primary reason for these small values is the f^{-2} dependence in the frequency range above 100 MHz.

Tropospheric effects will be appreciable only for transmission paths which graze the earth's surface and hence have not been considered at S-band. For Ku-band signals between a ground station and TDRS, the additional path delay can vary up to 9 nanoseconds. Between the user satellite and TDRS, this delay can increase to 50 nanoseconds for low elevation angle user satellites. For Ku-band signals, the major contribution to the additional delay $\delta\tau$ of a signal occurs in the high refractivity of the troposphere. Since the refractivity decreases with pressure and humidity, a high dry ground station site* is desirable. Also, operation during a rain storm may be undesirable. The variation in delay is less than 1 nanosecond.

---

* The TDRSS ground station site will be at White Sands, New Mexico. This location is not in a rainy area but rather in a desert area.

TABLE 5.2

SUMMARY OF TDRSS RADIO WAVE PROPAGATION DELAYS IN THE TROPOSPHERE AND IONOSPHERE

User to TDRS - S-band (nominally 2.2 GHz)

Propagation Region	Time Delay	Fluctuations in Time Delay
Troposphere (0-70 km)	Only applicable for transmission paths which graze the earth's surface.	Not considered to date.
Ionosphere (70-40000 km)	1 to 50 nanoseconds (one-way), highly dependent on orbit-TDRS geometry. Can be calculated with computer models.	$\sigma_{\delta\tau}$ = 1 nanosecond for time periods less than 1 second. Model inaccuracy is ± 20% of delay time.

TDRS to User and Ground - Ku-band (nominally 15 GHz)

Propagation Region	Time Delay	Fluctuations in Time Delay
Troposphere	Typically 9 nanosecond (one-way) ground station to TDRS path (elevation angle = 40°). Up to 50 nanoseconds for low elevation angle user satellites.	Further study required, preliminary results give $\sigma_{\delta\tau}$ = 0.006 nsec for periods less than 1 second.
Ionosphere	Less than 1 nanosecond for all geometries.	$\sigma_{\delta\tau} = 10^{-6}$ nsec for time periods less than 1 second. $\delta\tau = 10^{-2}$ nsec due to transmission path moving through ionosphere over a period of minutes.

VI. OSCILLATOR STABILITY CONSIDERATIONS

GENERAL CLOCK DEFINITIONS

Before considering the timing error associated with a particular user satellite using the TDRSS, it is useful to briefly summarize some of the basic characteristics or definitions associated with clocks. First, a clock is defined as a frequency standard (oscillator) coupled with a counter-divider. In a clock there are two major sources of error; (1) accuracy and stability of the frequency source, and (2) the accuracy of the establishment of initial setting sometimes referred to as epoch.

Accuracy

Accuracy is usually referred to as the degree of conformity of a measured and/or calculated value to some specified figure (see Chapter 8 of Reference 24 for further detailed definition). For example, consider a user satellite that time tags data on-board the spacecraft. Time accuracy in this case is the degree of conformity of the satellite clock's time with respect to some well defined ground time source. The principal causes of inaccuracy result from both random and non-random fluctuations. To determine the accuracy of a frequency standard it is necessary to consider the precision of the measurement process and parameter reproducibility. Precision is defined as the performance capability of a measurement process with contributions from the measurement equipment and the standard being measured. Generally, precision is the best consistently attainable indicator for the measurement process. As an example the precision of a frequency standard measurement is limited by the instability of either the standard or the measurement equipment, whichever is greater. In any event, accuracy can never be better than precision. Reproducibility is the degree of agreement across a set of independent frequency standards of the same design. A typical measure of reproducibility could be the following: given an average value for each of a set of measurements on a device, the reproducibility is the standard deviation of this set of measurements about the mean value. Reproducibility is a relative measure in contrast to accuracy which is an absolute measure. If a manufacturer provides nearly perfect reproducibility of a device, then its frequency accuracy will be primarily a problem of measurement precision.

Stability

Stability of a frequency source is defined as the frequency and/or time domain behavior of a process. The measure of stability is the spectral density of fractional frequency fluctuations, $S_y(f)$. In the time domain the measure of frequency stability (Reference 23) is the Allan variance (or its square root),

$$\langle \sigma_y^2 (N,T,\tau) \rangle = \frac{N}{N-1} \int_0^\infty S_y(f) \, \mathrm{sinc}^2(f\tau) \left\{1 - \frac{\sin^2(\pi r f N \tau)}{N^2 \sin^2(\pi r f \tau)}\right\} df \quad (6\text{-}1)$$

where

$\langle x \rangle \equiv$ denotes the infinite time average of x

$N \equiv$ number of samples

$f \equiv$ frequency

$T \equiv$ time between successive samples

$\tau \equiv$ sampling or averaging interval

$r \equiv T/\tau$

$\mathrm{sinc}(x) \equiv (\sin \pi x)/(\pi x)$

Manufacturers usually specify a frequency stability for N=2 samples and under the condition $T=\tau$. This stability is defined as $\sigma_y^2(\tau) = \langle \sigma_y^2 (2,\tau,\tau) \rangle$ and is given by

$$\sigma_y^2 (\tau) = 2 \int_0^\infty S_y(f) \frac{\sin^4(\pi f \tau)}{(\pi f \tau)^2} \, df \quad (6\text{-}2)$$

Since $\sigma_y(\tau)$ is usually specified by the manufacturer, an easy method for computing $\langle \sigma_y^2(N,T,\tau) \rangle$ is available through the use of bias functions (Reference 24),

$$\langle \sigma_y^2 (N,T,\tau) \rangle = B_1 (N,r,\mu) \, B_2 (r,\mu) \, \sigma_y^2 (\tau) \quad (6\text{-}3)$$

where $B_1(N,r,\mu)$ and $B_2(r,\mu)$ are tabulated bias functions and the parameter μ is related to the particular noise process occurring within the device.

In general, a measurement will be made of received frequency and compared to some ideal perfect reference clock to obtain the difference. The normalized fractional frequency deviation, $y(t)$, is then given by

$$y(t) = \frac{f(t) - f_o}{f_o} = \frac{\delta f}{f_o} + Dt + n(t) \quad (6\text{-}4)$$

where δf is the frequency offset with respect to the ideal frequency, f_0, D is the drift rate of the oscillator in fractional parts per unit time, and n(t) is the noise process. Both the frequency offset and drift terms are deterministic functions of time, which can be estimated, while the remaining noise term represents a random process. The variation in the measurement error is then dependent only on the noise portion of y(t) and is given by either equations (6-1) or (6-3). The computation approach for this error is given in the next paragraph for several distinct noise processes.

Noise Models

A useful composite noise model has been developed in the literature (References 23, 25, 26). This model consists of a set of five separate and independent noise processes, $z_\alpha(t)$ for $\alpha = -2, -1, 0, 1, 2$ such that

$$y(t) = \sum_{\alpha=-2}^{2} z_\alpha(t) \tag{6-5}$$

where the spectral density of z_α is given by

$$S_{z_\alpha}(f) = \begin{cases} h_\alpha f^\alpha & ; 0 \leq f \leq f_h \\ 0 & ; f > f_h \end{cases} \tag{6-6}$$

for n in the range (-2, -1, 0, 1, 2) where h_α are constants. For this composite noise model, $S_y(f)$ becomes

$$S_y(f) = \sum_{\alpha=-2}^{2} h_\alpha f^\alpha \tag{6-7}$$

for $0 \leq f \leq f_h$ and $S_y(f)$ is assumed to be negligible beyond this range. Each z_α contributes to both $S_y(f)$ and $< \sigma_y^2 (N,T,\tau) >$ independently. In the above expressions f_h is that frequency where a sharp cut-off in noise power occurs (i.e., perfect bandpass filtering). In actual practice the above model fits almost all real frequency sources. Usually, only two or three of the h_α coefficients are significant and the others can be neglected. Since the z_α are independent noises, it is sufficient to compute their effects separately and recognize that the superposition can be accomplished by simple additions of their contributions to either $S_y(f)$ or $< \sigma_y^2 (N,T,\tau) >$. It has been shown (References 25, 27) that if $S_y(f)$ is of the form denoted by equation (6-7), then the average of the Allan variance is proportional to the averaging interval

τ, according to the following relation,

$$< \sigma_y^2 (N,T,\tau) > \propto \tau^{\mu} \quad ; 2\pi\tau f_h >> 1 \tag{6-8}$$

for N and $r = T/\tau$ held constant. The parameter μ is related to α by the following mapping

$$\mu = \begin{cases} -\alpha - 1 & ; -3 < \alpha < 1 \\ -2 & ; 1 \leq \alpha \end{cases} \tag{6-9}$$

Table 6.1 denotes the five distinct noise processes and the proportionality dependence of τ on $< \sigma_y^2 (N,T,\tau) >$. Both frequency, y, and phase, x, noise processes are shown.

TABLE 6.1
NOISE MODELS

α	$S_y(f)$	$S_x(f)$	μ	$<\sigma_y^2 (N,T,\tau)>$ Dependency on τ	Frequency Noise Process	Phase Noise Process
-2	$h_{-2}f^{-2}$	$h_{-2}f_0^2 f^{-4}$	1	τ	Random Walk Y	---
-1	$h_{-1}f^{-1}$	$h_{-1}f_0^2 f^{-3}$	0	1	Flicker Y	---
0	$h_0 f^0$	$h_0 f_0^2 f^{-2}$	-1	τ^{-1}	White Y	Random Walk X
1	$h_1 f^1$	$h_1 f_0^2 f^{-1}$	-2	τ^{-2}	---	Flicker X
2	$h_1 f^2$	$h_2 f_0^2$	-2	τ^{-2}	---	White X

In order to compute the time domain stability, it is important to know the noise processes involved for the oscillator or clock under consideration. An illustrative example of this effect is shown in Figure 6.1 where $\sigma_y(\tau)$ is obtained from the manufacturer's frequency specification on the two sample Allan variance. This particular figure would be representative of a crystal oscillator. Other frequency standards such as Cesium beam clocks,

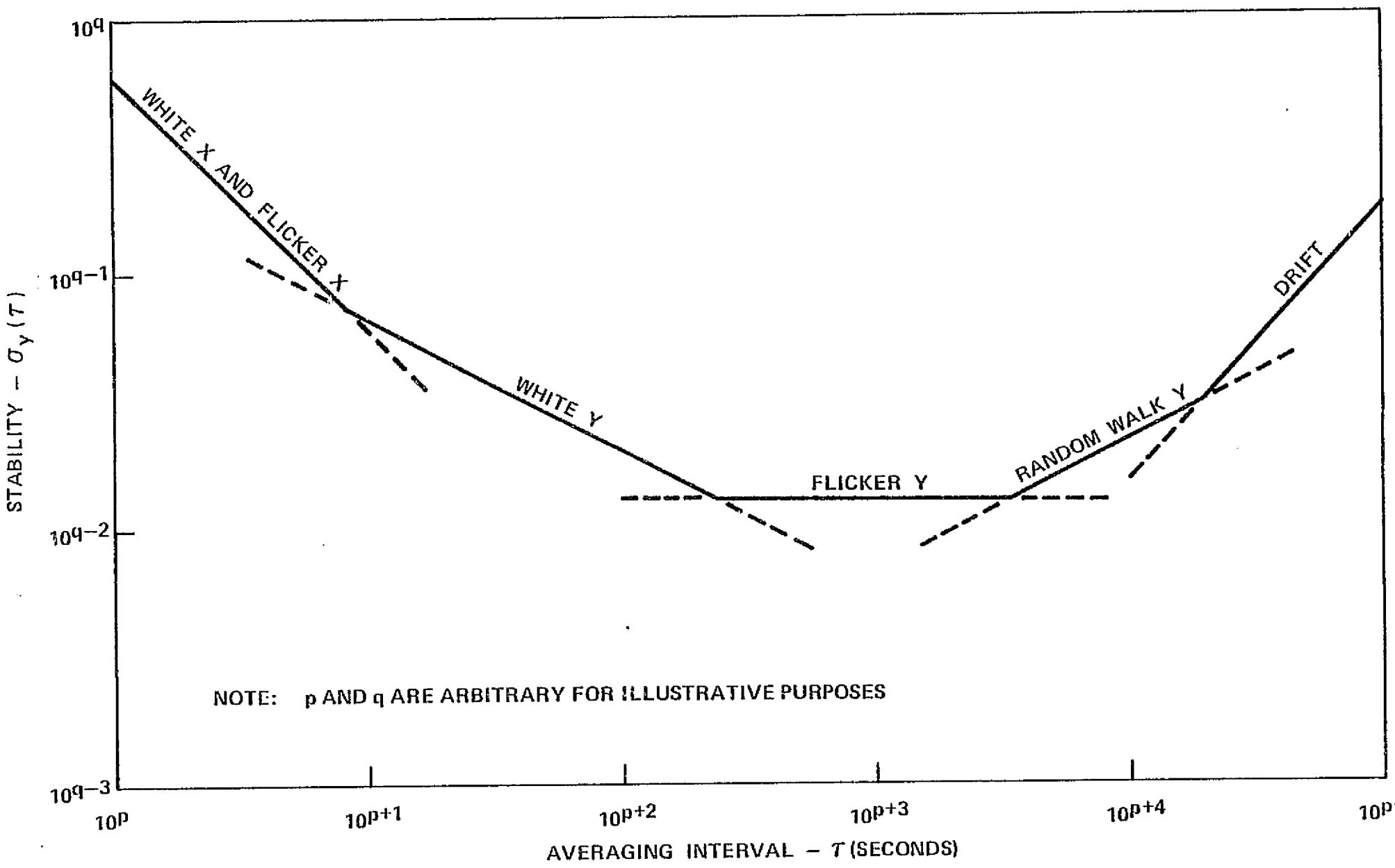

FIGURE 6.1. TYPICAL STABILITY CHARACTERISTIC FOR AN OSCILLATOR VERSUS AVERAGING INTERVAL

Rubidium standards or even hydrogen masers would not have all five noise processes present. Thus, it becomes necessary to consider each type of clock separately in so far as determining the appropriate noise models in the regions of interest. This type of analysis has been done and will be discussed in a subsequent paragraph.

TDRSS/USER CLOCK ERRORS

In the previous section general clock error theory was developed and the approach to computing the time domain stability, $< \sigma_y^2(N,T,\tau) >$, was outlined. The parameter y is defined by equation (6-4) as the normalized fractional frequency deviation of an oscillator. This oscillator (or clock) will provide a phase output, $\phi(t)$, during some time t. Relative to a given reference oscillator of frequency f_0, a phase error can be measured.

$$\phi_\varepsilon (t) = \phi (t) - 2\pi f_0 t \tag{6-9}$$

This phase error may be characterized as random and time varying. Over some interval of time, $t = \tau$ for example, the resulting clock timing error is given by

$$t_\varepsilon(\tau) = \frac{\phi_\varepsilon(\tau)}{2\pi f_0} = \frac{f(\tau) - f_0}{f_0} \cdot \tau = y(\tau) \cdot \tau \tag{6-10}$$

where the appropriate substitutions of (6-4) and (6-9) have been made. Based on this general procedure, the standard deviation of the clock timing error is, in general, given by

$$\sigma_c(\tau) = \tau \cdot \sigma_y(\tau) \tag{6-11}$$

Hence, the resulting clock timing error is proportional to the averaging interval upon which the measurement is made, and the standard deviation of fractional frequency fluctuations.

This theory must now be applied to a TDRSS/User system model to determine the impact of the clock placement and type as well as TDRS configuration upon the overall timing accuracy of the user data. All errors exclusive of clocks are not considered in this section, but must be added to form a composite error budget (see Section VII for details).

There are four basic timing problems that must be considered:

- Ground clock timing variations caused by propagation delay
- Ground/user clock timing variations
- Initialization of master clock - Ground/user calibration
- Measurement of the propagation delay (two-way or one-way)

The first type of clock error outlined above is that error caused by the finite two-way propagation delay of the ground clock. This error occurs only when the ground transmitted reference source is the same as that used to mix with the received signal (e.g., two-way Doppler tracking). Because of the finite time, τ_p, to propagate and receive a signal, this received replica of the original transmitted signal is at a slightly different frequency than our original reference source. When the two signals are mixed together, an error is introduced.

The second problem area is the variations in the ground and/or user clocks. First, it is desired to compute the timing error during an averaging interval τ when the time between successive samples is defined as T. This problem is referred to as the ground measurement timing error problem and applies to the TDRS operational tracking modes between ground, TDRS and user satellite. For this problem the clock is at the ground station only and the TDRS and user act as mere signal transponders in real time. Secondly, a problem of timing error exists when a clock is placed in a user satellite to obtain event time tagging. This clock will drift and not be continuously calibrated at all times. The ability of the user to accurately tag time with its clock will depend on the clock drift between calibrations. Hence, the problem is referred to as the ground/user clock timing error problem.

Our third problem is one of calibration of both the user and ground clocks. The remaining problem area will apply only to those designs requiring a measurement of the total propagation delay, τ_p. In some cases of interest (see Section VII for details), the propagation delay will determined separately using the PN ranging code. Since this is a ranging rather than a clock problem, this effect will not be considered in this section.

Ground Clock Timing Error Caused by Propagation Delay

This error is caused by the clock variations on the ground caused by the two-way propagation delay. TDRS will operate in several possible data relay modes. These operational modes have been outlined in Section IV. The determination of user event time can be accomplished through the TDRS range and range rate data. It is assumed that two-way range rate (Doppler tracking) with the user can be performed using the TDRSS.

For this operational mode, Reinhardt (Reference 28) has shown that the standard deviation of the N=2 sample range rate error is given by

$$\sigma_v(2,T,\tau) = \begin{cases} \frac{c}{\sqrt{2}}\,\sigma_y(2,T,\tau) & ; r \geq 1 \\ \frac{cr}{\sqrt{2}}\,\sigma_y(2,\tau,T) & ; r \leq 1 \end{cases} \qquad (6\text{-}12)$$

where $\tau_p = T$ and

$$\sigma_y^2(2,t_1,t_2) = \frac{1}{2t_2^2} < \left[\int_{t_0}^{t_0+t_2} y(t)dt - \int_{t_0+t_1}^{t_0+t_1+t_2} y(t)dt \right]^2 > \qquad (6\text{-}13)$$

Ranging error can be computed from the range rate error. The integral of range rate is range. Since the averaging process involves integration, not dividing the information stored in the counter by τ turns range rate data into range data (Reference 28). Thus, for random processes the ranging error is given by

$$\sigma_r(2,T,\tau) = \tau\, \sigma_v(2,T,\tau) \qquad (6\text{-}14)$$

Similarly, for this value of range error, the associated time error can be shown to be

$$\sigma_{t_\varepsilon} = \sigma_t(2,T,\tau) = \sigma_r(2,T,\tau)/c$$

$$= \begin{cases} \frac{\tau}{\sqrt{2}}\, \sigma_y(2,T,\tau) & ; r \geq 1 \\ \frac{\tau r}{\sqrt{2}}\, \sigma_y(2,\tau,T) & ; r \leq 1 \end{cases} \qquad (6\text{-}15)$$

Equation (6-15) represents the standard deviation of the timing error associated with a two-way Doppler tracking (range rate) system using two samples. The determination of the Allan variance in (6-15) must be done for each clock under consideration using the theory and noise models developed in the preceeding section. The resulting expressions for $\sigma_{t_\varepsilon} = \sigma_t(2,T,\tau)$, after having evaluated the Allan variance using equation (6-1) with the appropriate noise model, are shown in Table 6.2. The appropriate expressions must be used with the clock under consideration to evaluate the composite timing error. In order to determine the constants h_α the expression for $\sigma_y(\tau)$ must be fitted to the data given by the manufacturer on the clock. Since drift is not a random but rather a deterministic process, its' effect can be almost completely eliminated by proper calibration. The expression for drift timing error is shown in Table 6.2 only for completeness.

Ground/User Clock Timing Error

When a clock is placed on the ground or in the user spacecraft for time tagging of events, then this clock must be calibrated with a certain frequency in order to minimize the timing error that will occur between calibration intervals. This timing error will consist of both the deterministic and random processes previously discussed. Assume a calibration interval denoted by τ_c and some time interval, T_B, following the calibration. The time between the end of a calibration to the beginning of the next calibration is equal to T_B. Our

TABLE 6.2

GROUND CLOCK TIMING ERROR EXPRESSIONS FOR VARIOUS NOISE PROCESSES USING THE TWO-WAY RANGE RATE TDRSS MODE

Noise	$\sigma_y(\tau)$	$\sigma_{t_\varepsilon} = \sigma_t(2, T, \tau)$
White X	$(3h_2 f_h)^{\frac{1}{2}}/(2\pi\tau)$	$f_h^{\frac{1}{2}} / 2\pi$; $r \neq 1$ $(3f_h/2)^{\frac{1}{2}} / 2\pi$; $r = 1$
Flicker X	$\frac{h_1^{\frac{1}{2}}}{2\pi\tau} \left\{\frac{9}{2} - \ln 2 + 3 \ln (2\pi f_h \tau)\right\}^{\frac{1}{2}}$	$\frac{(h_1)^{\frac{1}{2}}}{2\pi} \left\{\frac{3}{2} + \ln (2\pi f_h T)\right\}^{\frac{1}{2}}$ $r \leq 1$ $\frac{(h_1)^{\frac{1}{2}}}{2\pi} \left\{\frac{3}{2} + \ln (2\pi f_h \tau)\right\}^{\frac{1}{2}}$ $r \geq 1$
White Y	$(h_0/2\tau)^{\frac{1}{2}}$	$(h_0 T)^{\frac{1}{2}}/2$; $r \leq 1$ $(h_0\tau)^{\frac{1}{2}}/2$; $r \geq 1$
Flicker Y	$(2 h_{-1} \ln 2)^{\frac{1}{2}}$	$\frac{h_{-1}^{\frac{1}{2}} T}{2} \left\{(1+\frac{1}{r})^2 \ln(1+\frac{1}{r}) + (1-\frac{1}{r})^2 \ln\left\lvert 1-\frac{1}{r}\right\rvert + \frac{2}{r^2} \ln r\right\}^{\frac{1}{2}}$; $r \leq 1$ $\frac{h_{-1}^{\frac{1}{2}} \tau}{2} \left\{(1+r)^2 \ln(1+r) + (r-1)^2 \ln\lvert r-1\rvert - 2r^2 \ln r\right\}^{\frac{1}{2}}$; $r \geq 1$
Random Walk Y	$\left(\frac{h_{-2}\tau}{6}\right)^{\frac{1}{2}} (2\pi)$	$\frac{\pi h_{-2}^{\frac{1}{2}} T^{3/2}}{\sqrt{6}} \left(\frac{3}{r} - 1\right)^{\frac{1}{2}}$; $r \leq 1$ $\frac{\pi h_{-2}^{\frac{1}{2}} \tau^{3/2}}{\sqrt{6}} (3r - 1)^{\frac{1}{2}}$; $r \geq 1$
Drift	$\frac{DT}{\sqrt{2}}$	$\frac{D\tau T}{\sqrt{2}}$

problem is to estimate the timing error during the interval T_B caused by clock instability. Reference 24 indicates that this error is given by

$$\sigma(\tau_C, T_B) = \frac{1}{\tau_C} \left[\tau_C(\tau_C + T_B)\, U(T_B) + T_B(\tau_C + T_B)\, U(\tau_C) - \tau_C\, T_B\, U(\tau_C + T_B)\right]^{\frac{1}{2}} \quad (6\text{-}16)$$

where $U(\beta)$ is the mean square value of the random time fluctuations, $x(t)$, of the clock given by

$$U(\beta) = < \left[x(t) - x(t + \beta)\right]^2 > \quad (6\text{-}17)$$

The function $U(\beta)$ has been calculated (Reference 24) and is shown in Table 6.3. Also shown in this table is the standard deviation of the time error during T_B caused by these random noise fluctuations. Only white, flicker and random walk in frequency noise processes are considered since these will be the primary causes of timing error. These expressions will be evaluated in subsequent paragraphs for various types of clocks and clock parameters.

User/TDRSS Clock Calibration Timing Error

Certain deterministic errors such as drift and frequency offset can be compensated for with appropriate clock calibration. If δf represents the frequency offset from the reference frequency, f_0, at some time t=0 and D is the drift or aging rate of the clock, then the total time error at some time t can be shown (Reference 29) to be given by

$$\varepsilon = \sigma_0 + \left(\frac{\delta f}{f_0} - 1\right) t + \frac{Dt^2}{2} \quad (6\text{-}18)$$

where σ_0 is the initial timing error. By properly setting the oscillator frequency because of the offset effect, the total timing error can be kept within σ_0 by recalibrating the clock according to (Reference 29)

$$T_C = 4\sqrt{\sigma_0/D} \quad (6\text{-}19)$$

where T_C is the time between oscillator recalibrations. Figure 6.2 shows the relationship between calibration error, σ_0, and time between calibrations for various drift rates reasonable for quartz oscillator and rubidium frequency standards.

TYPICAL OSCILLATOR STABILITY CHARACTERISTICS

Oscillators are generally grouped into two broad classes:

- Crystals
- Atomic standards
  - Cesium beam
  - Rubidium
  - Hydrogen maser.

TABLE 6.3

USER CLOCK TIMING ERROR EXPRESSIONS

Noise	$U(T_B)$	$\sigma(\tau_c, T_B)$
White Y	$h_o \; T_B/2$	$\left[\frac{h_o \; T_B}{2} \quad \left(\frac{T_B + \tau_c}{\tau_c}\right)\right]^{\frac{1}{2}}$
Flicker Y	$\lim_{\alpha \to -1} \frac{2h_{-1}\ln(2) \; T_B^{1-\alpha}}{2-2^{-\alpha}}$	$T_B \; h_{-1}^{\frac{1}{2}} \left[\frac{T_B}{\tau_c}\left(\frac{\tau_c}{T_B} + 1\right)^2 \ln\left(1 + \frac{\tau_c}{T_B}\right) - \left(1 + \frac{\tau_c}{T_B}\right)\ln\left(\tau_c/T_B\right)\right]^{\frac{1}{2}}$
Random Walk Y	$\frac{-h_{-2}T_B^{\,3}(2\pi)^2}{12}$	$\frac{2\pi \; T_B}{\sqrt{6}} \cdot \left[h_{-2}\left(T_B + \tau_c\right)\right]^{\frac{1}{2}}$

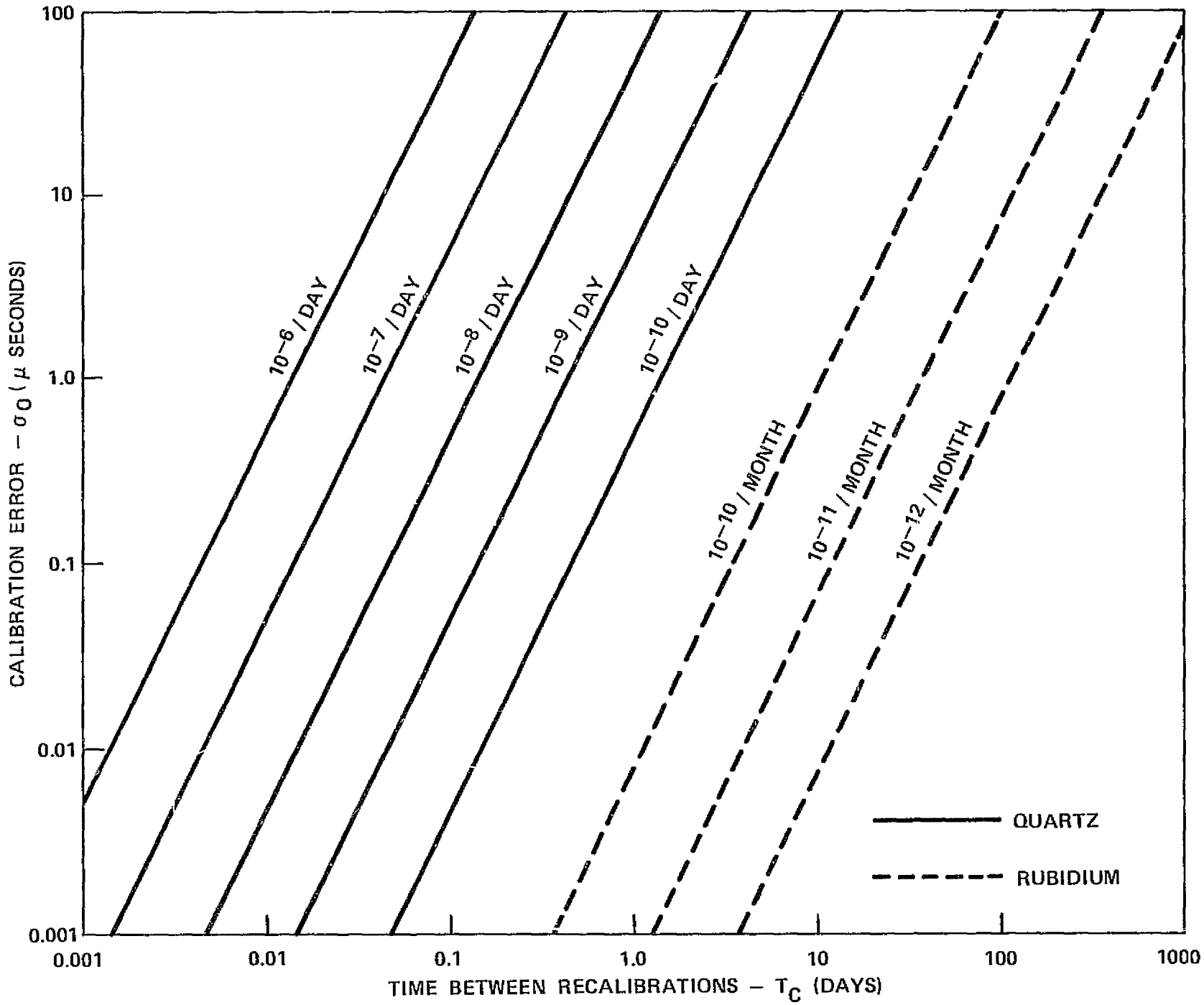

FIGURE 6.2. CALIBRATION ERROR VERSUS TIME BETWEEN CALIBRATIONS FOR CRYSTALS AND SUBIDIUM STANDARDS

Crystals oscillators are generally used in most electronic applications. They may be oven controlled to produce more precise stability characteristics. The need for even more accurate frequency sources brought about the atomic standard device. The three basic types of atomic standards include the Rubidium gas cell, hydrogen maser, and cesium beam clock.

A recent search through manufacturer's characteristics enabled us to select some representative standards. The respective two sample stability characteristic, $\sigma_y(\tau)$, is shown in Figure 6.3 for some crystal oscillators, rubidium and cesium standards.

The quartz crystals range from an inexpensive, lightweight (4 oz), low power (120 mw) device (FE 22-TV2D) to a costly, heavier (6½ pounds), and high power (8 watt) oscillator (FE 1800D). The first crystal with the poorest stability characteristic would be representative of what could be placed on a user spacecraft. Actually, better oscillators can be placed aboard satellites at the expense of cost through increased satellite weight and power requirements. Note that the crystal stability curves all tend to be flat (flicker Y noise) in the range of averaging intervals corresponding up to several seconds and then increase as τ is increased. The increase in stability is due to the random walk in oscillator frequency noise discussed earlier and aging (drift). For averaging intervals less than 1 second the crystal curves tend to increase again as the remaining noise processes take over. For purposes of selecting crystal oscillators to be used in subsequent analyses the following two devices have been chosen as representative:

- FE 22-TV2D ; $\sigma_y(1 \text{ sec}) = 2 \times 10^{-9}$
- HP 10544A ; $\sigma_y(1 \text{ sec}) = 10^{-11}$

Both of these oscillators weigh less than one pound. The Hewlett Packard (HP) standard does, however, require approximately an order of magnitude more power. With these constraints in mind, each oscillator is applicable to a user satellite. Of the two, the HP standard would be more expensive to place on a user satellite because of the increased power requirement.

The remaining two standards considered include the HP 5061A Cesium beam and HP 5065A Rubidium frequency standard. The manufacturer stability characteristics for these devices is also shown in Figure 6.3. Note that for these devices, it is primarily the Flicker Y and White Y noise effects that predominate. Improved stability characteristics have been obtained over the conventional quartz crystal at the expense of added weight (34 to 70 pounds) and power (~ 50 w). These units are more likely to be used on the ground than in a user satellite. Their inherent advantage is that they can obtain better stability over longer averaging intervals than the crystal oscillators. One final comment is worth mentioning concerning the rubidium device. Long term drift occurs in the HP rubidium standard with an aging rate equal to $D < 10^{-11}$ per month.

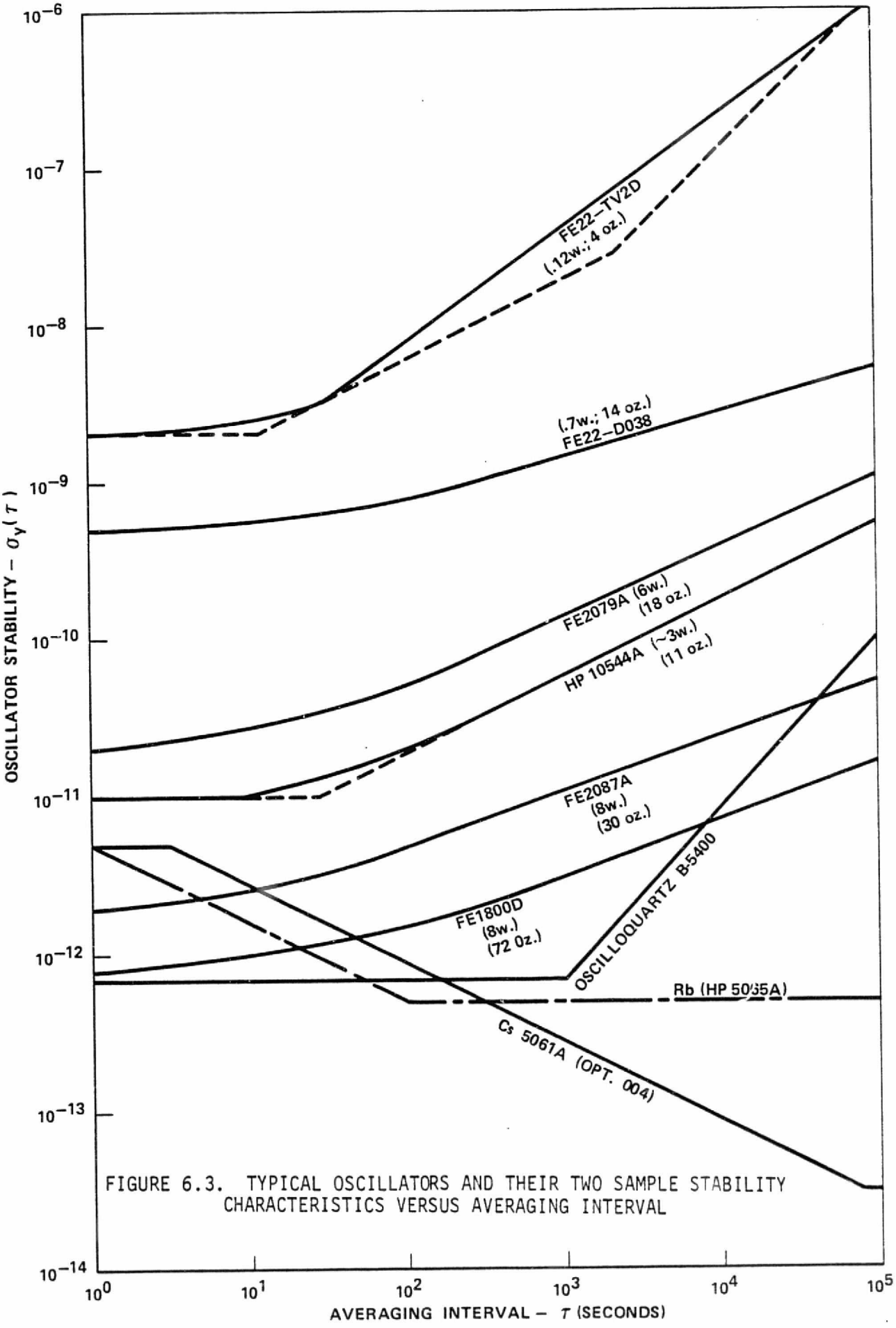

FIGURE 6.3. TYPICAL OSCILLATORS AND THEIR TWO SAMPLE STABILITY CHARACTERISTICS VERSUS AVERAGING INTERVAL

GENERAL CLOCK PERFORMANCE TRADEOFFS

In this paragraph various timing error tradeoffs are established for four basic oscillators whose stability characteristics are shown in Figure 6.3.

- Crystals (2)
  - FE 22-TV2D
  - HP 10544A
- Atomic Standards (2)
  - Rubidium: HP 5065A
  - Cesium: HP 5061A opt. 004

Other possible oscillators could be substituted for the above and their timing error characteristics can be computed using the same methodology. Also, since our four representative clocks represent extreme as well as mid-range stability characteristics, it is felt that our results could be used as gross estimates for similar (but not exactly the same) clocks.

Ground Clock Timing Error Caused by Propagation Delay

This timing error corresponds to the error resulting from a two way range rate measurement over an interval τ at the ground when the propagation time is equal to T. For this case Equation (6-15) has been evaluated for each of the five possible noise processes and the resulting expressions are given in Table 6.2. Evaluation of the constants, h_α, has been done for each of the above four oscillators. Following that, the timing error associated with the individual noise processes was determined.

Crystals. The individual noise component results are shown in Figures 6.4 and 6.5 for the two crystal oscillators. Note that for the averaging intervals of interest, only Flicker Y and Random Walk Y noise processes are present in addition to the deterministic drift effect. This is easily seen by referring to the appropriate portions of Figures 6.1 and 6.3. The composite timing error has been computed for both of these crystals as the root sum square (RSS) of the individual components. These composite timing error results are shown in Figures 6.6 and 6.7 respectively. Two cases are shown; (1) drift compensated by calibration, and (2) drift not compensated. In practice it is expected that the drift effect will be taken out by proper calibration (see Figure 6.2 for details). In terms of maintaining a timing error on the order of a μ second or greater, this can happen with the nominal crystal (FE 22-TV2D) primarily for either T large or τ large. For the higher quality crystal (HP 10544A), one μ second timing errors will occur only when both τ and T are large or small. Assuming 300 seconds as a maximum averaging interval (see Table 3.2) and a maximum time between samples equal to T=1 hr., the respective timing error associated with each crystal is:

$$\sigma_{t\varepsilon} = 9 \text{ microseconds (FE 22-TV2D)}$$

$$\sigma_{t\varepsilon} = 25 \text{ nanoseconds (HP 10544A)}$$

These above values represent reasonable worst case design. For most user orbits using the TDRSS, the value of T will be on the order of 1 second which will result in a timing error of nanoseconds or fractions of nanoseconds for the above two crystals.

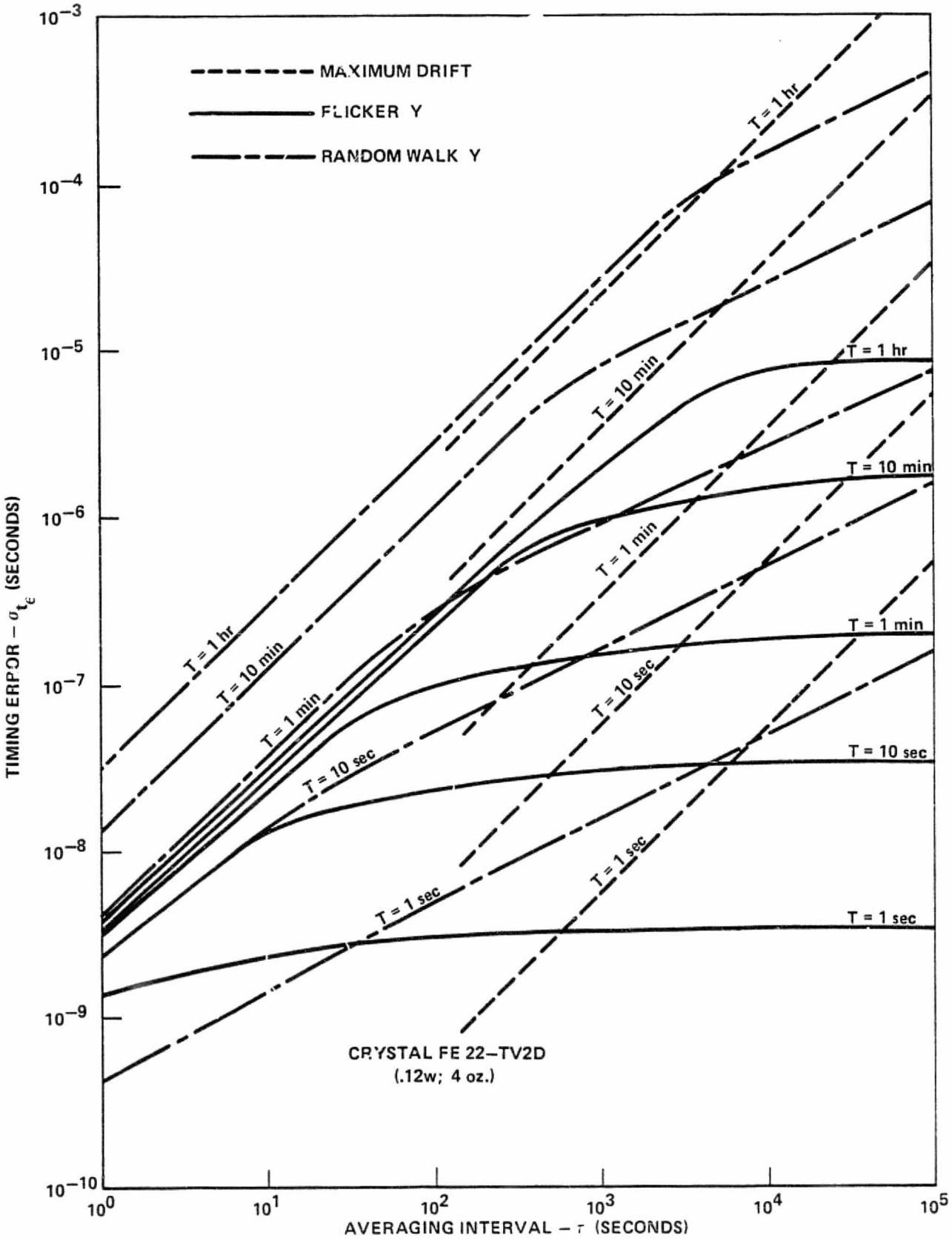

FIGURE 6.4. GROUND CLOCK TIMING ERRORS VERSUS AVERAGING INTERVAL FOR A NOMINAL CRYSTAL OSCILLATOR

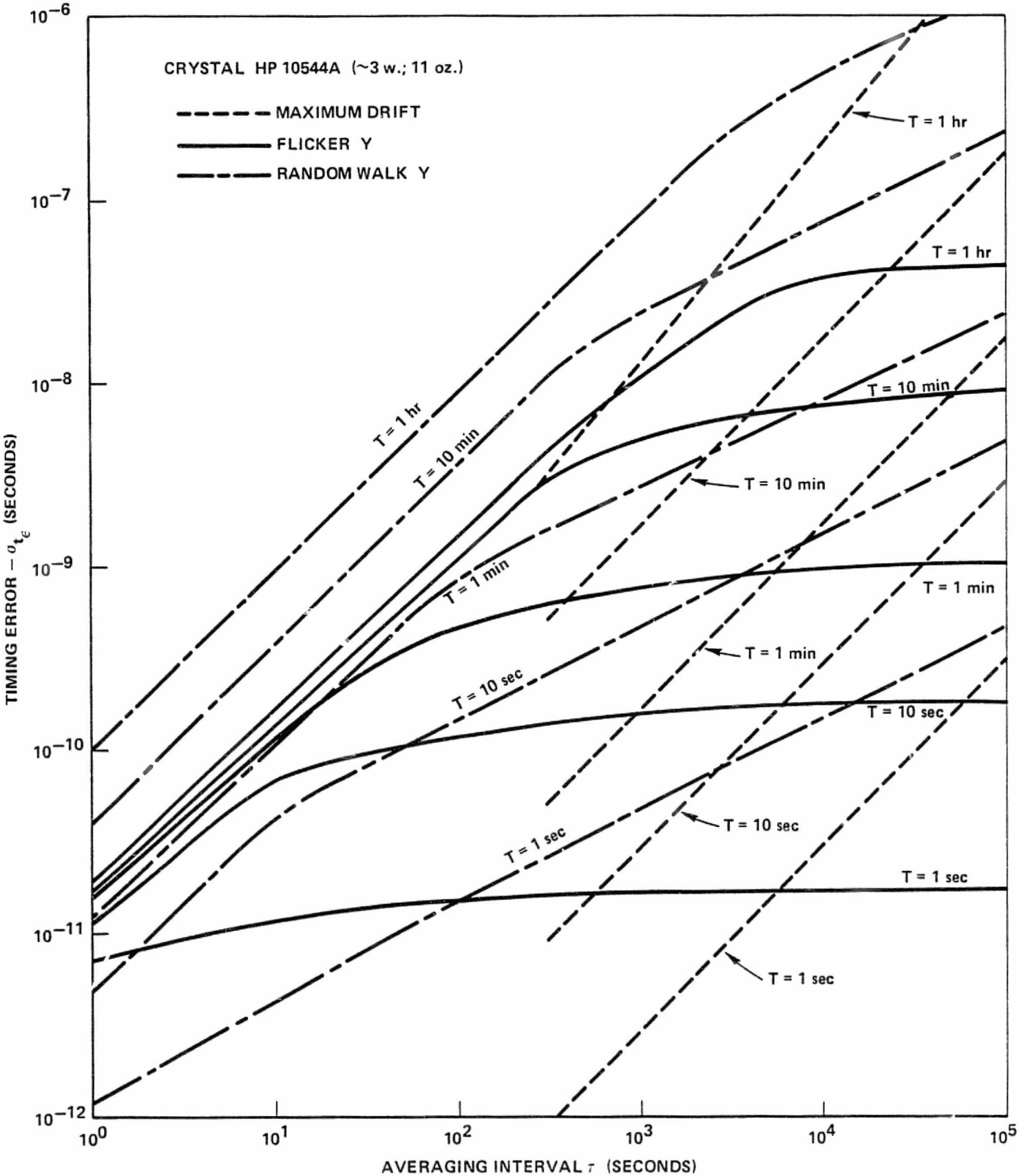

FIGURE 6.5. GROUND CLOCK TIMING ERRORS VERSUS AVERAGING INTERVAL FOR A HIGH QUALITY CRYSTAL OSCILLATOR

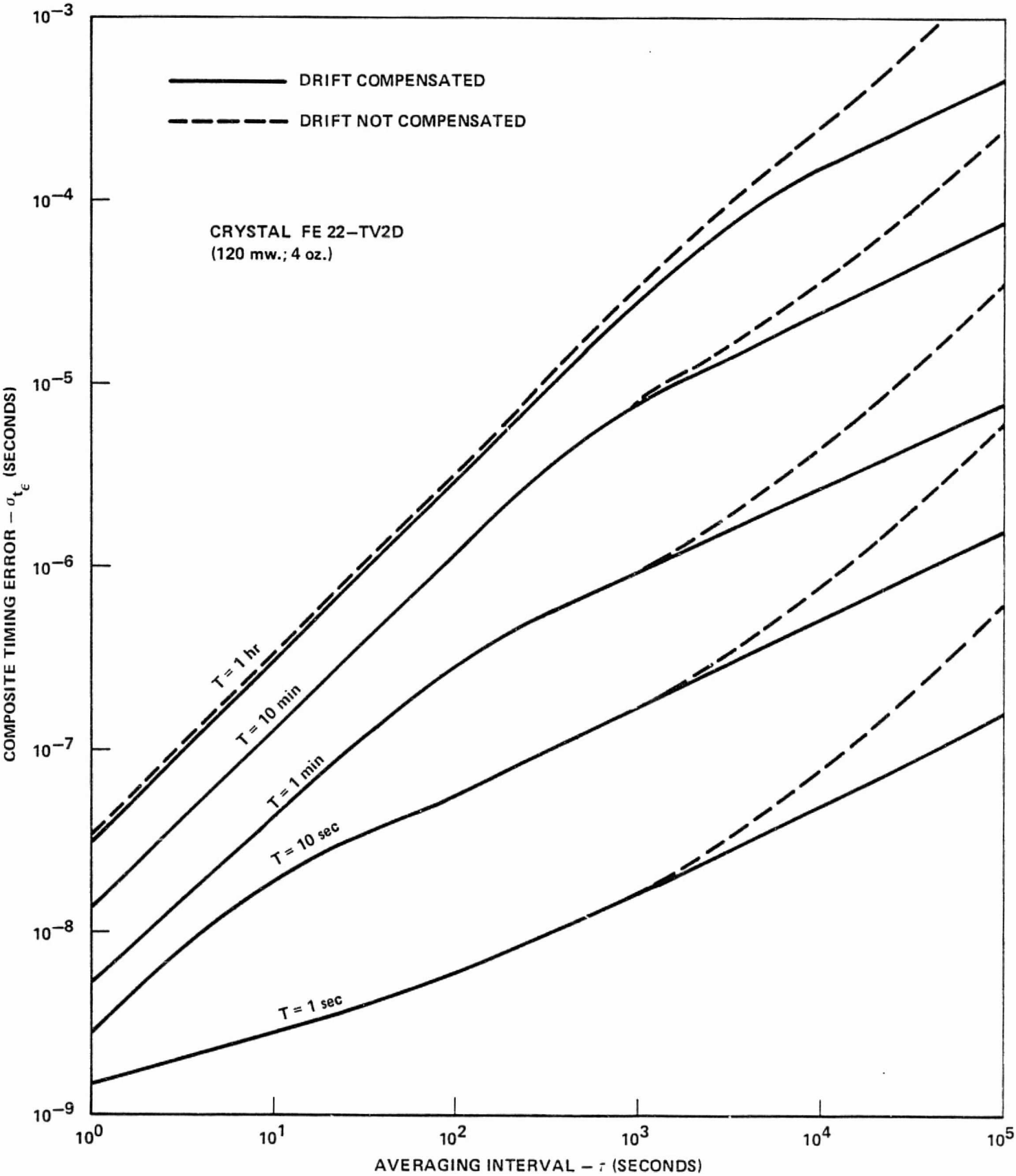

FIGURE 6.6. COMPOSITE GROUND CLOCK TIMING ERROR VERSUS AVERAGING INTERVAL FOR A NOMINAL CRYSTAL OSCILLATOR

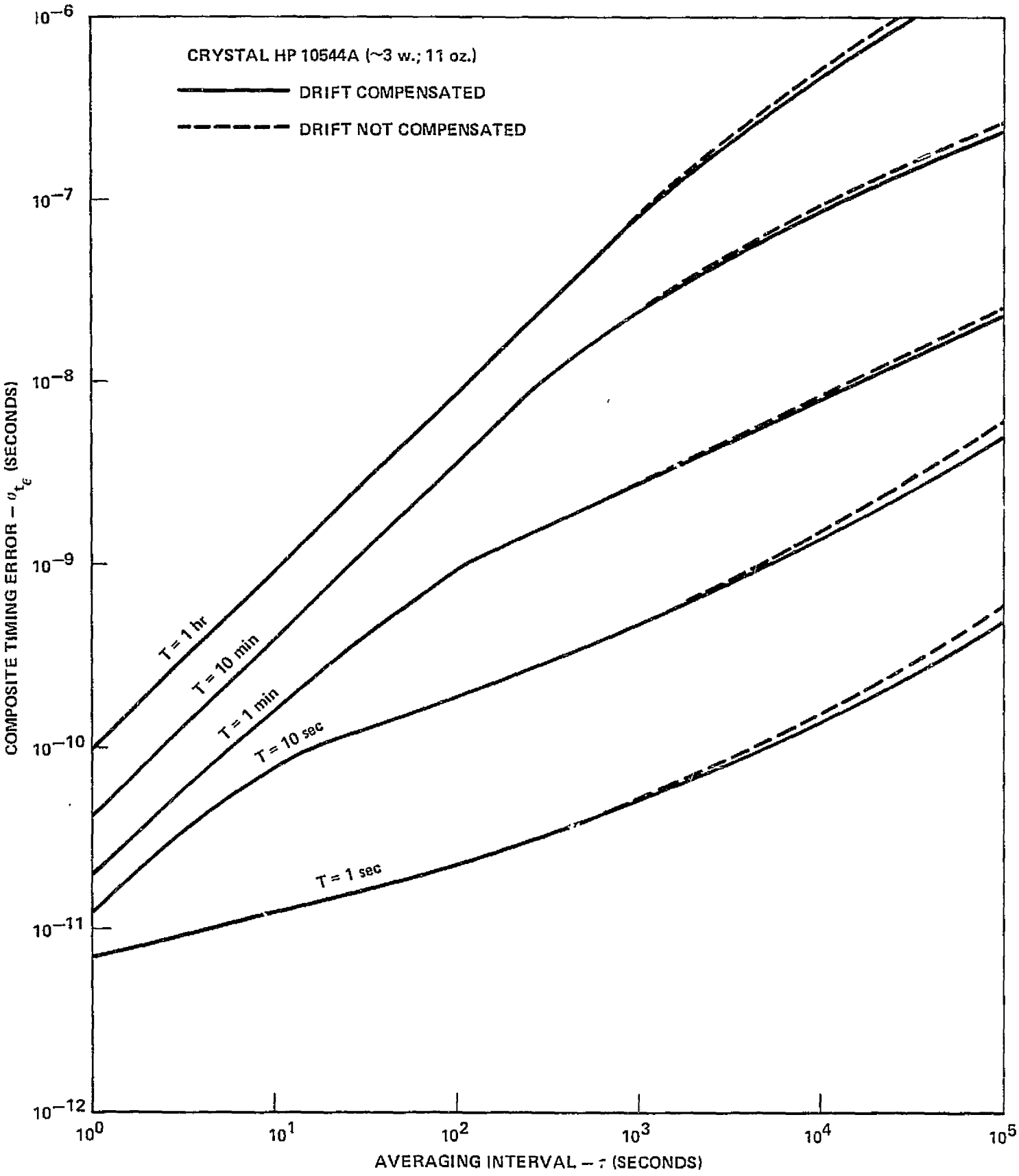

FIGURE 6.7. COMPOSITE GROUND CLOCK TIMING ERROR VERSUS AVERAGING INTERVAL FOR A HIGH QUALITY CRYSTAL OSCILLATOR

Atomic Standards. Using this same approach the composite timing error, σ_{t_ε}, has been evaluated for the rubidium and cesium beam frequency standards. These results are shown in Figures 6.8 and 6.9 respectively. Only Flicker Y and White Y noise effects are present for these devices for the averaging intervals of interest. Because the manufacturers' data on these devices indicates abrupt changes from white noise to flicker noise, the composite timing error is just the sum of each noise effect in its' particular region. In actual practice, it is expected that there would be some smoothing of these results around the value of τ where white noise changes to flicker noise. As is evident from these figures, the composite timing error will be approximately one nanosecond or less for all reasonable values of τ and T. These results show the resulting timing error that will be possible when cesium beam standards are placed in the TDRSS ground station. As before, assume T=1 hr and τ=300 seconds as a reasonable worst case implementation. Under this constraint the timing error associated with each atomic standard is equal to:

- σ_{t_ε} = 0.2 nanosecond (Rubidium HP 5065A)
- σ_{t_ε} = 0.1 nanosecond (Cesium HP 5061A opt. 004).

For more typical user orbits (T≈1 sec.) the timing error is in the order of picoseconds.

In summary, these atomic standards show an improvement over nominal crystals by reducing the timing error from 9μ seconds to tenths of nanoseconds. When compared to a high quality crystal the improvement is from tens of nanoseconds to tenths of nanoseconds. Other improvement factors could be calculated for different values of τ and T but the results would be similar.

Ground/User Clock Timing Error

As discussed in a preceeding section, the ground and/or user clock timing error under consideration corresponds to that error in an interval, T_B, following a calibration of duration, τ_C. This would relate to user satellites which are continuously time tagging events using an on-board clock and buffering the data when the satellite is not in communication with the TDRSS. If the user satellite were continuously in contact with the TDRSS, then a clock in the user satellite is not necessary for event time tagging since this process could then be done by the ground station clock in real-time.

For each of the four clocks under consideration, Equation (6-16) has been evaluated for each of the three principal noise processes (see Table 6.3) to yield the user clock timing error, $\sigma(\tau_C, T_B)$. The individual contributions to this timing error are shown in Figures 6.10 and 6.11 for crystals and in Figures 6.12 and 6.13 for atomic standards. The calibration interval, τ_C, has been allowed to vary from one second to one day. Within the TDRSS/User satellite format, it is expected that T_B will not be greater than two hours (which represents approximately an orbit of stored data from a low-medium altitude satellite). Practically speaking, it is anticipated that T_B will be on the order of minutes for most cases.

The composite timing error has been calculated as the root sum square of each of the contributing effects and is shown in Figures 6.14 and 6.15 for crystals and in Figures 6.16 and 6.17 for atomic standards. In this case the range of T_B has been allowed to vary from one second to one hour. As an example, consider a reasonable worst case design with a calibration time of 10 seconds and a value for T_B equal to 1 hour (e.g., approximately one-half

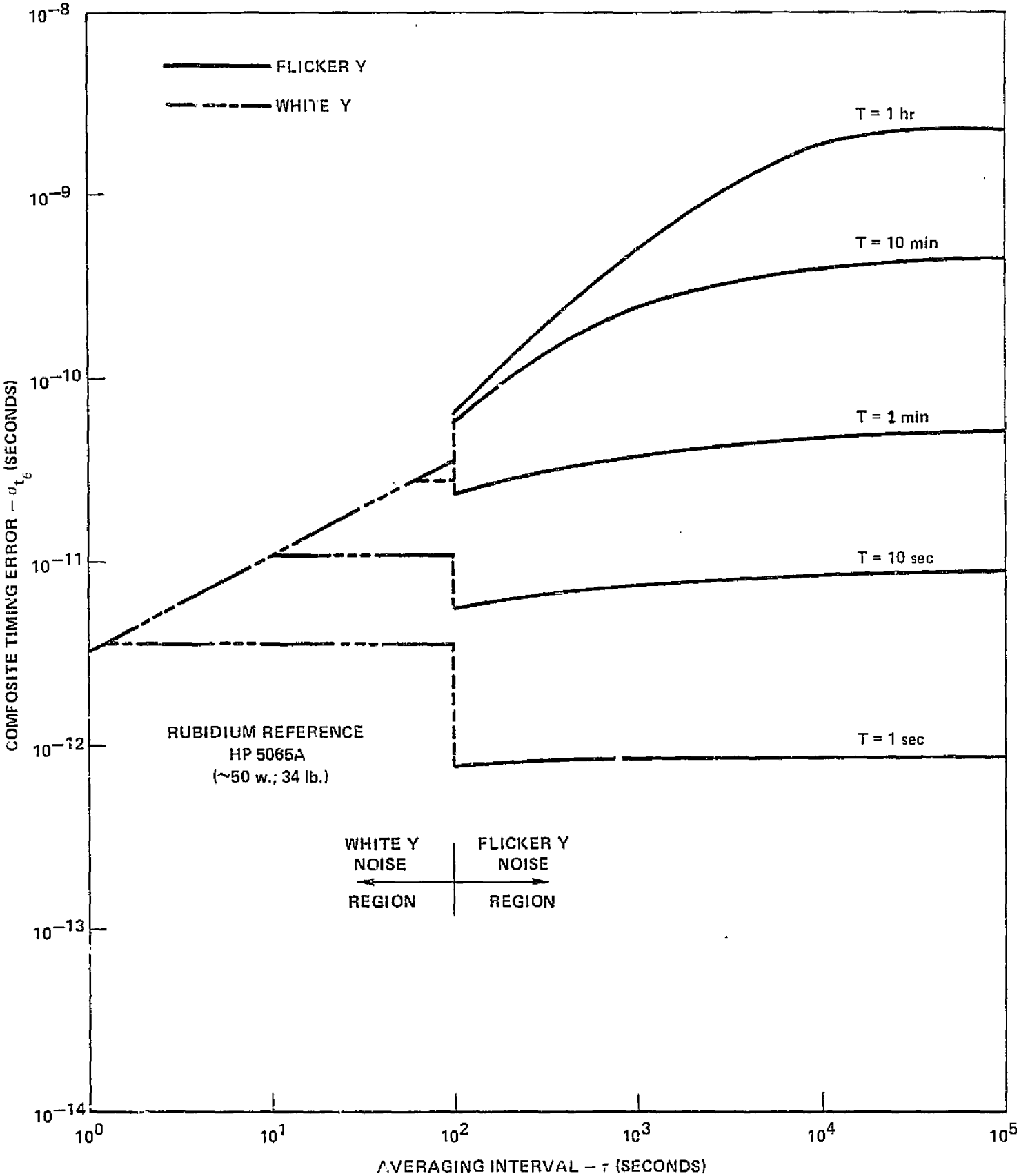

FIGURE 6.8. COMPOSITE GROUND CLOCK TIMING ERROR VERSUS AVERAGING INTERVAL FOR A RUBIDIUM STANDARD

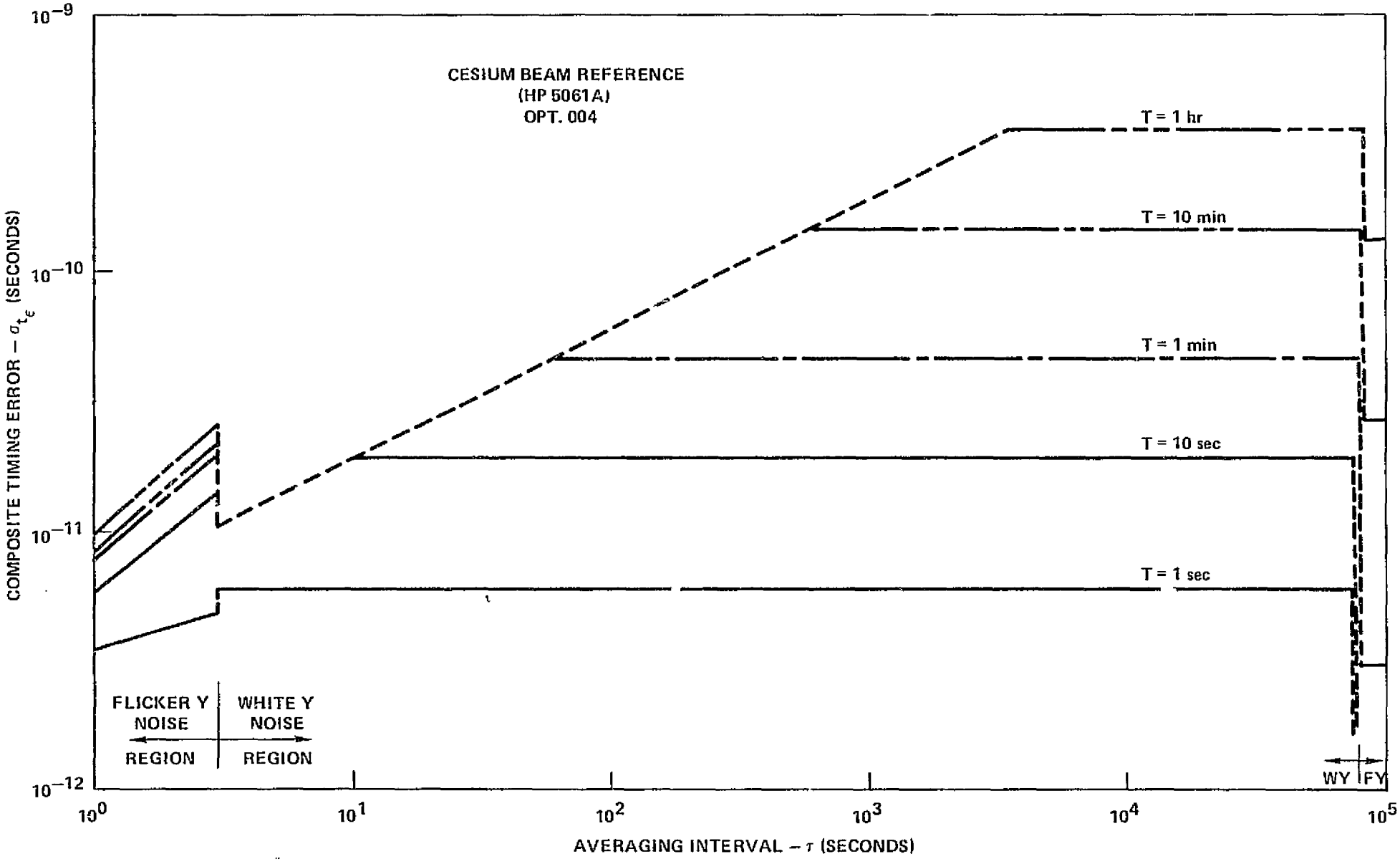

FIGURE 6.9. COMPOSITE GROUND CLOCK TIMING ERROR VERSUS AVERAGING INTERVAL FOR A CESIUM STANDARD

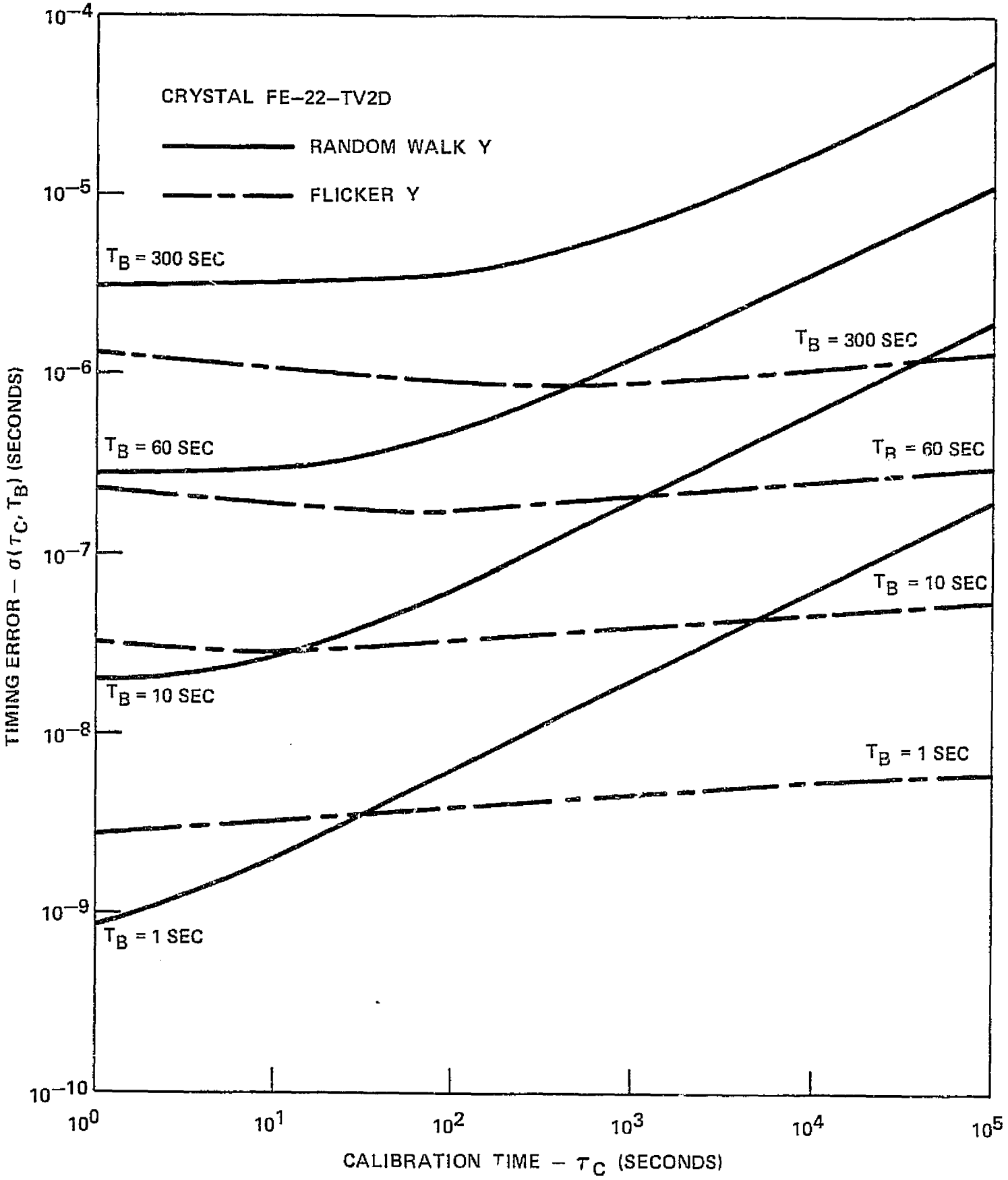

FIGURE 6.10. USER CLOCK TIMING ERRORS VERSUS AVERAGING INTERVAL FOR A NOMINAL CRYSTAL OSCILLATOR

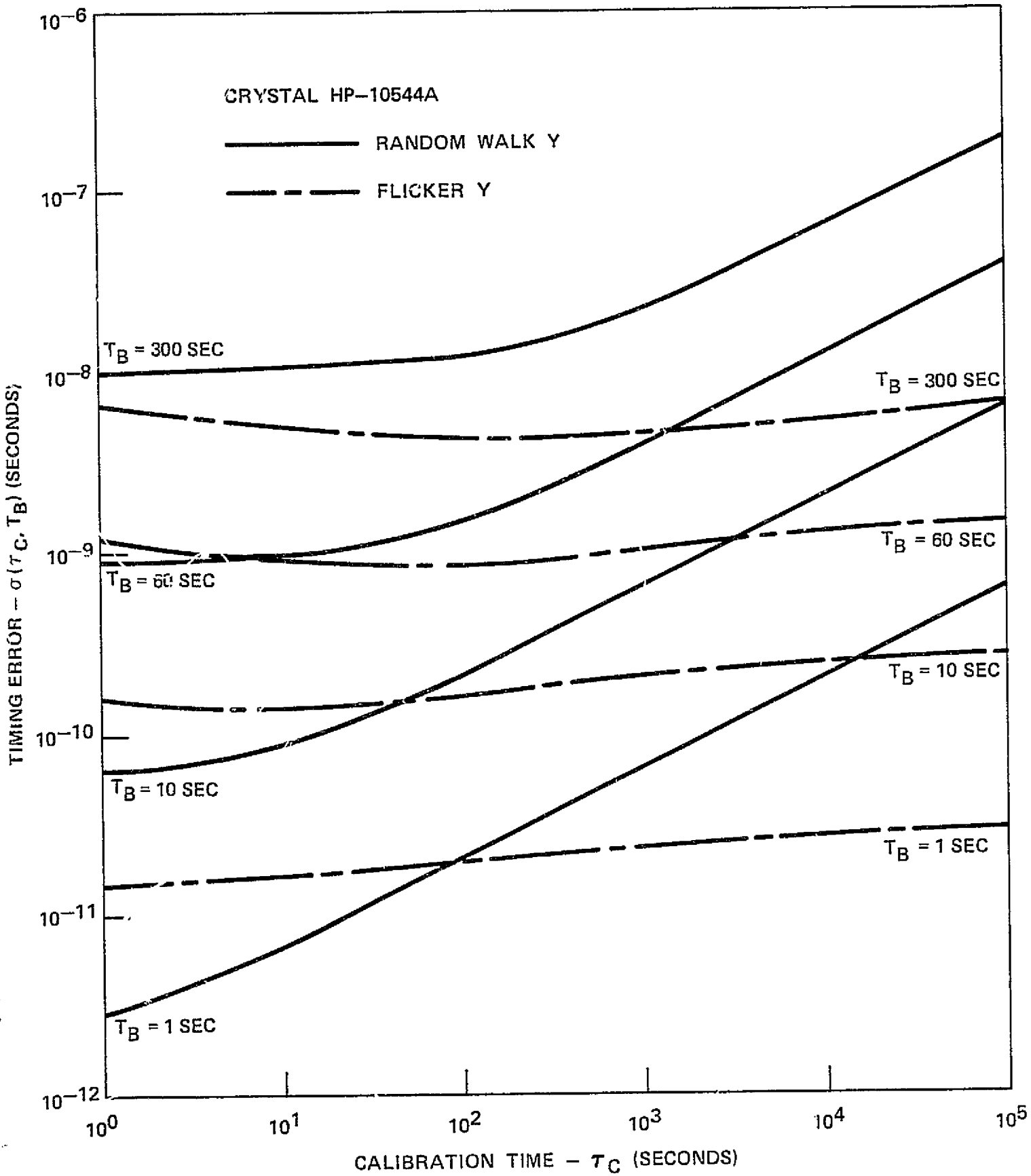

FIGURE 6.11. USER CLOCK TIMING ERRORS VERSUS AVERAGING INTERVAL FOR A HIGH QUALITY CRYSTAL OSCILLATOR

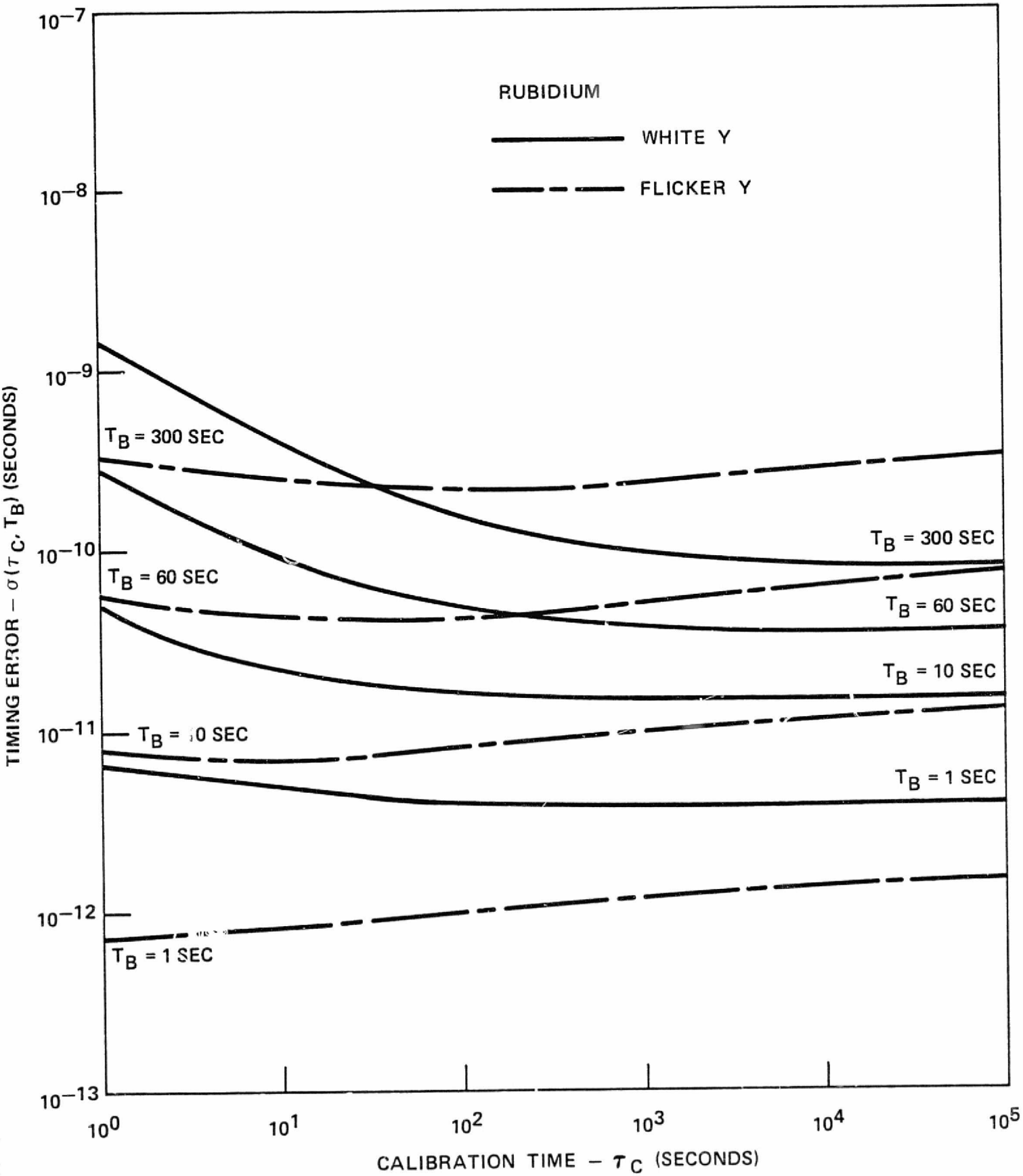

FIGURE 6.12. USER CLOCK TIMING ERRORS VERSUS AVERAGING INTERVAL FOR A RUBIDIUM STANDARD

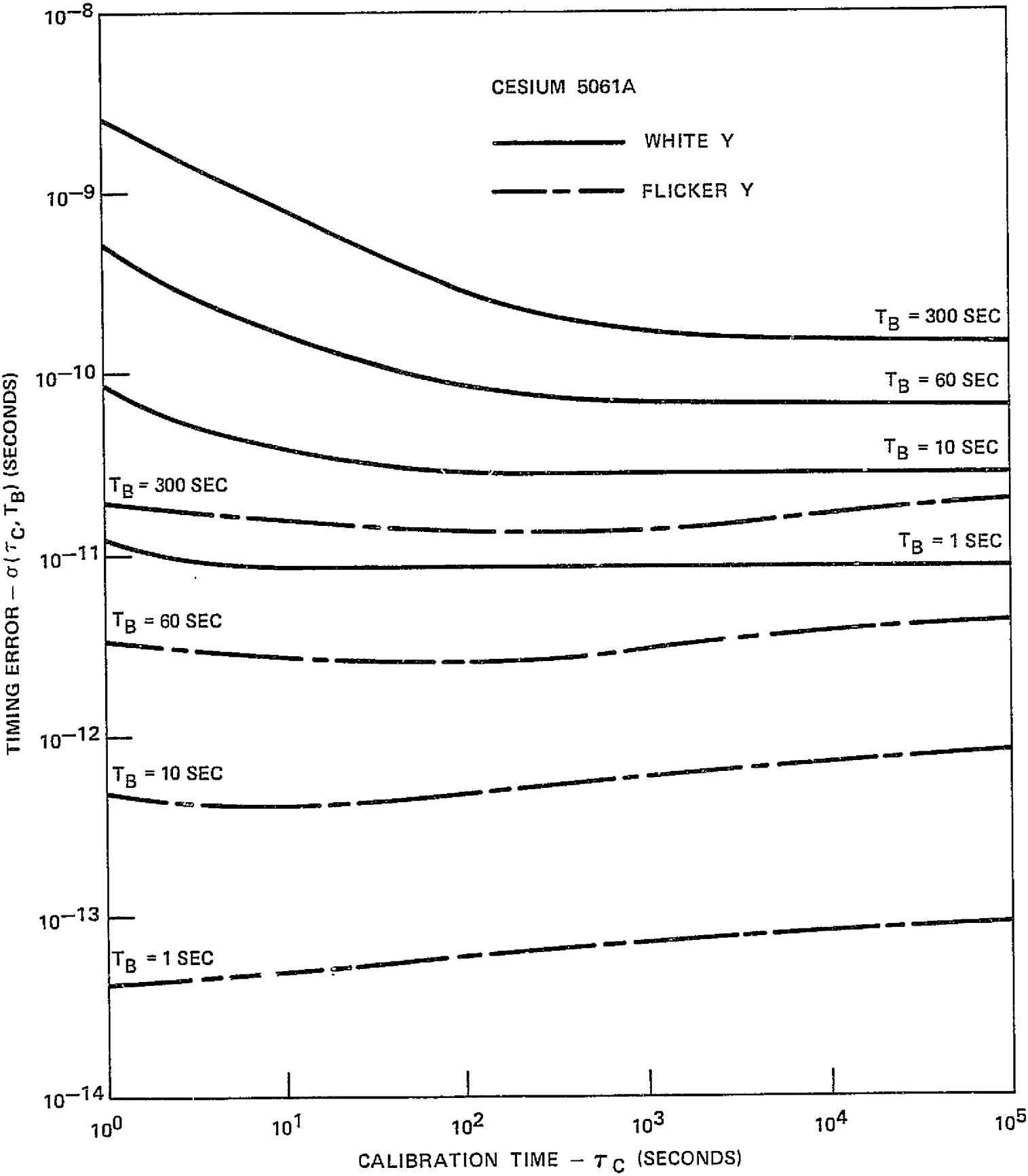

FIGURE 6.13. USER CLOCK TIMING ERRORS VERSUS AVERAGING INTERVAL FOR A CESIUM STANDARD

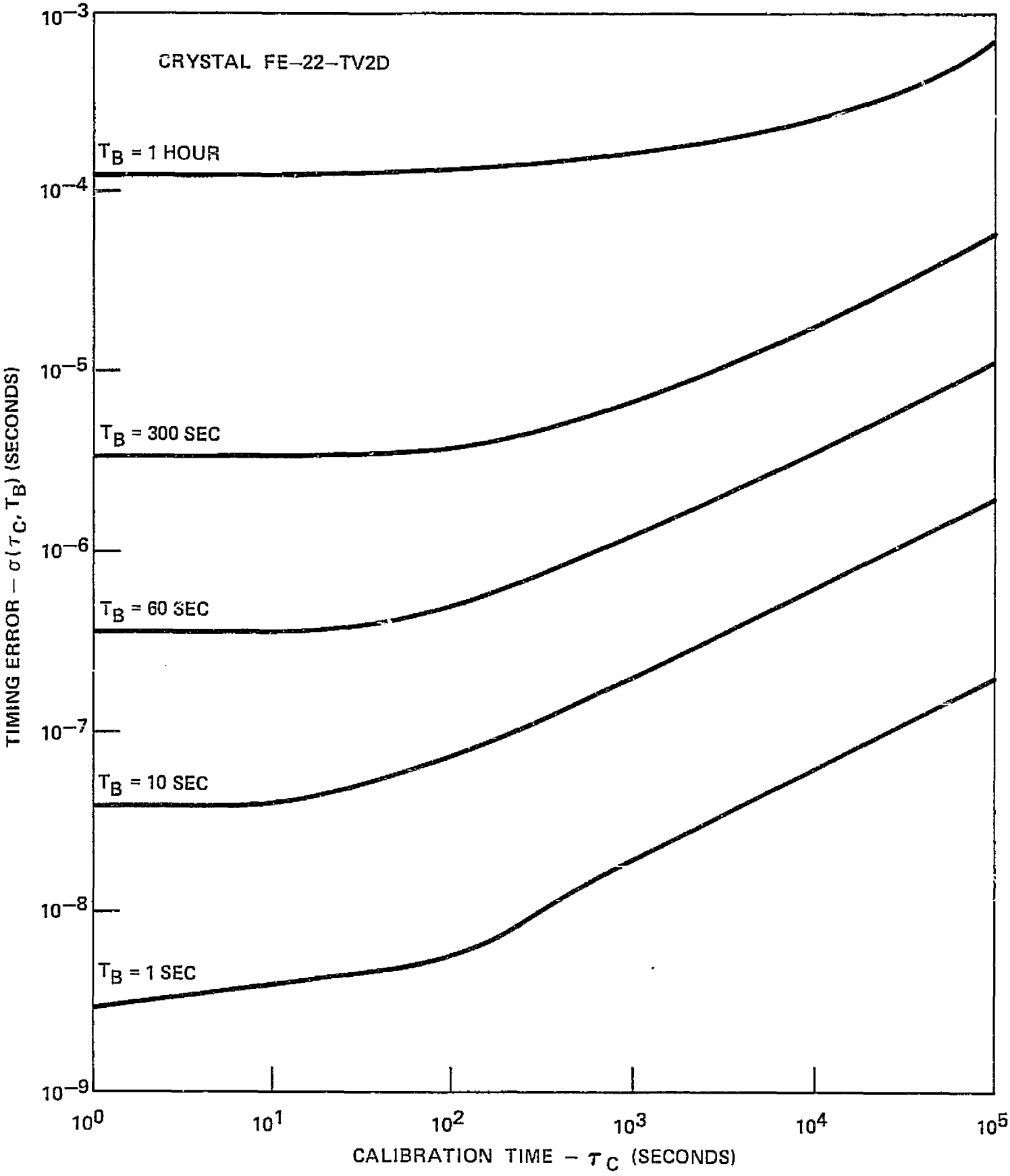

FIGURE 6.14. COMPOSITE USER CLOCK TIMING ERROR VERSUS AVERAGING INTERVAL FOR A NOMINAL CRYSTAL OSCILLATOR

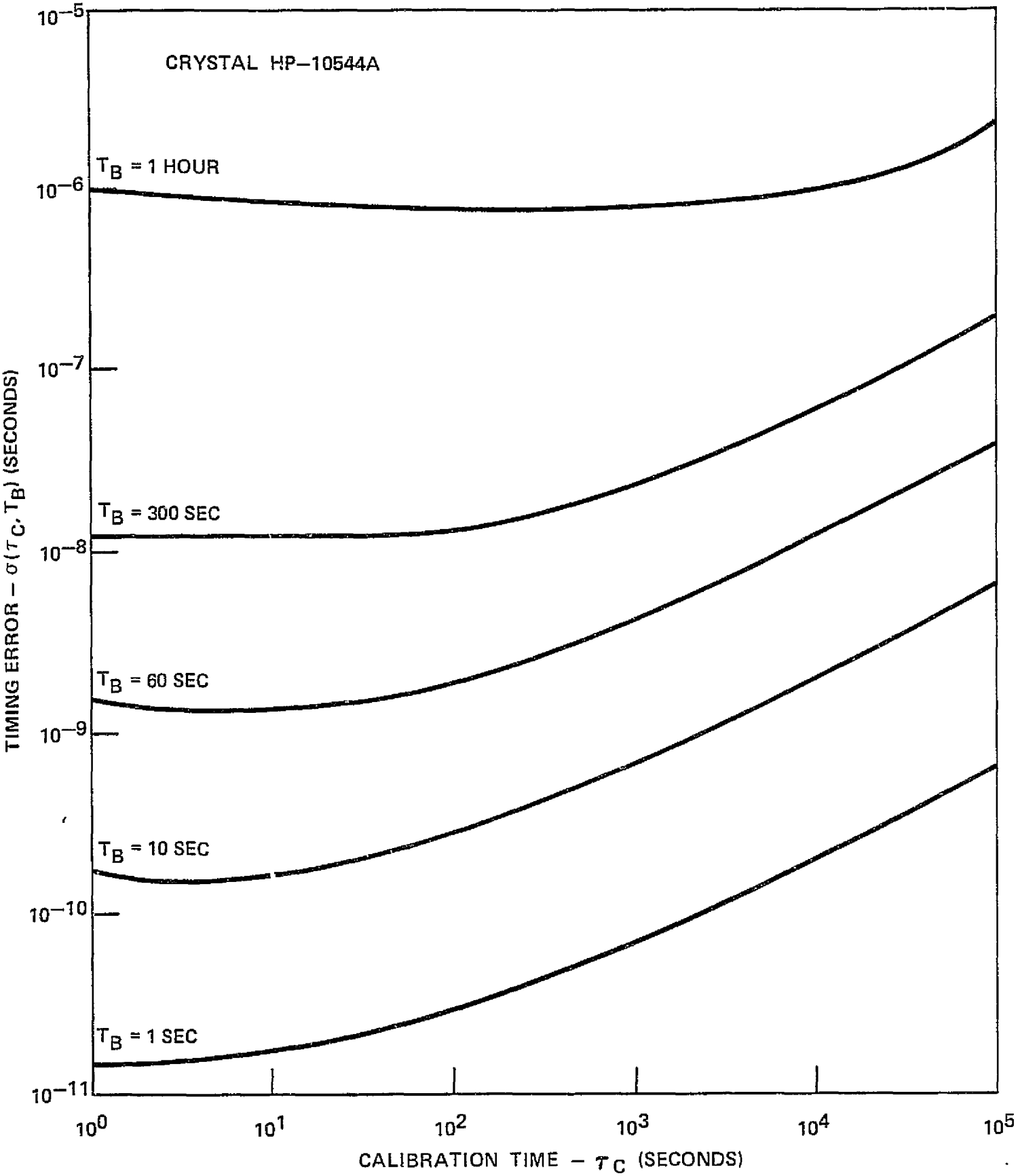

FIGURE 6.15. COMPOSITE USER CLOCK TIMING ERROR VERSUS AVERAGING INTERVAL FOR A HIGH QUALITY CRYSTAL OSCILLATOR

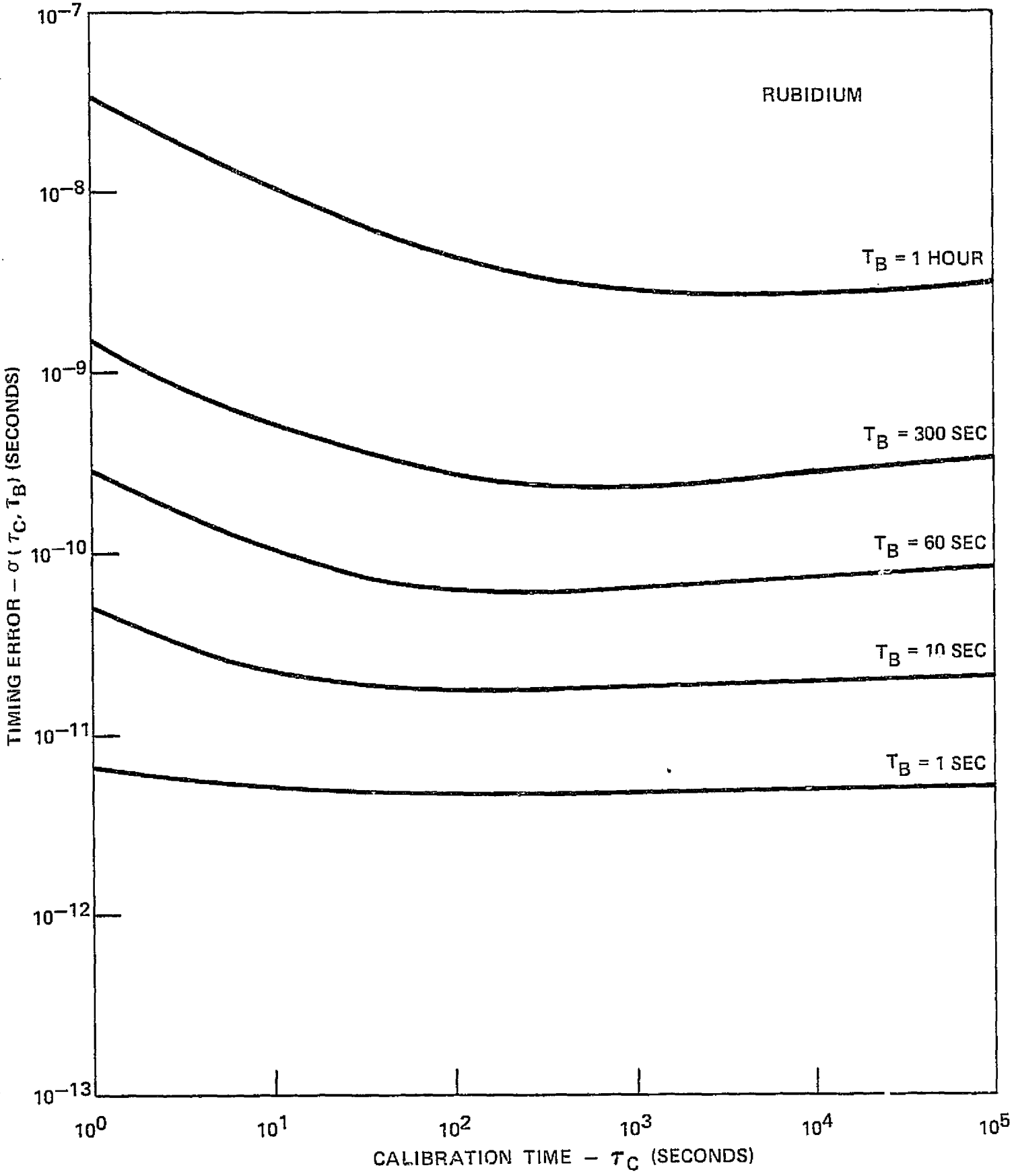

FIGURE 6.16. COMPOSITE USER CLOCK TIMING ERROR VERSUS AVERAGING FOR A RUBIDIUM STANDARD

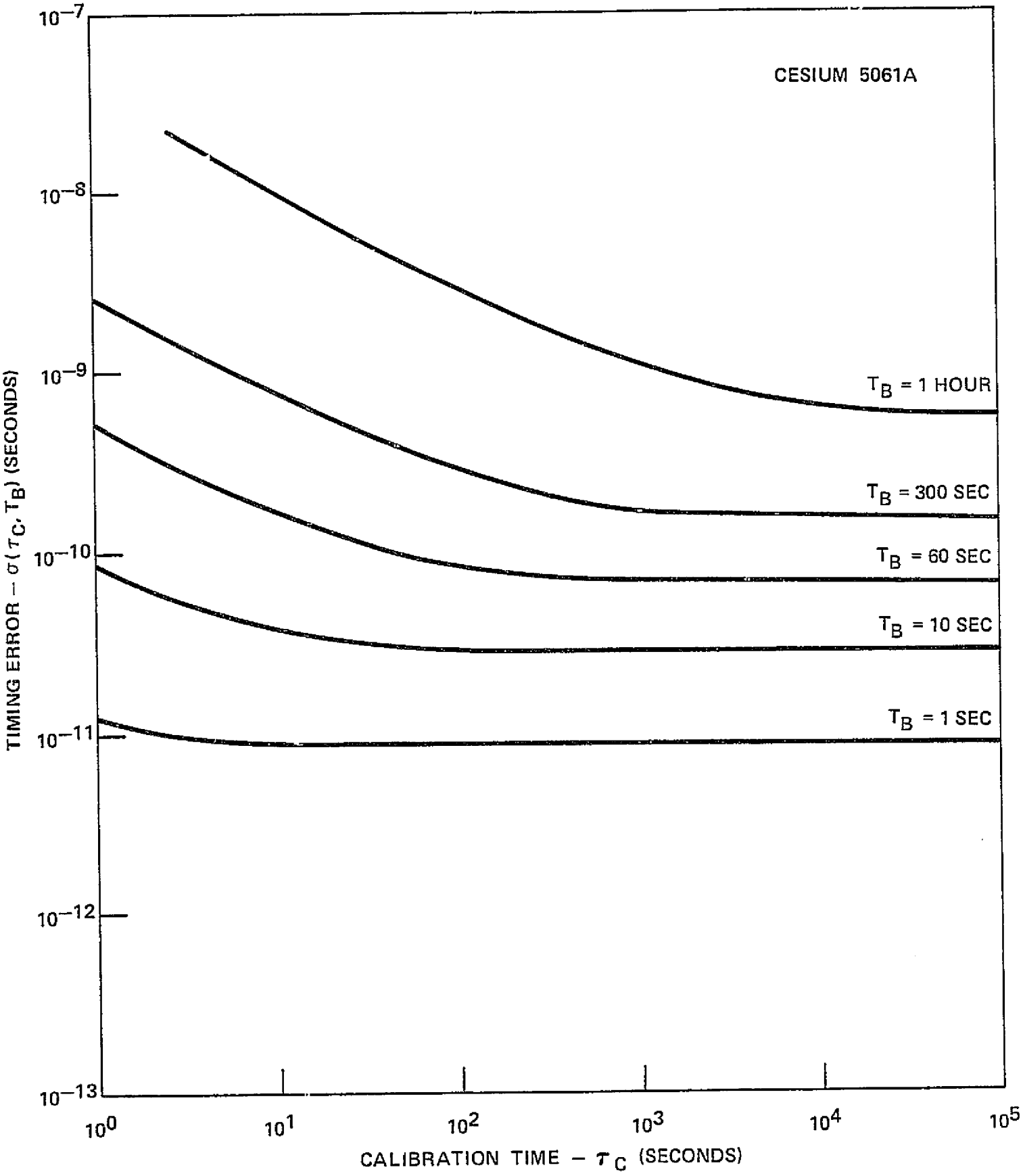

FIGURE 6.17. COMPOSITE USER CLOCK TIMING ERROR VERSUS AVERAGING INTERVAL FOR A CESIUM STANDARD

orbit of stored data). Under these conditions Figures 6.14 through 6.17 yield a composite timing error equivalent to that shown in the table below.

TABLE 6.4

WORST-CASE DESIGN FOR USER TIMING ERROR

Frequency Standard		$\sigma(\tau_C$=10 sec, T_B=1 hr)	
Crystal:	FE 22-TV2D	130.	microseconds
Crystal:	HP 10544A	.85	microseconds
Rubidium:	HP 5065A	10.6	nanoseconds
Cesium:	HP 5061A opt. 004	10.	nanoseconds

From this table it is clear that for the worst case design, the user satellite cannot rely on a nominal crystal oscillator such as FE 22-TV2D in order to obtain microsecond timing of events. If, however, a user can only have a clock of this type then Figure 6.14 indicates that maximum time between calibrations must be on the order of T_B=2 minutes or less in order to obtain microsecond time tagging. This could, in turn, impose a severe limitation on the user satellite data collection system.

CLOCK ERROR SUMMARY

A methodology for computing one sigma timing errors assocaited with oscillator instability has been developed in the preceeding paragraphs. General expressions for the Allan variance, $\sigma_y^2(N,T,\tau)$, which is the time domain measure of frequency stability, are given for various noise processes. This parameter was then related to the TDRSS/USER operational system. Both ground and user clock timing error expressions have been given (Table 6.2 and 6.3). The effect of frequency drift on the recalibration cycle was also developed with results shown in Figure 6.2 for typical crystal and rubidium standards.

Some typical oscillators were then summarized with respect to their two sample frequency stability, $\sigma_y(\tau)$. Both atomic standards (rubidium and cesium) and crystalswere considered. A nominal and a high quality crystal were selected. Although these four clocks are not all inclusive in terms of market availability, they do represent reasonable bounds on what is available. Practically any other oscillator that might be chosen would fall somewhere within the stability curves of Figure 6.3 for these devices.

Following this, the ground and user clock timing error were computed for each of the four standards. The composite ground clock timing error caused by propagation delay is shown in Figures 6.6 through 6.9. In general, the atomic clocks provide approximate worst case (τ=300 sec and T=1 hr) timing errors on the order of tenths of nanoseconds, whereas the timing error associated with our two crystals ranges from nanoseconds to microseconds. Similarly, the composite ground and/or user clock timing error has been determined and is shown in Figures 6.14 through 6.17 for the four frequency standards. On a reasonable worst case basis (τ_C= 10 sec and T_B=1 hr), the atomic clocks both provided about 10 nanosecond timing error while the timing error of the two crystals was in the 1-100 microsecond

range. Other errors could be calculated for different values of τ, T, τ_C, T_B and the above values would have to be scaled accordingly. In the next section, this will be done for some specific TDRSS and user orbit operational modes.

VII. DATA TIMING ERROR CALCULATION APPROACH

TDRSS/USER CONFIGURATIONS

It was difficult, in view of the number of variables involved, to decide on the configurations for which data timing error calculations should be made. The decision was made to base a general set of operational cases on the majority of user satellites as shown in Figure 4-1b. The periods of User/TDRSS non-visibility would not be considered in the general set of cases but in a limited set of cases. This was done because the periods of non-visibility vary widely with orbital inclination and altitude and also, the user may not require data during these periods.

In the timing error calculations for the general cases, the following assumptions were made:

- The Orbital period for all user satellites is 95 minutes,
- Each TDRS operates with a user for half the orbital period during continuous data acquisition,
- For non-continuous data acquisition, the contact period is 25 minutes (this may be high for most SA users - probably on the order of 10 minutes for a tape recorder data dump),
- If timing accuracy is critical, and continuous R&RR data is not available due to the user operating mode, TDRSS will schedule additional R&RR contacts if operational time allows. This will be most applicable to MA users where the forward beam is pointed electronically, rather than SA users where the forward beam must be mechanically slewed.

With these general assumptions in mind, our TDRSS/USER configurations were chosen according to whether the user event data is time tagged and transferred to the ground station in real time or non-real time (stored data mode).

REAL TIME (RT) USER EVENT TIME TAGGING AND DATA TRANSFER

For this configuration, four separate operational concepts have been considered:

Continuous Two-way R&RR

In this example the forward link is available so that 2-way R&RR or coherent 2-way RR can be made through the contact period. This applies to the low rate SA users and high rate SA users that have simultaneous low rate operations or coherent carrier operations when high rate data is transmitted.

Continuous One-way RR With R&RR Calibration

In this case the forward link is available, generally, only at the start of a pass for two-way R&RR measurements. For the balance of the pass one-way RR measurement data is available. This applies particularly to the MA users since the forward link is shared. It would also apply to the high rate SA users that operate the low data rate during the initial R&RR measurement period and thereafter operate at the high data rate using the user satellite frequency reference. Five subcases are considered: one, two and three calibrations per TDRS pass and 25 minute contact periods per TDRS pass and per user satellite orbit.

R&RR Calibration With Ephemeris Data

This is similar to the previous case with the difference that position data from orbit computations is used to determine the propagation delay between calibrations instead of one-way RR measurement data.

One-Way Only Tracking

This configuration differs from the preceeding cases because the user satellite is assumed to be equipped with a transmitter only. Hence, a forward link to the user (for calibration or any other purpose) is never available. Time tagging, however, is still performed on the ground for the RT data. It is required to have ephemeris data from the satellite to accurately determine the propagation delay.

NON-REAL TIME (NRT) DATA TRANSFER OF USER EVENTS

The primary difference between the NRT and the RT modes is the insertion of a clock in the user satellite for time tagging. A larger number of SA users will employ tape recorders to store data for readout through TDRSS. Tape recorders will not be a general requirement for MA users since they can transmit data nearly continuously in real time. Four sub-cases are considered: a data dump each TDRS pass, each user satellite orbit and every two user satellite orbits, and a short record segment of 20 minutes. Five minutes is allowed for acquisition and five or ten minutes for tape recorder readout during the contact period. One orbit of data can be read out in five minutes at a 20:1 dump rate and ten minutes allows two orbits of data to be read out. The corresponding R&RR calibration periods are assumed to be five or ten

minutes. The above four operational configurations will be assumed for the non-real time data transfer mode.

- NRT Data Transfer - Continuous 2-way R&RR
- NRT Data Transfer - Continuous 1-way RR with R&RR calibration
- NRT Data Transfer - R&RR calibration with ephemeris data
- NRT Data Transfer - Continuous 1-way only tracking.

TOTAL TIMING ERROR

The total timing error associated with a particular configuration is equal to the RSS of the equipment and propagation errors, σ_e, and the total RSS clock error, σ_{ci}.

$$\sigma_\varepsilon = (\sigma_e^2 + \sigma_{ci}^2)^{\frac{1}{2}} \qquad (7\text{-}1)$$

The subscript i is used to refer to the operational mode under consideration. From the previous discussion there are a total of eight operational modes.

Sections VIII and IX develop the appropriate values for σ_{ci} for both RT and NRT data transfer modes. The following paragraph summarizes the values for the equipment and propagation errors σ_e. Substitution of the appropriate values of σ_e and σ_{ci} into equation (7-1) will then result in an overall system timing error.

Computation of Overall Equipment Error, σ_e

This error consists of the RSS of all equipment and propagation errors exclusive of the system clocks. Typical time delay variations were determined in Sections III and V. These include the following variations:

Error Source	Timing Error, (nsec.)
User Data Delay	3.3
User PN ranging error	2.4
User Transponder Delay	20.0
TDRS Delay	17.3
Ground Station Ranging Bias	11.5
Ground Station Delay Deviation	10.0 (MA)
	5.0 (SA)
Propagation	10.0

The RSS of these variations is 32.4 nsec. (MA), and 31.2 nsec. (SA). Thirty-two nsec. is a good approximation for use in both cases and will be used in our calculations.

Ground Station data delay measurement accuracy is 577 nsec. and time code resolution is 289 nsec., for an RSS total of 645 nsec. There will also be the bit synchronizer delay variation which was calculated as .00207 bits. The following bit rates result in the delay variations shown:

Mode	Bit Rate	Delay Variation, σ (nsec.)
MA low	5 kbps	414
MA high	50 kbps	41
SA low	50 kbps	41
SA high	1 Mbps	2

Only the delay at 50 kbps will be used in calculations to reduce the number of combinations of parameters to be considered. The timing errors for MA systems at low bit rates will be slightly higher than given by the final calculations. These contributing effects can be conveniently summarized in the following table.

TABLE 7.1
OVERALL EQUIPMENT TIMING ERROR, σ_e

OVERALL ERROR SOURCES	TIMING ERROR, σ (nsec.)
General Equipment	32
Ground Station Data Delay Measurement & Time Resolution	645
Bit Synchronizer	41
Total Equipment RSS Timing Error, σ_e	647

It should be noted that the ground station data delay measurement and time code resolution are the limiting factors in the above computation of σ_e. If more accurate data delay measurements and time codes were available, the overall equipment error would reduce to a minimum value of $\sigma_e \sim 52$ nanoseconds. This value of approximately 50 nanoseconds probably represents the best achievable value for σ_e and, as such, would result in an upper bound on total system timing error, σ_e. Hence, our upper bound on total system timing error would be $\sigma_e \geq 50$ nanoseconds assuming an optimum ground station design for the time code and data delay measurement. For the purpose of our analysis based on assumed TDRSS parameters, the upper bound on σ_e would be 647 nanoseconds. From this analysis it is evident that further and more detailed efforts in this area of ground station time code design and measurement are worthwhile and needed since the benefits are extremely desirable.

VIII. COMPUTATION OF OVERALL CLOCK ERROR -RT DATA TRANSFER

In this section real-time (RT) user event time tagging and data transfer is considered. For this case the actual time tag is done at the ground station. Each of the previously mentioned four TDRS/USER operational modes discussed in Section VII will now be examined with respect to computing the overall clock error, σ_{c_i} .

RT CONTINUOUS 2-WAY R&RR

For this configuration it is assumed that only user event data which can be transferred in real time is available. In this way, both the user satellite and the TDRS act as simple transponders. All time tagging is referenced at the ground station and no event clock is necessary in the user satellite. The ground clock must be calibrated at a certain interval T_c in order to preserve the overall timing accuracy. For this configuration the overall timing error is given by

$$\sigma_{c_1} = \left[\sigma_0^2 + \sigma_{t_\varepsilon}^2 + \sigma^2(\tau_c, \tau)\right]^{\frac{1}{2}} \tag{8-1}$$

where σ_0 is given by equation (6-19), which depends on the clock drift rate D and time between calibrations T_c, and σ_{t_ε} is given by the equations of Table 6.2 and depends on the averaging interval and the propagation delay T. Finally, the remaining quantity $\sigma(\tau_c, \tau)$ is the ground clock timing error and is given by the equations of Table 6.3 with the substitution $T_B = \tau$. Figures 6.2 and 6.6. to 6.9 are used to determine the values for σ_0 and σ_{t_ε} while figures 6.14 to 6.17 can be used to determine $\sigma(\tau_c, \tau)$. A tabulation of these results are given in Table 8.1 for each of the four frequency standards under consideration. For our parameters of interest the term σ_0 is essentially negligible.

TABLE 8.1

TABULATION OF σ_{c_1} AND σ_0 (nanoseconds) for τ_c = 10 seconds

Frequency Standard	σ_{c_1} (T = 1 hr.)		σ_{c_1} (T = 10 min.)		σ_{c_1} (T = 1 min.)		σ_{c_1} (T = 1 sec)		σ_0	
	τ = 1 sec	τ = 5 min	τ = 1 sec	τ = 5 min	τ = 1 sec	τ = 5 min	τ = 1 sec	τ = 5 min	τ = 1 sec	τ = 5 min
Crystal 1	32.2	9590.	14.5	4670.	6.5	3340.	4.0	3300.	0	60.
Crystal 2	0.12	28.6	0.05	15.8	0.03	12.1	0.02	12.	0	0.06
Rubidium	0.01	0.59	0.01	0.56	0.01	0.55	0.01	0.55	0	0
Cesium	0.01	0.86	0.01	0.86	0.01	0.85	0.01	0.85	0	0

For the TDRS/USER modes of interest, the propagation delay will not, in general, be greater than T = 1 second. Hence, equation (8-1) has been solved for the T = 1 second case for all four oscillators of interest. The resulting overall clock timing error, σ_{C1}, is plotted in Figures 8-1 through 8-4 as a function of averaging interval, τ, with the calibration interval τ_C ranging from 10 seconds to 10^4 seconds. If continuous monitoring of the ground station clock is possible using TDRS, then $\sigma_{C1} \rightarrow \sigma t_\varepsilon$. For Rubidium and Cesium standards, the continuous calibration lower bound would be approximately several picoseconds as shown in Figures 8.3 and 8.4. For the two crystal standards the continuous calibration lower bound is given by Figures 6-6 and 6-7 with T = 1 second. In the case of crystal 1, the continuous calibration lower bound would be approximately $1 < \sigma_{C1} < 100$ nanoseconds. Similarly, for crystal 2, the range would be $.01 < \sigma_{C1} < .5$ nanoseconds.

The summarize, assume a worst case averaging interval of τ = 5 minutes and a propagation delay of T = 1 second. This results in an overall clock timing error shown below.

TABLE 8.2
RT CONTINUOUS 2-WAY R&RR TIMING ERROR FOR τ = 5 MINUTES, τ_C = 10 SECONDS, and T = 1 SECOND

Oscillator		Timing Error, σ_{C1}
Crystal:	FE 22-TV2D	$\leq$ 3.3 microseconds
Crystal:	HP 10544A	$\leq$ 12.0 nanoseconds
Rubidium:	HP 5065	$\leq$ 0.6 nanoseconds
Cesium:	HP 5061A Opt. 004	$\leq$ 0.9 nanoseconds

The values shown in Table 8.2 can be obtained directly from Figures 8-1 to 8-4. Since cesium clocks are anticipated for the TDRSS ground stations, the overall clock timing error will be on the order of 1 nanosecond or less. This represents a substantial improvement over crystals as shown in Table 8.2. Further, if continuous ground station clock calibration could be made, this clock timing error could be further reduced by about a factor of one-hundred.

RT CONTINUOUS 1-WAY RR WITH R&RR CALIBRATION

In this mode a calibration of the ground-clock can be made frequently with the TDRS only. However, when the user satellite is in view of TDRS, its' transponder clock, which will be used subsequently for one-way range rate data, must be calibrated during an interval τ_C and then recalibrated again after some elapsed time interval T_B. Thus, the overall timing error for this operational configuration is given by

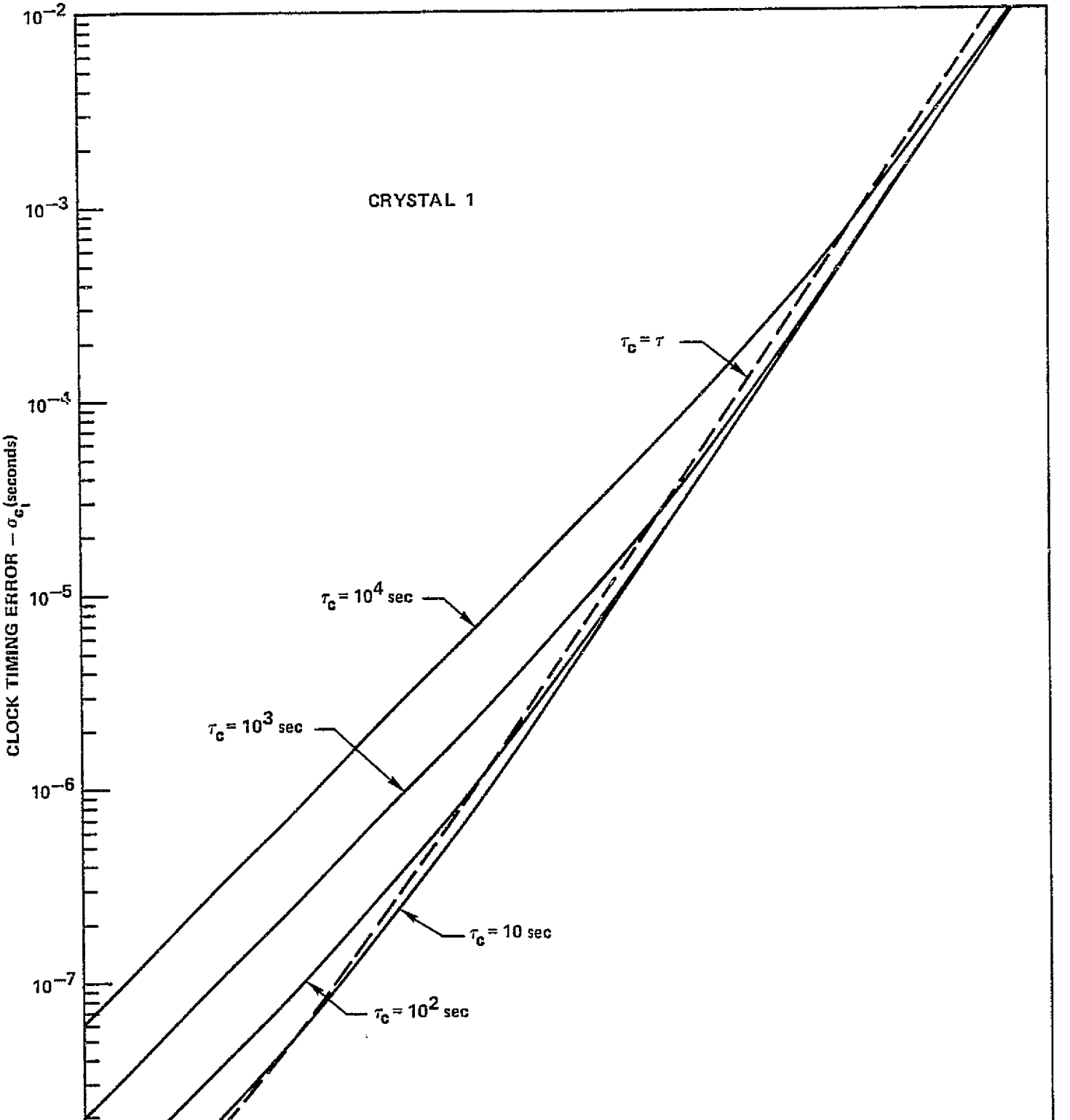

FIGURE 8.1. OVERALL GROUND CLOCK TIMING ERROR VS. AVERAGING INTERVAL FOR RT CONTINUOUS 2-WAY TRACKING WITH T=1 SECOND AND USING CRYSTAL 1

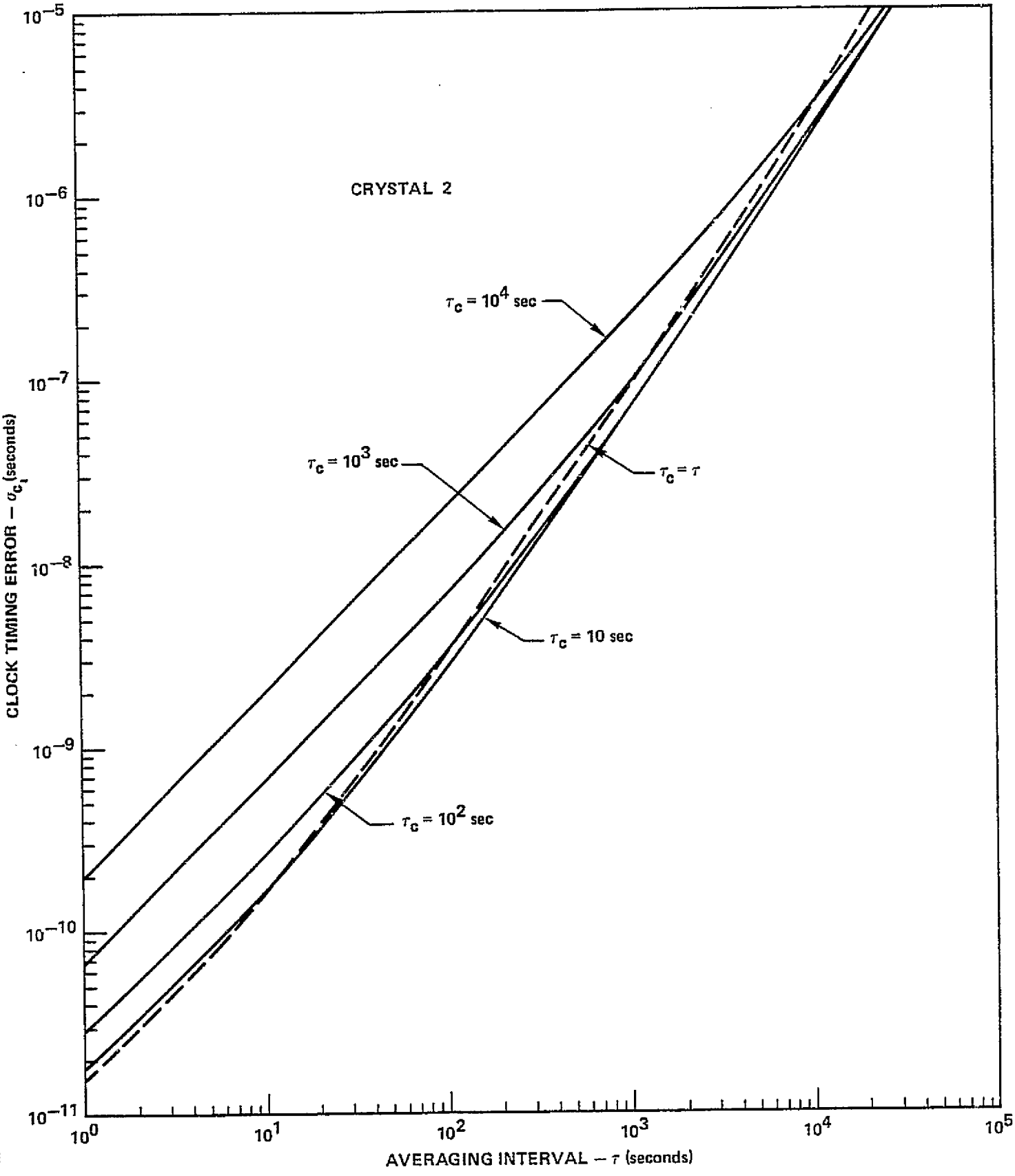

FIGURE 8.2. OVERALL GROUND CLOCK TIMING ERROR VS. AVERAGING INTERVAL FOR RT CONTINUOUS 2-WAY TRACKING WITH T=1 SECOND AND USING CRYSTAL 2

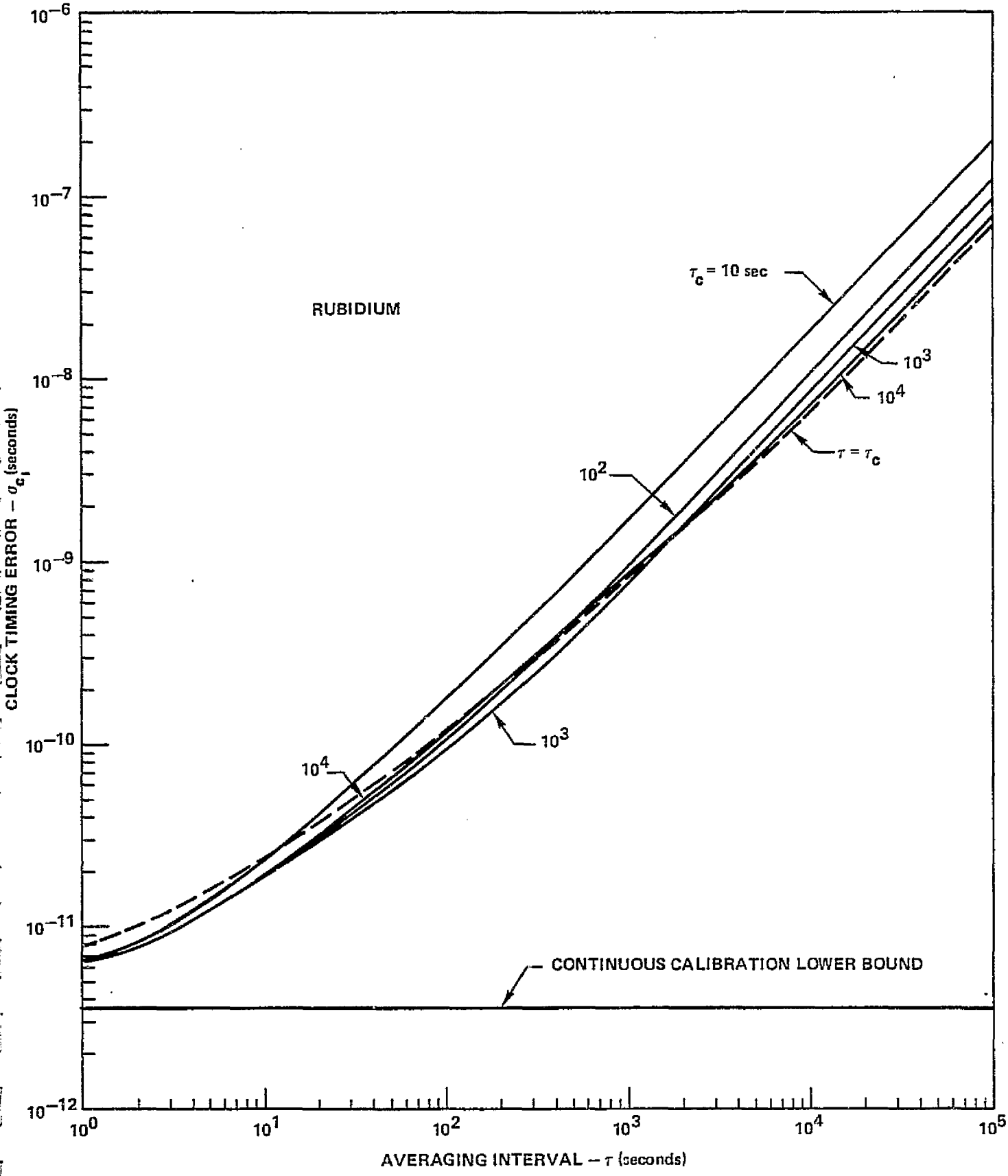

FIGURE 8.3. OVERALL GROUND CLOCK TIMING ERROR VS. AVERAGING INTERVAL FOR RT CONTINUOUS 2-WAY TRACKING WITH T=1 SECOND AND USING A RUBIDIUM STANDARD

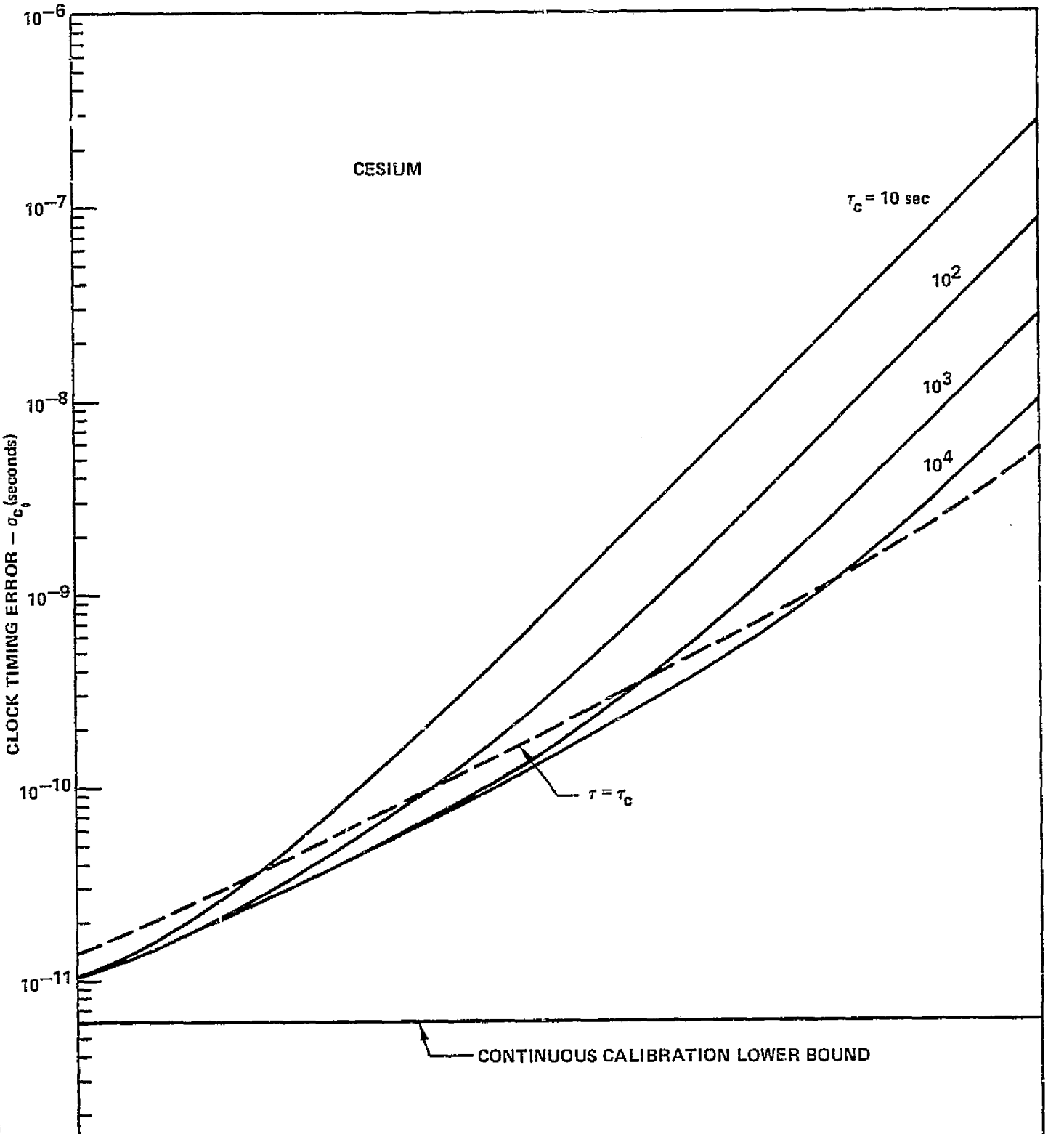

FIGURE 8.4. OVERALL GROUND CLOCK TIMING ERROR VS. AVERAGING INTERVAL FOR RT CONTINUOUS 2-WAY TRACKING WITH T=1 SECOND AND USING A CESIUM STANDARD

$$\sigma_{C_2} = \left\{ \sigma_{C_1}^2 + \sigma_0^2 + \sigma^2(\tau_C, T_B) \right\}^{\frac{1}{2}} \qquad (8\text{-}2)$$

σ_{C_1}: ground clock error

σ_0: transponder drift error

$\sigma^2(\tau_C, T_B)$: transponder clock error during T_B

At this point, it will be assumed that a cesium clock will be used in the ground station yielding $\sigma_{C_1} < 1$ nanosecond. Thus Equation (8-2) reduces to

$$\sigma_{C_2} \leq \left\{ 10^{-18} + \sigma_0^2 + \sigma^2(\tau_C, T_B) \right\}^{\frac{1}{2}} \qquad (8\text{-}3)$$

For a calibration interval of τ_C = 2 minutes, Equation (8-2) has been evaluated for various values of T_B by using Figures 6.2 and 6.14 thorugh 6.17. The results are shown in Table 8.3. For cesium, $\sigma_0 = 0$ and for rubidium clocks $\sigma_0 \rightarrow 0$ for the values of T_B (assume $T_C = T_B$ for this case). For the crystals, however, σ_0 becomes appreciable for our parameters of interest. In Table 8.3 it is evident that if a nominal crystal is placed in a user satellite, event time tagging will be in error in the range of tens of microseconds. Using a better crystal will decrease the timing error to fractions of a microsecond. If atomic standards were available (possible in the future case) in the user satellite, then event time tagging could be made to within 3 nanoseconds or less.

RT R&RR CALIBRATION WITH EPHEMERIS DATA

This case is similar to the previous case except that position data from orbit computations is used to determine the propagation delay between calibrations instead of one-way range rate measurement data. For this operational mode, the total clock timing error is equal to

$$\sigma_{C_3} = \left\{ \sigma_{C_1}^2 + \sigma_{pos}^2 \right\}^{\frac{1}{2}} \qquad (8\text{-}4)$$

where σ_{pos} is the position error estimate and σ_{C_1} is the error associated with the two way RR link during calibration. Reference 5 provides estimates of orbital accuracy determination in the TDRSS era. Detailed computations are performed for two satellites with the orbital parameters as given below:

Satellite	Altitude	Inclination
EOS-B	980 km	99
SATS-H	300 km	20

EOS-B provides a best case in that atmospheric drag is negligible at its orbital altitude and the high orbital inclination provides optimum tracking geometry through TDRSS. SATS-H represents a near worst case in that atmospheric drag introduces uncertainties in the orbital calculations and low inclinations provide the most disadvantageous TDRSS tracking geometry. Reference 5 estimates

TABLE 8.3

RT CONTINUOUS ONE-WAY RR WITH R&RR CALIBRATION FOR τ_c=2 MINUTES

Operational Mode	Timing Error, σ_{C_2} (microseconds)					
	T_B (Minutes)	T_C (Minutes)	Crystal 1	Crystal 2	Rubidium	Cesium
Continuous (One calibration/ TDRS pass)	46	46	90.	0.3	0.003	0.002
Continuous (Two calibration/ TDRS pass)	22	22	32.	0.11	0.002	0.002
Continuous (Three calibration/ TDRS pass)	14	14	17.	0.06	0.001	0.001
25 Minute contact per TDRS pass	25	46	36.	0.13	0.002	0.002
25 Minute contact per user orbit	25	93	41.	0.13	0.002	0.002

that the total TDRS position error, taking an RSS of all error contributions, will be 100 meters. The position uncertainty is 25 m for EOS-B and 566 m for SATS-H. Combining the position errors and determining corresponding delay uncertainties gives the following results:

Satellies	Combined Position Error (RSS m)	Position Time Error σ_{pos} (nsec)
EOS-B	103	344
SATS-H	575	1917

The errors are based on tracking data which provides a good distribution for orbit determination. The tracking data samples can be widely spaced, however, such as 2 minutes per 2 hours or per 4 hours and scheduling should not present difficulties. It will be necessary to have sufficient tracking data available in the same general time period as the data operations since propagating data forward or backward in time will result in larger errors. Substituting the above values for σ_{pos} into Equation (8-4) and recalling our earlier assumption of cesium clocks at the ground station (σ_{c_1} = 1 nanosecond), the total timing error becomes

- σ_{c_3} = 0.344 microseconds (high inclination orbit)
- σ_{c_3} = 1.917 microseconds (low inclination orbit).

On the surface it appears that this approach would be better than the previous operational mode using a nominal crystal for the user satellite. However, since there are numerous types of orbits (σ_{pos} varies a great deal as shown in Reference 5), many other cases would have to be considered before any definitive conclusions could be reached regarding using orbit position data for time tagging during real time operations.

ONE WAY ONLY TRACKING

In this configuration the user satellite does not have a receiver and, hence, only 1-way transmission occurs. The time tagging of data is done on the ground using the clock at the ground station. The error caused by the propagation delay upon the ground clock (as in 2-way tracking links) is not present in this configuration resulting in σ_{t_ε}=0. Thus, the resulting total clock timing error is equal to

$$\sigma_{c_4} = \left[\sigma_0^2 + \sigma^2(\tau_c, \tau) + \sigma_{pos}^2 \right]^{\frac{1}{2}} \qquad (8\text{-}5)$$

In Equation (8-5) the quantity $\sigma(\tau_c,\tau)$ has been evaluated and the results are shown in Figures 8-5 through 8-8 for our frequency standards of interest. The calibration error σ_0 is negligible for most parametric cases but the values of σ_{pos} are a dominant component part. Substituting the values of σ_{pos} from the

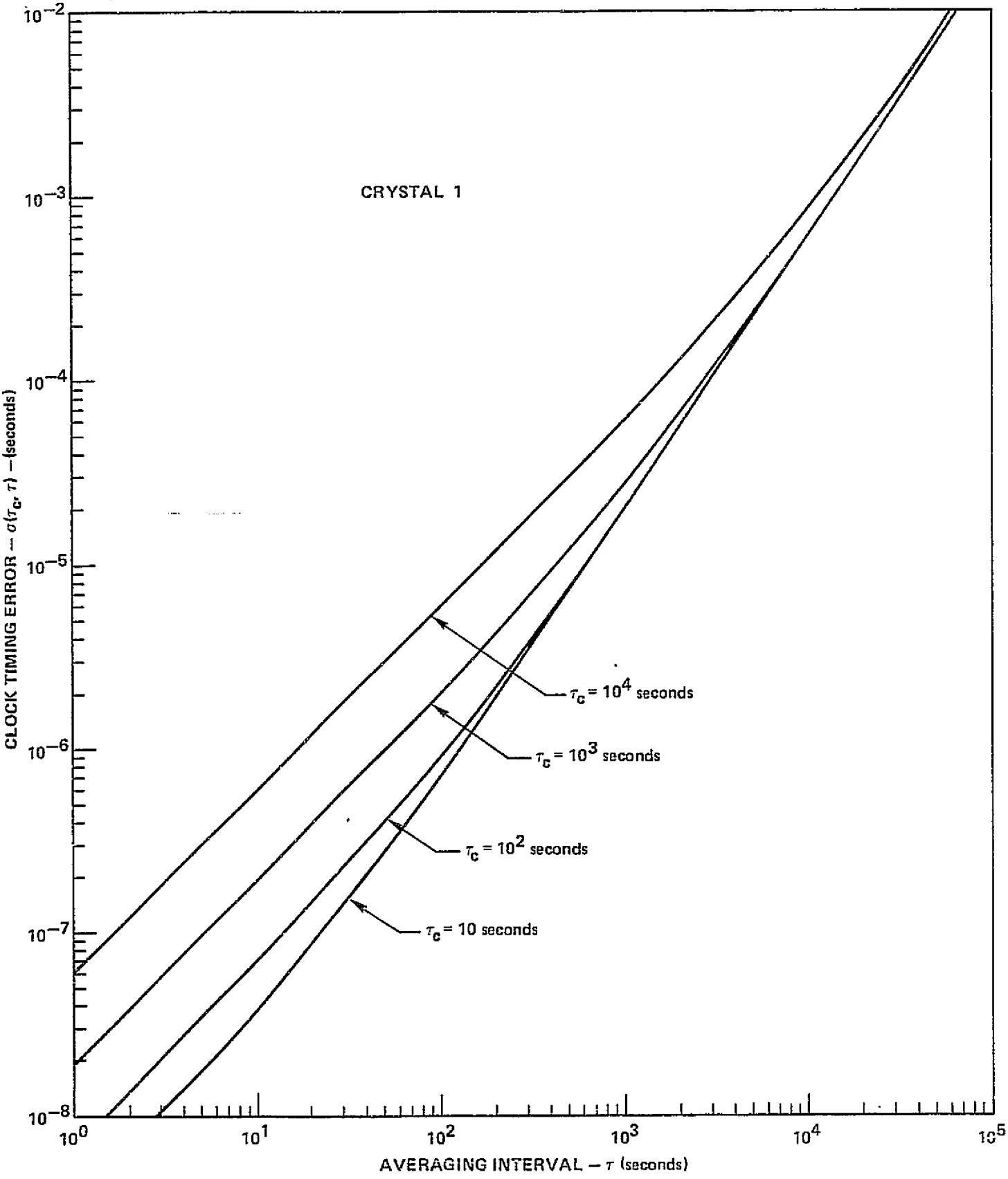

FIGURE 8.5. OVERALL GROUND CLOCK TIMING ERROR VS. AVERAGING INTERVAL FOR RT CONTINUOUS 1-WAY ONLY TRACKING USING CRYSTAL 1

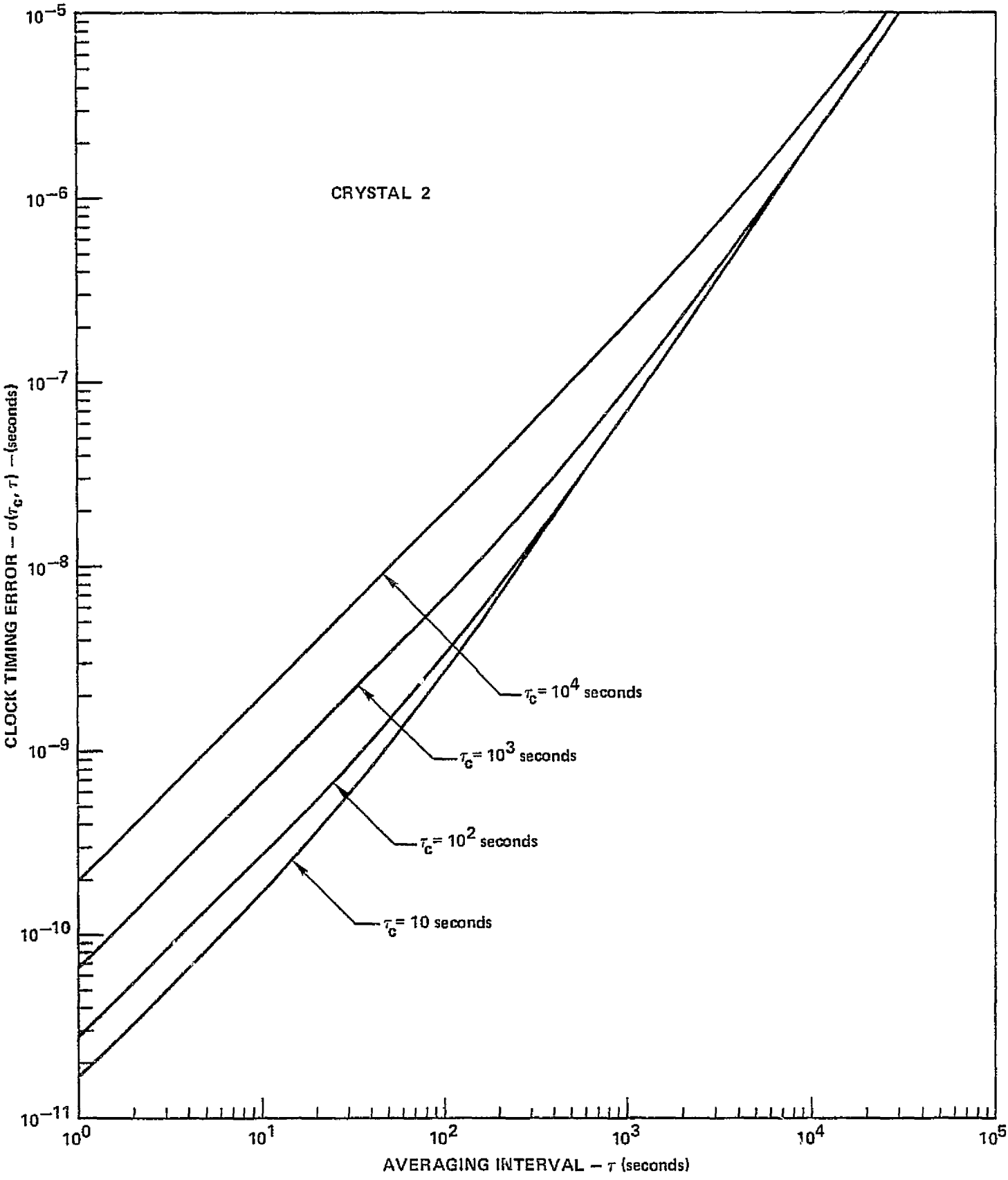

FIGURE 8.6. OVERALL GROUND CLOCK TIMING ERROR VS. AVERAGING INTERVAL FOR RT CONTINUOUS 1-WAY ONLY TRACKING USING CRYSTAL 2

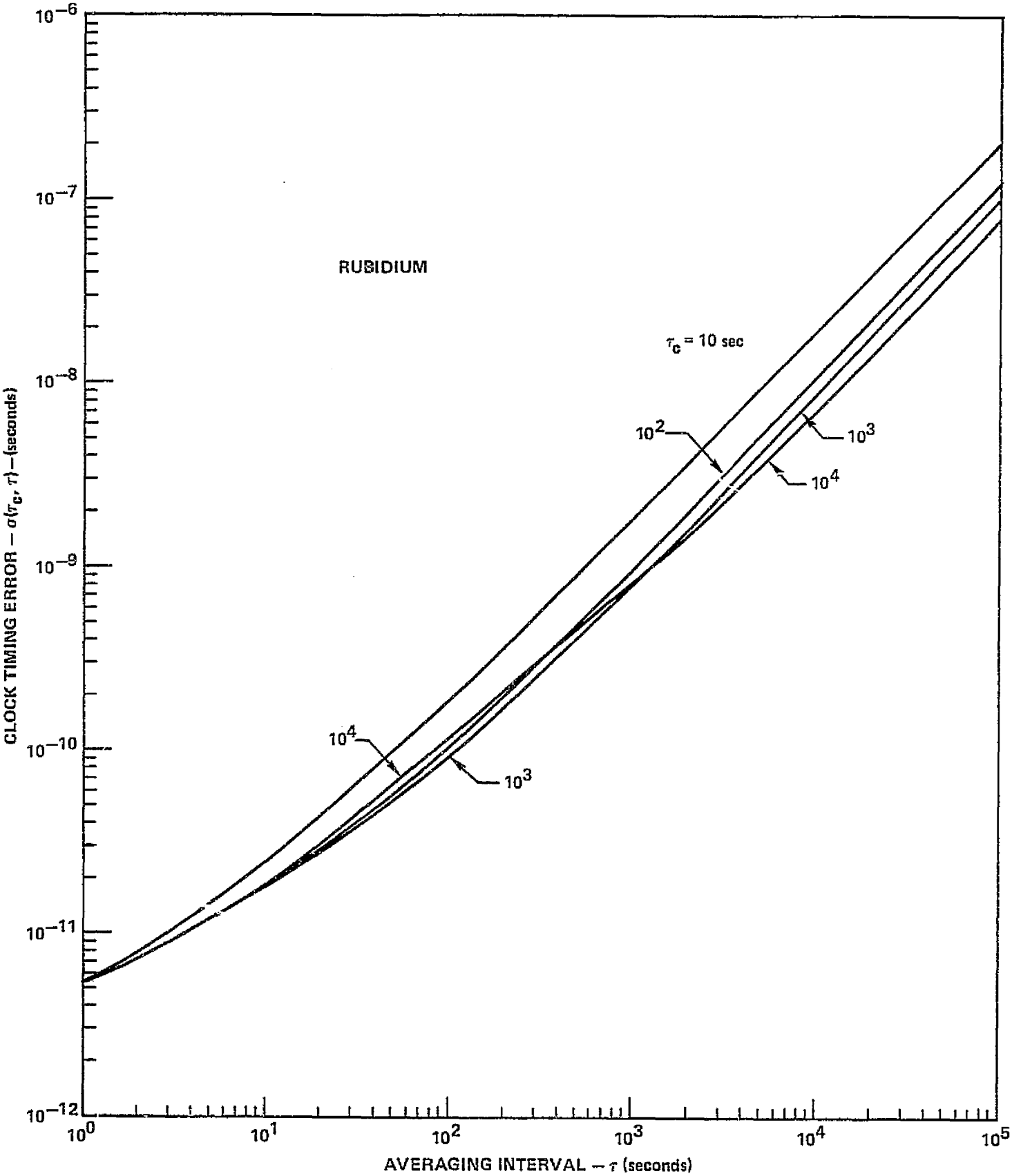

FIGURE 8.7. OVERALL GROUND CLOCK TIMING ERROR VS. AVERAGING INTERVAL FOR RT CONTINUOUS 1-WAY ONLY TRACKING USING A RUBIDIUM STANDARD

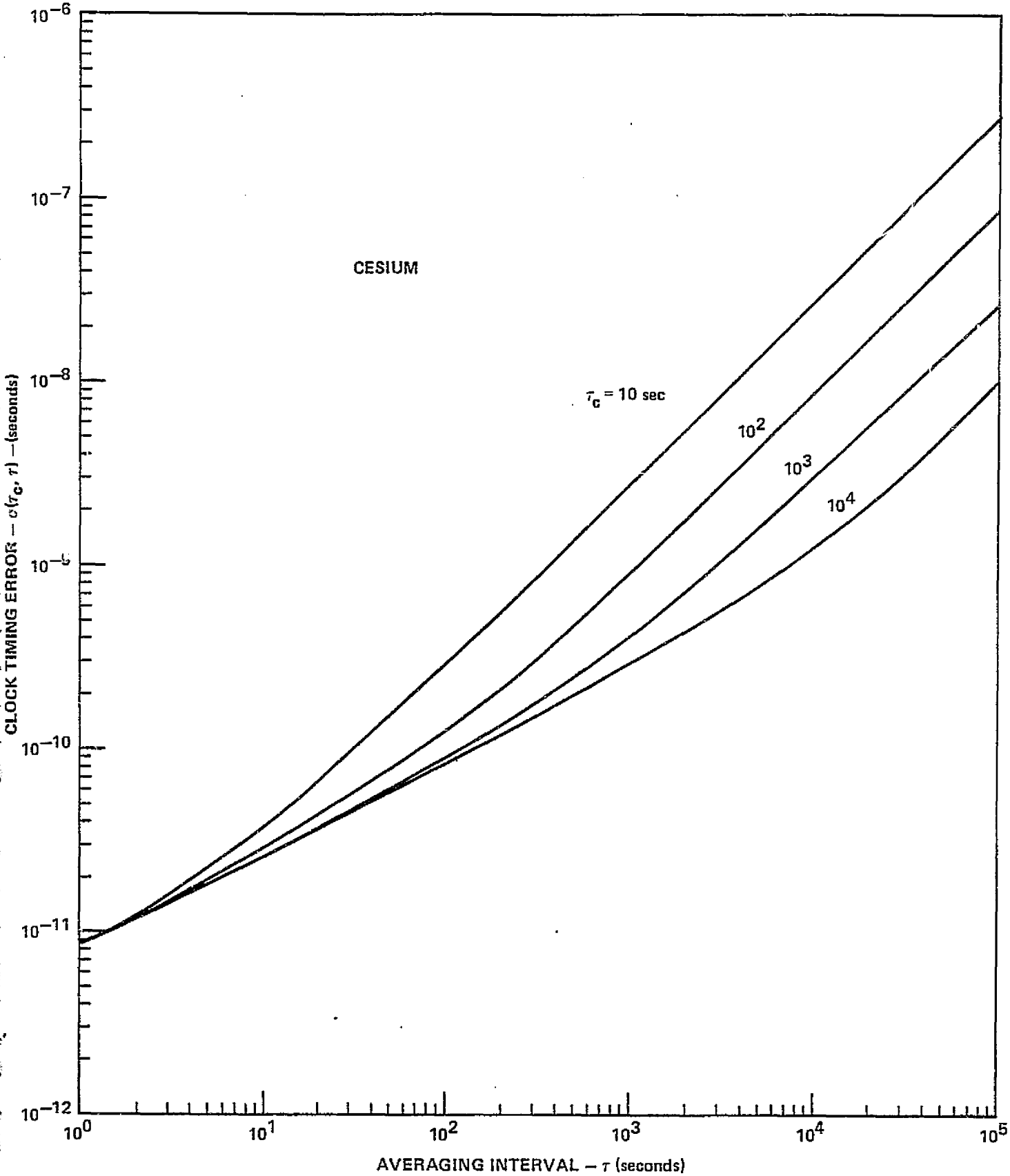

FIGURE 8.8. OVERALL GROUND CLOCK TIMING ERROR VS. AVERAGING INTERVAL FOR RT CONTINUOUS 1-WAY ONLY TRACKING USING A CESIUM STANDARD

previous paragraphs into equation (8-5) and using the results of Figures 8-5 through 8-8, the total timing error (for an averaging interval of τ= 300 seconds) becomes

- Cesium, Rubidium, or high quality crystal clock
  - σ_{C_4} = 0.344 microseconds (high inclination orbit)
  - σ_{C_4} = 1.917 microseconds (low inclination orbit)
- Nominal crystal clock
  - $\sigma_{C_4} \approx$ 3.5 microseconds or greater (high/low inclination orbit)

Since cesium clocks will be used at the ground stations, our results for this configuration are identical to those of the previous case (i.e., $\sigma_{C_4} = \sigma_{C_3}$). The resulting timing error associated with the cesium standard is completely masked by the poor ephemeris data error.

IX. COMPUTATION OF OVERALL CLOCK ERROR - NRT DATA TRANSFER

In the previous section the overall clock timing error was calculated for the case of real-time data event time tagging. The following paragraphs extend these earlier results to the case of time tagging events that are stored on-board a user spacecraft. The event time estimate will be performed by the clock on-board the user satellite. Tape recorders will be used to store the user event data prior to data dumpting through the TDRS. As before in Section VII, a total of four operational configurations are considered. In the following paragraphs the computation of overall clock error, σ_{c_i}, is given.

NRT DATA TRANSFER - CONTINUOUS 2-WAY R&RR

The only difference between this scheme and the proceeding operational model is that a clock is place aboard the user satellite for time tagging of events which are then stored in a buffer and transfered to the ground station at a later time. Based on this approach, the total clock timing error is equal to

$$\sigma_{c_5} = \left\{ \underbrace{\sigma_{c_1}^2}_{\substack{\text{ground}\\ \text{clock}\\ \text{error}}} + \underbrace{\sigma_0^2}_{\substack{\text{user}\\ \text{clock}\\ \text{calibration}\\ \text{error}}} + \underbrace{\sigma^2(\tau_c, T_B)}_{\substack{\text{user}\\ \text{clock}\\ \text{error}\\ \text{during}\\ T_B}} \right\}^{\frac{1}{2}} \qquad (9\text{-}1)$$

where σ_0 is the calibration error associated with the user clock when the time between recalibrations is equal to T_C. During an interval T_B, after calibration, the user clock will drift. For simplicity we will assume that $T_C = T_B$ which means that a calibration interval of duration τ_C will precede data dumping. Again using our assumption that a cesium clock will be in the ground station, equation (9-1) becomes

$$\sigma_{C_5} = \left\{10^{-18} + \sigma_o^2 + \sigma^2(\tau_C, T_B)\right\}^{\frac{1}{2}} \qquad (9\text{-}2)$$

Note that this expression is equal to equation (8-3), the only difference being in the chosen values for τ_C, $T_C = T_B$. Equation (9-2) has been evaluated for the four basic clocks for four separate operational modes. These results were obtained through the use of Figures 6.2 and 6.14 through 6.17 and the results are shown in Table 9.1. From Table 9.1 we see that the nominal crystal yields poor timing error (tens to hundreds of microseconds). The higher quality crystal is somewhat better (σ_{C_5} on the order of a few microseconds or less). The atomic standards are much better with timing errors on the order of 20 nanoseconds or less. However, it is doubtful that a typical user could place one of these atomic frequency sources aboard the satellite because of size, weight, and cost constraints.

NRT DATA TRANSFER - CONTINUOUS 1-WAY RR WITH R&RR CALIBRATION

For this scheme a transponder clock is required in the user in addition to an event time tagging clock. This transponder clock must be calibrated so that continuous one-way range rate data can be transmitted after a suitable calibration interval. The composite timing error for this mode is equal to

$$\sigma_{C_6} = \left\{\sigma_{C_1}^2 + \sigma_{O_1}^2 + \sigma_{O_2}^2 + \sigma^2(\tau_{C_1}, T_{B_1}) + \sigma^2(\tau_{C_1}, T_{B_2})^2\right\}^{\frac{1}{2}} \qquad (9\text{-}3)$$

where

$\sigma_{C_1} \equiv$ ground clock error (10^{-9} sec)

$\sigma_{O_1} \equiv$ user transponder clock calibration error

$\sigma_{O_2} \equiv$ user event clock calibration error

$\sigma(\tau_{C_1}, T_{B_1}) \equiv$ user transponder clock error during T_{B_1}

$\sigma(\tau_{C_2}, T_{B_2}) \equiv$ user event clock error during T_{B_2}

Equation (9-3) has been evaluated for the case when T_{B_1} = 20 minutes, τ_{C_1} = 2 minutes, $T_{C_1} = T_{C_2}$ and $T_{B_2} = \tau_{C_2}$. These results are obtained by using the appropriate figures in Section VI and are shown in Table 9.2. From Table 9.2 we note that this operational mode has approximately the same time tagging accuracy as the previous case for NRT data transfer using continuous 2-way R&RR data. The effect of having to calibrate the transponder clock is almost negligible when compared to the user event clock timing error. It should be noted that for different values of T_{B_1}, T_{B_2}, T_{C_1}, T_{C_2}, τ_{C_1}, and τ_{C_2}, this may not be true in general. One has to analyze the specific case in hand and be careful about making general statements.

TABLE 9.1

TOTAL CLOCK TIMING ERROR FOR NRT DATA TRANSFER

USING THE CONTINUOUS 2-WAY R&RR DATA

Operational Mode	τ_C (minutes)	$T_B = T_C$ (minutes)	σ_{C_5} (microseconds)			
			Crystal 1	Crystal 2	Rubidium	Cesium
Data dump/TDRS pass	5	43	95.	0.3	0.003	0.002
Data dump/User orbit	5	90	240.	0.8	0.007	0.004
Data dump/2 user orbits	10	180	620.	2.1	0.010	0.006
Record 20 minutes from calibration	5	20	34.	0.10	0.001	0.001

TABLE 9.2

TOTAL CLOCK TIMING ERROR FOR NRT DATA TRANSFER

USING CONTINUOUS 1-WAY RR DATA WITH R&RR CALIBRATION

Operational Mode	τ_{C_2} (minutes)	$T_{B_2} = T_{C_2}$ (minutes)	σ_{C_6} (microseconds)			
			Crystal 1	Crystal 2	Rubidium	Cesium
Data dump/TDRS pass	5	43	98.	0.31	0.003	0.002
Data dump/User orbit	5	90	241.	0.8	0.007	0.004
Data dump/2 user orbits	10	180	620.	2.1	0.010	0.006
Record 20 minutes from calibration	5	20	42.	0.11	0.002	0.002

NRT DATA TRANSFER - R&RR CALIBRATION WITH EPHEMERIS DATA

This mode is similar to an earlier RT operational mode using orbit position data instead of one-way RR measurement data. The only difference is that an event clock is placed aboard the user. Based on this fact, the resulting timing error is equal to

$$\sigma_{c_7} = \left\{ \sigma_{c_1}^2 + \sigma_{pos}^2 + \sigma_o^2 + \sigma^2(\tau_c, T_B) \right\}^{\frac{1}{2}} \qquad (9\text{-}4)$$

where

σ_{pos} ≡ position time error from orbit data (see earlier paragraph in Section VIII)

σ_o ≡ calibration error of user event clock

$\sigma(\tau_c, T_B)$ ≡ user event clock error during T_B

σ_{c_1} ≡ ground clock error (10^{-9} sec)

Substitution of the appropriate values into the above expression (and noting that $T_C = T_B$) from the figures of the previous sections yields the composite timing error shown in Table 9.3. The total timing error must be greater than or equal to the position data timing error. For satellite users with crystals Table 9.2 indicates that position error is not the dominant contributor in most cases. On the other extreme, there is no point in placing atomic standards in the user satellite if position data is to be used to obtain time tagging because the capability or accuracy of the atomic standard is masked by the poor position data error.

NRT DATA TRANSFER - ONE WAY ONLY TRACKING

This particular configuration is much different from the three previous cases since a forward link to the user is never available. The user takes event data as necessary (at any orbitrary time), time tags this data and places it in storage. When in view of TDRS, the user can elect to dump this data which has been stored for some time duration denoted by T_S. The ground station must receive the user signal and estimate the transmitted clock frequency. The contributing time error sources for this case include:

- Time reference user calibration error
  - User clock drift error, σ_o
  - User clock frequency offset, $\sigma_{\delta f}$
- User clock time error during T_S, $\sigma(\tau_{cs}, T_S)$
- Ground reference clock time error, $\sigma(\tau_{cg}, \tau)$
- Ephemeris error in the determination of the propagation delay, σ_{pos}

TABLE 9.3

TOTAL CLOCK TIMING ERROR FOR NRT DATA TRANSFER USING R&RR CALIBRATION WITH POSITION DATA

Operational Mode	τ_C (Minutes)	$T_B = T_C$ (Minutes)	σ_{C_7} (microseconds)							
			Crystal 1		Crystal 2		Rubidium		Cesium	
			Lo	Hi	Lo	Hi	Lo	Hi	Lo	Hi
Data Dump/TDRS Pass	5	43	96.	95.	1.94	0.46	1.92	0.34	1.92	0.34
Data Dump/User Orbit	5	90	240.	240.	2.08	0.87	1.92	0.34	1.92	0.34
Data Dump/2 User Orbits	10	180	620.	620.	2.84	2.13	1.92	0.34	1.92	0.34
Record 20 Minutes from Calibration	5	20	35.	34.	1.92	0.38	1.92	0.34	1.92	0.34

The resulting expression for the total clock timing error is then given by

$$\sigma_{c_B} = \left\{ \sigma_o^2 + \left(\frac{\delta f}{f_o} T_s\right)^2 + \sigma^2\left(\tau_{cs}, T_s\right) + \sigma^2\left(\tau_{cg}, \tau\right) + \sigma_{pos}^2 \right\}^{\frac{1}{2}} \quad (9\text{-}5)$$

user drift error	user frequency offset error	user clock error during T_s	ground clock error during τ	ephemeris error

where

$f_o \equiv$ user transmit frequency

$\delta f \equiv$ frequency offset error

$T_s \equiv$ data storage time on-board the user

$\tau_{cs} \equiv$ calibration time of the user and the TDRSS

$\tau_{cg} \equiv$ calibration time of the ground clock

$\tau \equiv$ averaging interval

For convenience, equation (9-5) has been broken into two parts; the first part dealing with clock errors only, σ_{cL}, and the second part dealing with ephemeris data.

$$\sigma_{c_B} = \left\{ \sigma_{cL}^2 + \sigma_{pos}^2 \right\}^{\frac{1}{2}} \quad (9\text{-}6)$$

In equation (9-6), the term σ_{cL}^2 is merely the sum of the first four terms of equation (9-5). This quantity, σ_{cL}, has been evaluated for each of our four frequency standards of interest. Figure 9.1 depicts this error and the component parts for crystal 1 as a function of user satellite data storage time, T_s. The frequency offset error is constrained to $\delta f \leq 5$ Hz, and the user satellite calibration time to $\tau_{cs} = 30$ minutes. Our ground calibration interval is defined as $\tau_{cg} = \tau$ and has a range of values from one second to 300 seconds. From Figure 9.1 it is evident that the user satellite clock error masks all other error sources for crystal 1. In Figure 9.2, σ_{cL} is plotted versus T_s for various values of frequency offset error ($\delta f \leq 20$ Hz) and user satellite calibration interval (1 min. $\leq \tau_{cs} \leq$ 30 min.). In order to achieve a one microsecond timing accuracy, Figure 9.2 indicates that the maximum allowable user data storage time is on the order of $T_s = 2$ minutes or less. In order for a typical user to store an entire orbit of data ($T_s \simeq 100$ min.), crystal 1 would only allow for a timing accuracy of approximately 300 μseconds.

Similar results for σ_{cL} have been developed for the higher quality crystal 2 and the Rubidium and Cesium standards. These characteristics are shown in Figures 9.3, 9.4 and 9.5 respectively. Unlike the previous case with crystal 1 where the user clock error was predominant, it is the frequency offset error term that represents our major source of timing error.

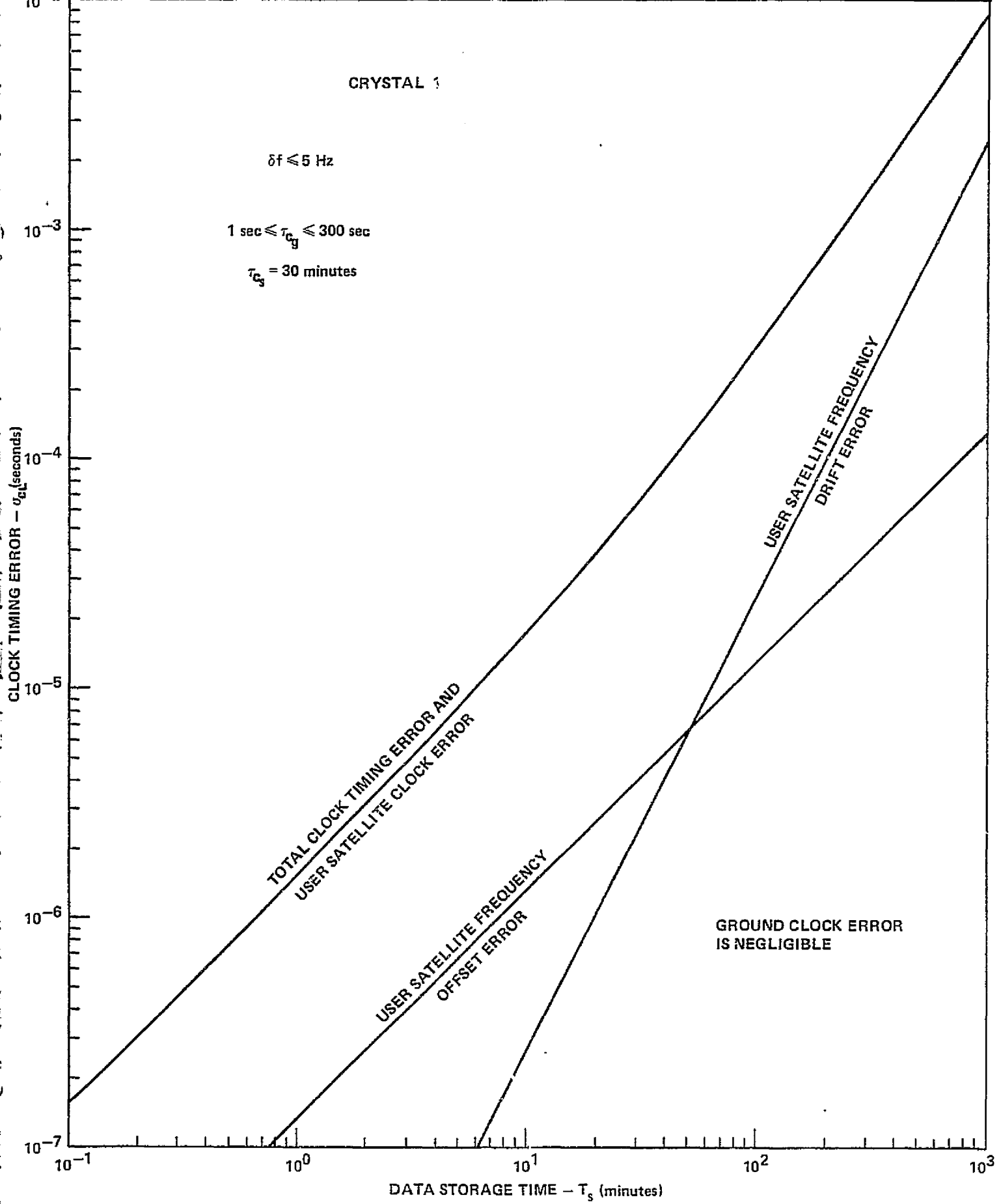

FIGURE 9.1. CLOCK TIMING ERROR VERSUS USER DATA STORAGE TIME FOR CRYSTAL 1 AND $\delta f \leq 5$ Hz

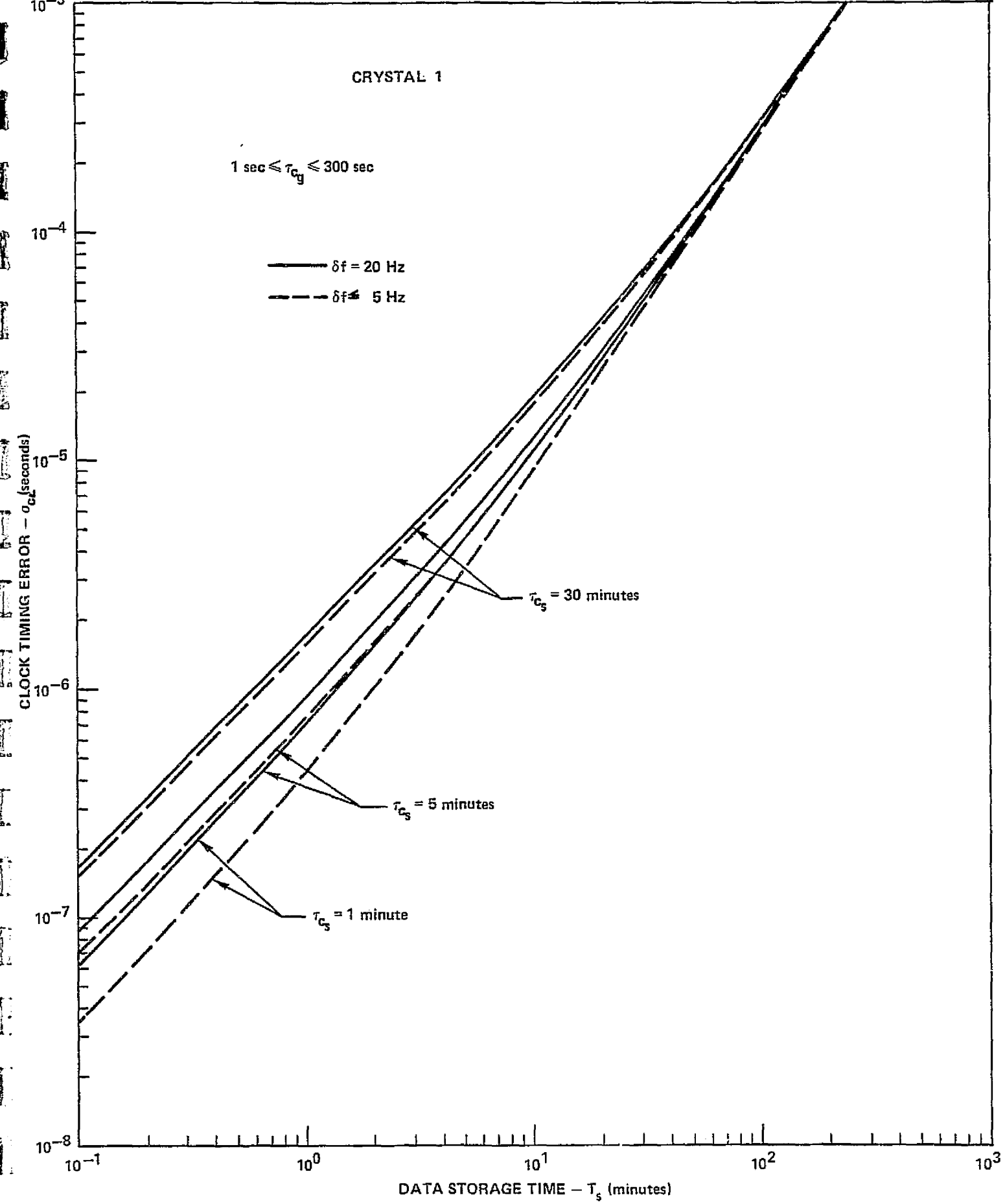

FIGURE 9.2. CLOCK TIMING ERROR VERSUS USER DATA STORAGE TIME FOR CRYSTAL 1 AND $\delta f \leq 20$ Hz and $\tau_{CS} \leq 30$ MINUTES

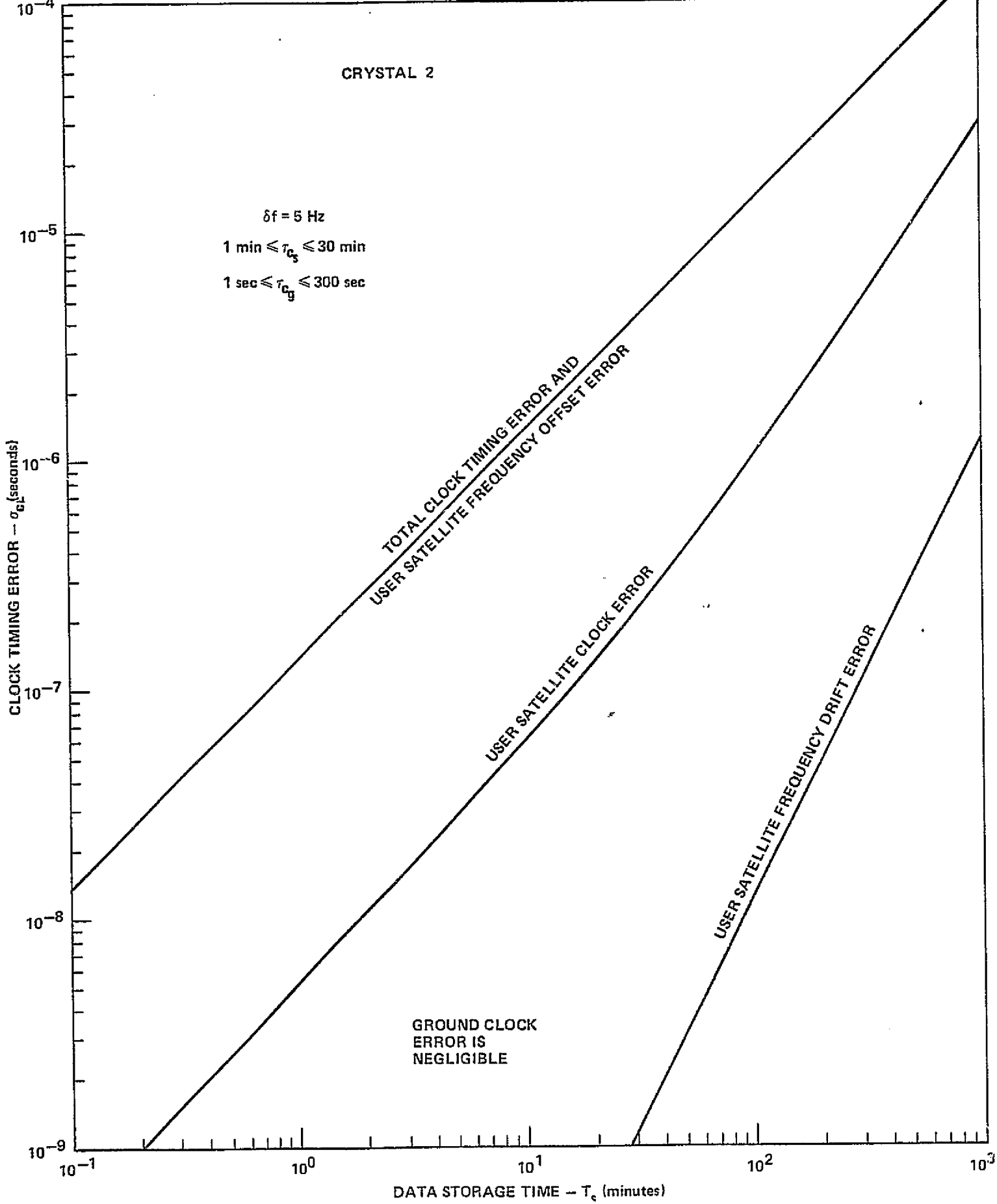

FIGURE 9.3. CLOCK TIMING ERROR VERSUS USER DATA STORAGE TIME FOR CRYSTAL 2 AND $\delta f \leq 5$ Hz

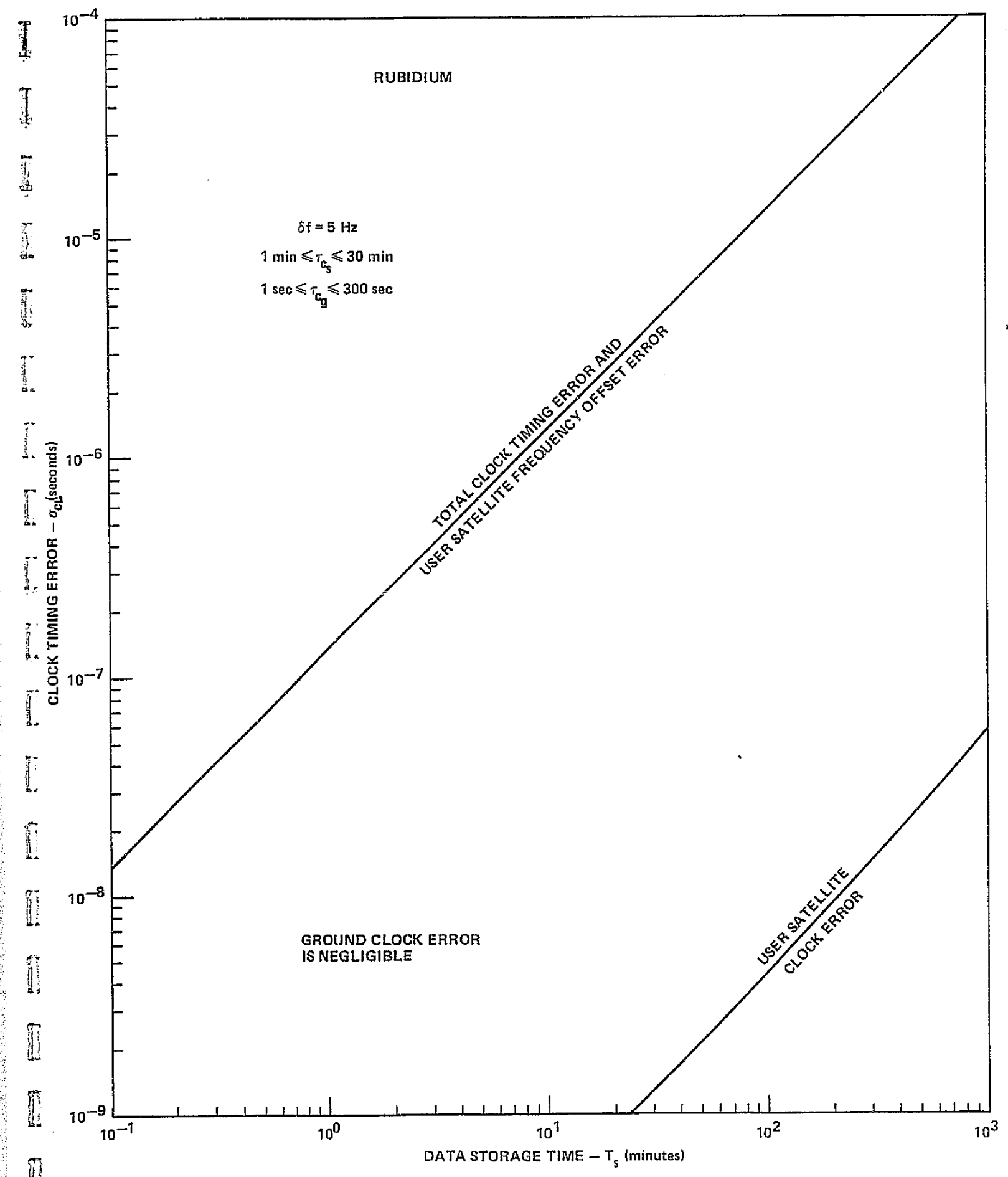

FIGURE 9.4. CLOCK TIMING ERROR VERSUS USER DATA STORAGE TIME FOR A RUBIDIUM STANDARD AND $\delta f \leq 5$ Hz

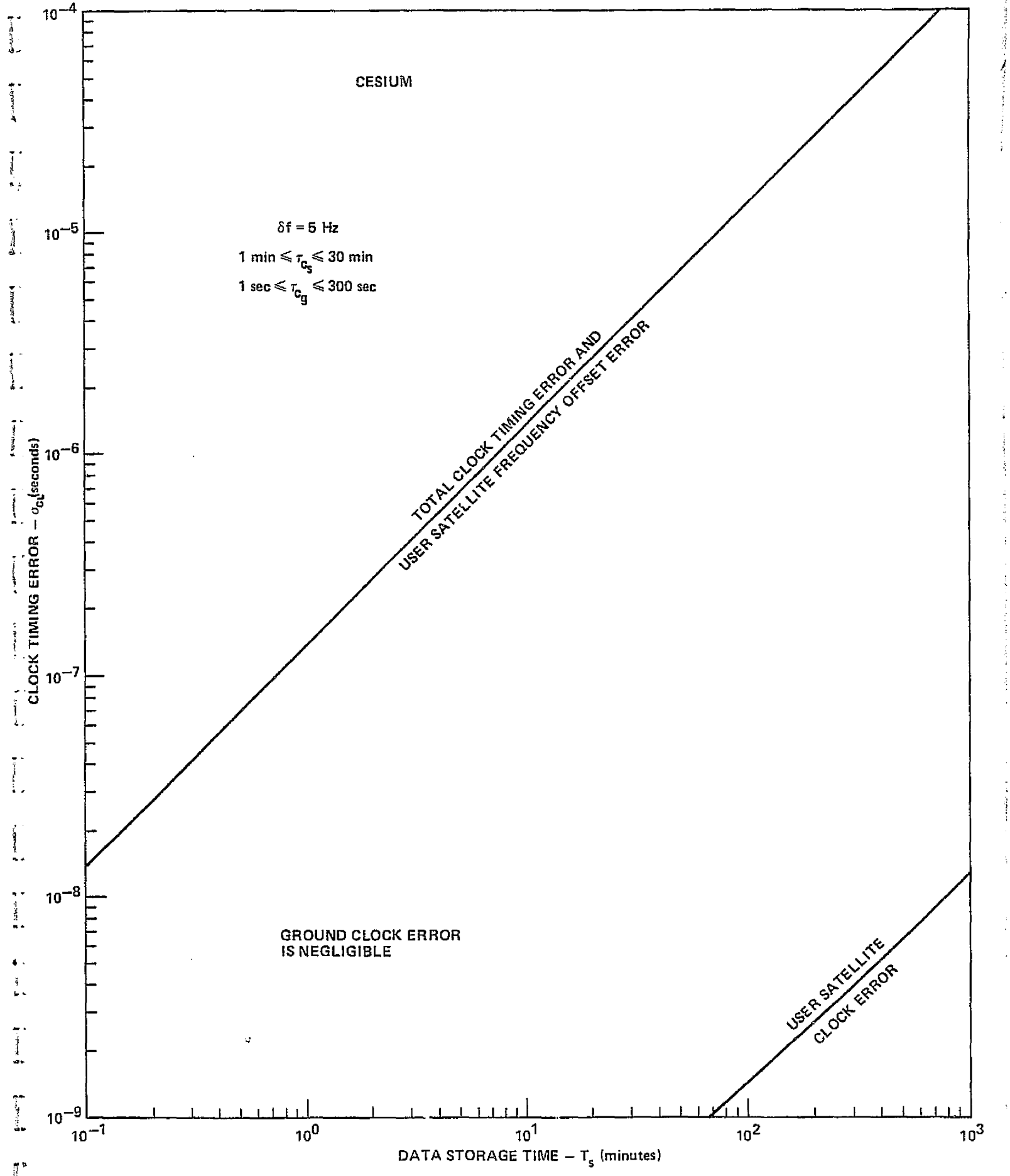

FIGURE 9.5. CLOCK TIMING ERROR VERSUS USER DATA STORAGE TIME FOR A CESIUM STANDARD AND $\delta f \leq 5$ Hz

More specific results for these three clocks are given Figure 9.6 for crystal 2 and Figure 9.7 for the atomic clocks. The frequency offset error has been allowed to vary from 0.2 Hz to 20 Hz. Since this is our dominant error source the results are insensitive to user calibration time, τ_{cs}, and ground calibration time, τ_{cg}. An expected value for δf is on the order of 5 Hz for S-band frequencies. For this case, microsecond clock timing accuracy is achieved for user data storage times on the order of $T_s \approx 7$ to 8 minutes. This would severely limit some of the user satellites in terms of their scientific applications. For a typical user to store an entire orbit of data ($T_s \approx 100$ minutes), the resulting timing error would be approximately $\tau_{c_8} \simeq$ 14 μseconds for a frequency offset error corresponding to δf=5 Hz.

The total clock timing error, σ_{c8}, is shown in Table 9.4 for the four operational modes considered to date. Basicly, the poor quality crystal 1 yields poorer timing accuracy than the other three clocks by a factor of about 15:1. Also, in order to allow for storage of nominal 90-100 minute orbits of data, the resulting timing accuracy is upper bounded by approximately $\sigma_{c8} \approx$ 12-14 μseconds. The fundamental timing accuracy of this NRT 1-way only tracking configuration is limited to 12-14 μseconds no matter how accurate a clock is placed in the user satellite. Possibly more sophisticated ground frequency tracking (δf=0.2 Hz) would allow for an overall timing accuracy of 1 μsecond using the high quality clocks. This, however, is a subject warranting further investigation.

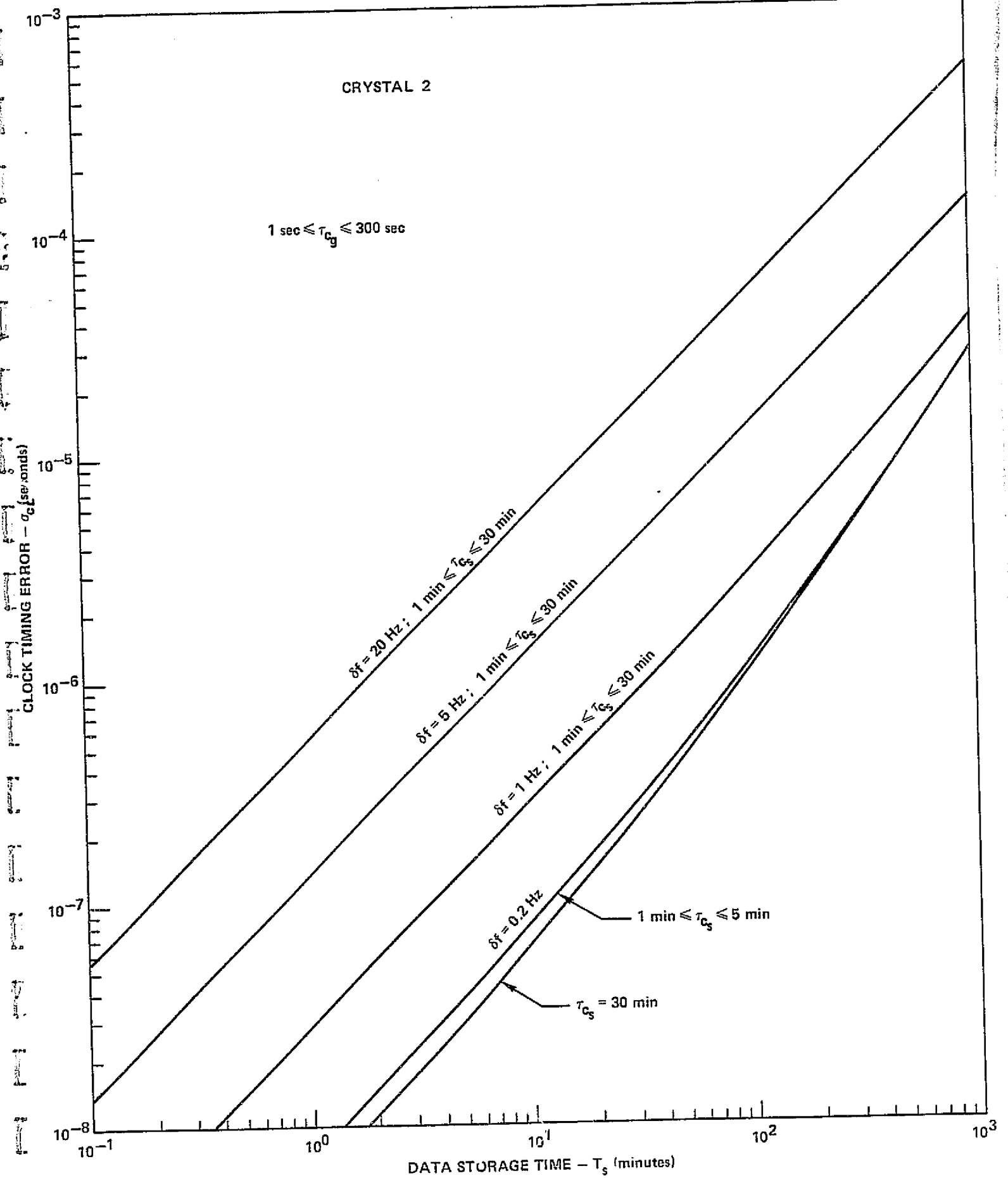

FIGURE 9.6. CLOCK TIMING ERROR VERSUS USER DATA STORAGE TIME FOR CRYSTAL 2 AND $\delta f \leq 20$ Hz AND $\tau_{CS} \leq 30$ MINUTES

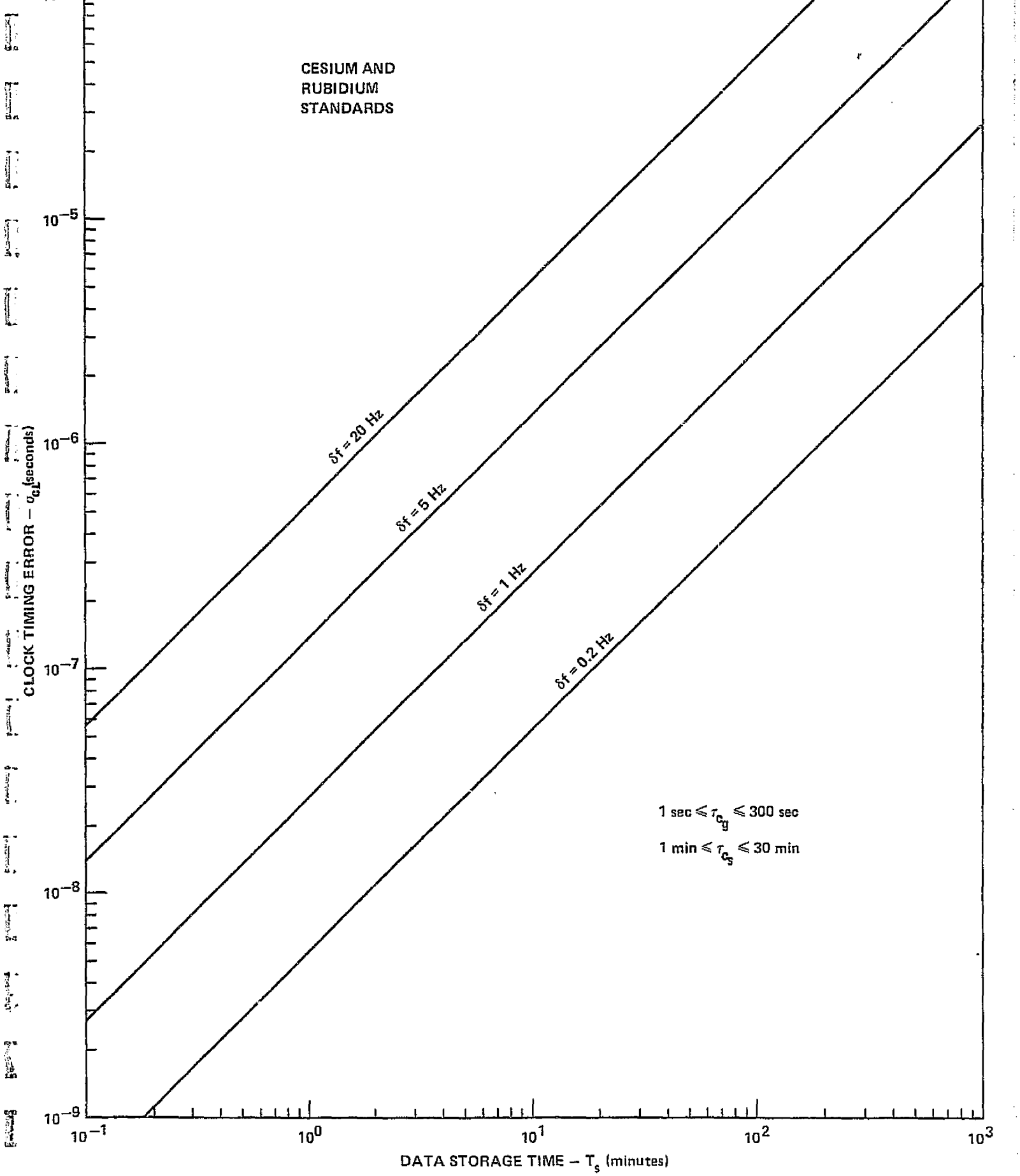

FIGURE 9.7. CLOCK TIMING ERROR VERSUS USER DATA STORAGE TIME FOR A CESIUM OR RUBIDIUM STANDARD AND $\delta f \leq 20$ Hz AND $\tau_{CS} \leq 30$ MINUTES

TABLE 9.4

TOTAL CLOCK TIMING ERROR FOR NRT ONE-WAY ONLY TRACKING (δf=5Hz)

Operational Mode	τ_{C_s} (Minutes)	T_s (Minutes)	σ_{C_g} (microseconds)		
			Crystal 1 Lo/Hi Inclination	Crystal 2, Rubidium or Cesium	
				Lo Inclination	Hi Inclination
Data Dump/TDRS Pass	5	43	96.	6.1	5.8
Data Dump/User Orbit	5	90	270.	12.2	12.0
Data Dump/2 User Orbits	10	180	750.	24.1	24.0
Record 20 Minutes from Calibration	5	20	28.	3.3	2.7

X. SUMMARY OF USER/TDRSS TIMING ERRORS

In the last two sections, the respective clock and equipment errors have been computed for some potential operational modes of interest. Based on these analyses, the total system timing error, σ_ε, has been computed according to equation (7-1). The results along with the contributing error components are shown in Table 10.1. These results were prepared for a reasonable worst-case operational implementation. Refer to the earlier sections on clock error for these details. In Table 10.1 the shaded regions represent "reasonable and practical" implementations. Other specific cases would have to be examined for different user clocks, but the methodology has been given and tradeoff curves are provided in Sections VI, VIII and IX.

In terms of satisfying our initial goal of $\sigma_\varepsilon < 1$ μsecond timing error, only operational modes 1 and 2 are fully acceptable using an atomic standard as the ground clock and at least a high quality crystal clock in the user satellite for mode 2. Modes 3 and 4 would also be acceptable for certain high inclination orbits. All of these first 4 modes deal with time tagging real-time event data only. For non real-time event time tagging, the next 4 modes are basicly unacceptable (for $\sigma_\varepsilon = 1$ μsec) without some modifications of parameters, such as reducing the user data storage time or placing an atomic standard aboard the user spacecraft. One additional comment worth noting is that one-way links from the user through TDRS generally provide either poor timing accuracy or small data storage time.

TABLE 10.1

SUMMARY OF USER/TDRSS TIMING ERRORS

Operational Mode	Equipment Timing Error, σ_e	Clock Timing Error, σ_{c_i}				Total System Timing Error, σ_ε			
		Nominal Crystal	High Quality Crystal	Rubidium	Cesium	Nominal Crystal	High Quality Crystal	Rubidium	Cesium
1*	647 nsec.	$\leq$ 3.3 μsec	$\leq$ 12 nsec	$\leq$ 0.6 nsec	$\leq$ 0.9 nsec	$\leq$ 3.4 μsec	$\leq$ .65 μsec	$\leq$ .65 μsec	$\leq$ .65 μsec
2*	647 nsec.	$\leq$ 90 μsec	$\leq$ 0.3 μsec	$\leq$ 3 nsec	$\leq$ 2 nsec	$\leq$ 90 μsec	$\leq$ .71 μsec	$\leq$ .65 μsec	$\leq$ .65 μsec
3* and 4*	647 nsec.	← $\leq$ .34** (1.9) μsec*** →				← $\leq$ .73** (2.02) μsec*** →			
5* and 6*	647 nsec.	$\leq$ 620 μsec	$\leq$ 2.1 μsec	$\leq$ 10 nsec	$\leq$ 6 nsec	$\leq$ 620 μsec	$\leq$ 2.2 μsec	$\leq$ .65 μsec	$\leq$ .65 μsec
7*	647 nsec.	$\leq$ 620 μsec	$\leq$ 2.9 μsec	$\leq$ .34** (1.9) μsec***		$\leq$ 620 μsec	$\leq$ 3.0 μsec	$\leq$ .73** (2.02) μsec***	
8*	647 nsec.	$\leq$ 750 μsec	$\leq$ 24.1 μsec			$\leq$ 750 μsec	$\leq$ 24.2 μsec		

*1 - RT Continuous 2-way R&RR
2 - RT Continuous 1-way RR with R&RR Calibration
3 - RT R&RR Calibration with Position Data
4 - RT One Way Only Tracking
5 - NRT Data Transfer - Continuous 2-way R&RR
6 - NRT Data Transfer - Continuous 1-way RR with R&RR Calibration
7 - NRT Data Transfer - R&RR Calibration with Position Data
8 - NRT Data Transfer - One Way Only Tracking

** For High inclination orbits.

*** For Low inclination orbits.

REFERENCES

1. Tracking and Data Relay Satellite System (TDRSS) Users' Guide, STDN No. 101.2, Revision 2, May 1975.

2. Performance Specification for Telecommunications Services Via the Tracking and Data Relay Satellite System, S-805-1, Revised November 1975.

3. TDRSS Telecommunications Study Phase 1 - Final Report, 15 September 1974, Advanced Products Division, The Magnavox Company.

4. TDRSS Alternate vs. Barcline System Study, Final Report, ORI Tech Report 1019, 27 February 1976.

5. Bertrand T. Fang, Brice P. Gibbs, TDRSS Era Orbit Determination System Review Study, Planetary Sciences Department Report No. MTO10-75, December 1975, Wolf Research and Development Group.

6. K. Davies, R. B. Fritz, R. N. Grubb and J. E. Jones, IEEE AES, vol. 11, p. 1103 (Nov. 1975).

7. F. J. Gorman Jr. and H. Soicher, Proc. PTTI 1974, p. 441.

8. L. J. Ippolito, NASA/GSFC Doc. No. X-951-75-211, August 1975.

9. G. H. Millman and R. E. Anderson in Phase and Frequency Instabilities in Electromagnetic Wave Propagation, AGARD Conf. Proc. No. 33, July 1970, p. 545.

10. G. H. Millman, in Propagation Factors in Space Communications, AGARD Conf. Proc. No. 3, 1967, p. 24.

References:

11. P. E. Schmid, R. B. Bent, S. K. Llewellyn, G. Nesterczrek, and S. Rangaswamy, "NASA-GSFC Ionospheric Corrections to Satellite Tracking Data," Doc. No. X-591-73-281, December 1973.

12. A brief summary of the ionospheric models may be found in "Total Electron Content and Scintillation Studies of the Ionosphere," ed. by J. Aarons, AGARDograph No. 166, ph. 13.

13. P. Schmid, GSFC, (301) 982-5320, private communication, April 1976.

14. R. Anderson, GE, Schenectady, (518) 374-2211 X52746, private communication, April 1976.

15. K. Davies, R. B. Fritz, R. N. Grubb, J. E. Jones, "ATS-6 Radio Beacon Experiment: The First Year," IEEE Trans. Aerosp and Elect. Systems, Vol. AES-11, pg. 1103, November 1975.

16. G. M. R. Winkler, Proc. IEEE 60, 526 (1972).

17. J. W. Marini, NASA/GSFC Doc. No. X-551-72-277, 1972.

18. J. W. Marini, Radio Science 7, 223 (1972).

19. J. W. Marini, NASA/GSFC Doc. No. X-551-71-122, 1971.

20. "Propagation Delay Statistics for Earth-Space Paths," CCIR (1974-1978), DOC. 5/23-E, 22 October 1975.

21. D.A. Gray, "Transmit-Time Variations in Line-of-Sight Tropospheric Propagation Paths," B.S.T.J. 49, July-August 1970, pp. 1059-1068.

22. Robert M. Cunningham, "Meteorological Aspects of Range and Range Rate Error," AFCRL Report ESD-TD4-64-103.

23. Cutler, L. and Searle, C., "Some Aspects of the Theory and Measurement of Frequency Fluctuations in Frequency Standards," Proc. of the IEEE, February 1966, pp. 136-154.

24. Blair, B., ed. Time and Frequency: Theory and Fundamentals, NBS Monograph 140, 1974.

25. Allan, D., "Statistics of Atomic Frequency Standards, Proc. IEEE, February 1966, pp. 221-230.

26. Barnes, J., et al, "Characterization of Frequency Stability," IEEE Trans. IM-20, May 1971, pp. 105-120.

27. Vessut, R., et al, "An Intercomparison of Hydrogen and Cesium Frequency Standards," IEEE Trans. IM-15, December 1966, pp. 165-176.

References:

28. Reinhardt, V., "Frequency Stability Requirements for Two Way Range Rate Tracking," Proc. of the 7th Annual Precise Time and Time Interval (PTTI) Applications and Planning Meeting, December 1975, pp. 265-283.

29. Hewlett Packard Applications Note 52-2, Timekeeping and Frequency Calibration, November 1975.